

# **An in-line measuring technique with tool error detection in an automotive production line**

By

**Florian Viol**

Submitted in fulfilment of the requirements for the degree of  
Masters of Engineering at the Nelson Mandela Metropolitan  
University

**December 2010**

**Promoter: Professor Theo van Niekerk**

**Co-Promoter: Professor Hinrich Holdack-Janssen**



## **Confidential content**

This project has been carried in cooperation with the Volkswagen AG. The content of this project is confidential and the information shall not be provided to third parties.

## Author's declaration

I, Florian Viol with student number 210227648, hereby declare that the thesis for "Master of Engineering" is my own work and that it has not previously been submitted for assessment to another University or for another qualification.

Signature: \_\_\_\_\_

Date: April 6<sup>th</sup>, 2011

## **Abstract**

The modern automobile industry faces an increasing demand on personalized high quality products. In order to stay competitive the automobile manufacturers have to ensure the customers high quality demands. With the increasing amount of applied parts and components manufacturing processes are becoming more complex. The recent quality assurance of the manufacturers considers only the product quality. Furthermore are with the recent quality assurance methods only punctual integrations of quality assurance tools in production chains possible. These limitations cause a large quality control loop. This leads in case of defective parts to an enormous time and money effort to track the cause for the defect.

This project presents an innovative measurement strategy of quality assurance within the modern automobile production which will minimize the control loop and identify the tool causing the defect in the part. It highlights the possibility to integrate equipment for quality assurance directly into the production cell itself and analyse the geometrical conditions within the manufacturing processes. The result of this thesis is a fully automated prototype which is installed into the actual production of the Volkswagen Golf assembly. The prototype system consists on the one hand out of different on the market free available hardware and software components. On the other hand there are specifically for this prototype developed hardware components and software tools. For the first time it is possible to inspect the geometrical conditions of one tool continuously during production and identify, if occurring, deviations in the tool in position direction and size.

The installation of similar systems in the production will minimize the control loops of the production. The chance of early recognition of errors will reduce the efforts and cost of error backtracking. In ideal conditions this instrument will identify defective tools before a product is manufactured. This innovative quality tool is the ideal addition to the current quality assurance and is the first link between the product quality and the geometrical conditions of the tools.

## **Acknowledgement**

I want to acknowledge my promoters Professor Theo van Niekerk and Professor Hinrich Holdack-Janssen for their guidance, support and encouragement.

This research has been carried out in 2010 in the cooperation project CarMetric at the institute for vehicle engineering in cooperation with the Volkswagen AG. I want to acknowledge all those who supported and guided me in this duration. I abdicate listing people by name since support, guidance, encouragement has many faces. I hope in this way to bypass to miss somebody.

Further I want to acknowledge my father and my girlfriend for their support and patience during this project period.

## Table of content

Confidential content.....	I
Author's declaration .....	II
Abstract .....	III
Acknowledgement .....	IV
Table of content.....	V
List of Figures.....	VIII
List of Tables .....	X
List of Equations.....	XI
List of Abbreviations .....	XII
1. Introduction to current quality strategy .....	1
1.1. RPS standard of Volkswagen .....	2
1.2. Quality assurance in production.....	4
1.2.1. Product path.....	4
1.2.2. Measurement tools .....	6
1.2.2.1. Perceptron inline measurement .....	6
1.2.2.2. Coordinate measuring machine .....	8
1.2.2.3. Software analysis.....	11
1.2.3. Control loop and error detection.....	12
1.2.4. Error elimination .....	13
1.3. Disadvantages of current strategy .....	14
2. Innovative quality strategy .....	16
2.1. Measurement principle of innovative strategy .....	17
2.2. Principle laser triangulation .....	19
2.3. Principle of photogrammetry .....	19
2.4. Measurement method .....	23
2.5. Advantages & Disadvantages of measurement method .....	24
3. State of Technology .....	26
3.1. Components.....	26
3.1.1. Optical sensors .....	26
3.1.1.1. CMOS sensor .....	27
3.1.1.2. 2D and 3D sensors .....	28
3.1.2. Laser.....	29

---

3.1.3.	Industrial robots .....	33
3.2.	Software .....	36
3.3.	Required interfaces .....	38
3.3.1.	Framegrabber .....	38
3.3.2.	Controller .....	38
4.	System implementation .....	39
4.1.	Production cell .....	39
4.2.	Hardware .....	41
4.3.	Software .....	44
4.4.	System setup .....	48
5.	Measurement with innovative system.....	52
5.1.	General settings .....	52
5.2.	System configuration.....	54
5.3.	Calibration of system.....	56
5.4.	Definition of nominal data.....	57
5.5.	Alignment.....	58
5.5.1.	Best fit registration .....	59
5.5.2.	3-2-1 registration.....	60
5.6.	Measuring procedure .....	61
5.6.1.	Manual measurements .....	61
5.6.2.	Automated measurements.....	63
5.7.	Display of the results.....	64
6.	Testing and data analysis.....	66
6.1.	Test setup .....	66
6.2.	Test object .....	67
6.3.	Testing procedure .....	68
6.4.	Data transformation.....	69
7.	Verification of results .....	71
7.1.	Points of interest for analysis .....	71
7.2.	Errors .....	72
7.3.	Theoretical evaluation of measurements .....	72
7.4.	Analysis of measurements .....	76
7.4.1.	Arithmetic average of measurements .....	76
7.4.2.	Standard deviation .....	77

---



---

7.4.3.	Interval of confidence .....	78
7.4.4.	Total deviation in three- dimensional space .....	82
8.	Discussion and conclusion .....	84
9.	Future developments and recommendations .....	<b>Fehler! Textmarke nicht definiert.</b>
10.	List of reference .....	89
Appendix A	.....	A 1
Appendix B	.....	B 1
Appendix C	.....	C 1
Appendix D	.....	D 1
Appendix E	.....	E 1
Appendix F	.....	F 1
Appendix G	.....	G 1
Appendix H	.....	H 1
Appendix I	.....	I 1

## List of Figures

Figure 1.1: Vehicle coordinate system (Volkswagen AG 1996).....	3
Figure 1.2: Degrees of freedom.....	3
Figure 1.3: Product path side panel (Barthen 2009).....	5
Figure 1.4: Laser triangulation principle .....	6
Figure 1.5: PSD element (Schnell 1998).....	7
Figure 1.6: Perceptron (Perceptron 2010).....	8
Figure 1.7: Tactile sensing mechanism .....	9
Figure 1.8: Mechanical trigger device.....	10
Figure 1.9: Quirl report (Hoffmann 2009) .....	11
Figure 1.10: Quirl colour plot (Hoffmann 2009) .....	12
Figure 1.11: Geometrical welding drums "Wilder Mix ".....	13
Figure 1.12: Geometry elements of tool .....	14
Figure 2.1: Principle of measurement.....	18
Figure 2.2: Robot installation.....	19
Figure 2.3: Central projection .....	20
Figure 2.4: Point projection.....	21
Figure 2.5: Collinearity condition .....	22
Figure 2.6: System setup.....	24
Figure 3.1: Digital image processing .....	26
Figure 3.2: Photon- to- electron conversion .....	28
Figure 3.3: Principle function of laser .....	29
Figure 3.4: Wave length (Sipex 2007) .....	30
Figure 3.5: Harmonic wave.....	31
Figure 3.6: Gauß model of intensity .....	32
Figure 3.7: Spectral bandwidth of laser and of light.....	32
Figure 3.8: Industrial robot .....	33
Figure 3.9: Modes of movement.....	34
Figure 3.10: Angle single axis during movement.....	35
Figure 3.11: Robot parameters during movement.....	36
Figure 3.12: Sensor read out algorithm .....	36
Figure 4.1: Layout tailgate Golf+ (Labahn 2010) .....	39
Figure 4.2: Robot grab in production cell.....	40

---

Figure 4.3: Hardware components .....	41
Figure 4.4: Sensor capabilities .....	42
Figure 4.5: Laser module.....	43
Figure 4.6: Atmel controller .....	43
Figure 4.7: Pattern.....	44
Figure 4.8: Software processes.....	45
Figure 4.9: Peakfinder processing.....	46
Figure 4.10: Merge process of range maps.....	46
Figure 4.11: Cloud of points .....	47
Figure 4.12: Hardware integration .....	49
Figure 4.13: Implemented sensor unit.....	50
Figure 4.14: Robot grab with calibration pattern.....	50
Figure 5.1: Optimal sensor constellation .....	52
Figure 5.2: General software overview .....	53
Figure 5.3: Setting dialogue.....	55
Figure 5.4: Result of merger calibration .....	56
Figure 5.5: Result of metric calibration .....	57
Figure 5.6: Configuration of nominal data .....	58
Figure 5.7: Best fit alignment.....	59
Figure 5.8: 3-2-1 preselection.....	60
Figure 5.9: Result with 3-2-1 registration.....	61
Figure 5.10: Manual mode .....	62
Figure 5.11: Automatic mode .....	63
Figure 5.12: Display of Z deviation .....	64
Figure 5.13: Display of X-Y deviation .....	65
Figure 6.1: Angle between sensor and object .....	66
Figure 6.2: Focusing of laser line .....	67
Figure 6.3: ATOS measurement result.....	68
Figure 6.4: Scheme of robot test cycle .....	69
Figure 7.1: Points of interest.....	71
Figure 7.2: Gaussian distribution curve .....	75
Figure 7.3: Gaussian distribution curve x .....	80
Figure 7.4: Gaussian distribution curve Y.....	81
Figure 7.5: Gaussian distribution curve Z.....	82

---

## List of Tables

Table 1: 3-2-1 rule .....	4
Table 2: Requirements for innovative system.....	17
Table 3: Advantages and limits .....	25
Table 4: Level of confidence (Papula 2003) .....	74
Table 5: Arithmetic average.....	76
Table 6: Standard deviation and deviation of average .....	78
Table 7: Interval of confidence for different level of confidence.....	79

## List of Equations

Equation 1:1: geometrical relation (Schießle 1991:96) .....	7
Equation 1:2: Isosceles triangle (Schießle 1991: 97) .....	7
Equation 1:3: Determination of distance (Schießle 1991:98) .....	7
Equation 1:4: Calculation of position (Schnell 1998) .....	8
Equation 1:5: Sphere (Papula 2003) .....	9
Equation 1:6: Lever equation case 2 (Papke 2010).....	10
Equation 1:7: Lever equation case 1 (Papke 2010).....	10
Equation 2:1: Inner Orientation (Luhmann 2003) .....	21
Equation 2:2: Point of object (Luhmann 2003) .....	22
Equation 2:3: Substitution (Lumann 2003) .....	23
Equation 2:4: Reproduction (Luhmann 2003).....	23
Equation 2:5: Collinearity condition (Luhmann 2003) .....	23
Equation 3:1: Quantum efficiency (Luhmann 2003) .....	27
Equation 3:2: Data amount (Schlitter 2010) .....	28
Equation 3:3: Harmonic wave (Donges, Noll 1993).....	30
Equation 3:4: Circular frequency (Donges, Noll 1993) .....	30
Equation 3:5: Number of waves (Donges, Noll 1993).....	31
Equation 3:6: Dispersions relation (Donges, Noll 1993) .....	31
Equation 3:7: Wave intensity (Donges, Noll 1993) .....	31
Equation 3:8: Threshold algorithm (Stemmer 2009).....	37
Equation 3:9: Position of centre of gravity .....	37
Equation 7:1: Arithmetic average (Blüm 2002) .....	73
Equation 7:2: Standard deviation (Bourier 2011).....	73
Equation 7:3: Average deviation (Papula 2003) .....	74
Equation 7:4: Interval of confidence (Papula 2003).....	74
Equation 7:5: Gaussian distribution curve (Papula 2003).....	75
Equation 7:6: Gaussian error propagation (Papula 2003) .....	76

## List of Abbreviations

$\gamma$	[%]	confidence level
$\lambda$	[ $\mu\text{m}$ ]	wave length of light
$\vartheta$	[mm]	confidence interval
$\Phi_{(x)}$	[1]	Gaussian distribution function
$\omega t$	[1/s]	circular frequency
$\Phi_0$	[rad]	
$b$	[mm]	basis between photo sensing device and laser diode
$d$	[m]	difference of height between object and sensor
$c$	[mm]	orthogonal distance projection centre and centre of projection
$c_0$	[m/s]	speed in vacuum
$c_w$	[m/s]	speed of phase of electro magnetic wave
$e$	[1]	eulersche number
$h$	[mm]	height between object and sensor
$m$	[1]	scale factor for rotational matrix
$p$	[ $\mu\text{m}$ ]	distance of change on photo sensing device
$r$	[mm]	radius of tripod
$r_{\text{laser}}$	[mm]	radius of laser beam
$\Delta r'$	[deg]	radial symmetrical deviation in projection
$s_x$	[mm]	standard deviation of single measurement from arithmetic average
$s_{\bar{x}}$	[mm]	naccuracy of arithmetic average
sec	[1]	second
$t$	[1]	factor for calculation of interval of confidence
$x$	[1]	x coordinate of projected point of object
$x_i$	[mm]	result of single measurement
$\bar{x}$	[mm]	arithmetical average of measurements
$x'$	[1]	x coordinate of vector of projection
$x'_0$	[1]	x coordinate of projection centre
$x'_p$	[1]	x coordinate of projected point of object
$\Delta x'$	[1]	translational x correction of deviation

---

$Y$	[1]	y coordinate of point of object
$y'$	[1]	y coordinate of vector of projection
$y'_0$	[1]	y coordinate of projection centre
$y'_p$	[1]	y coordinate of projected point of object
$\Delta y'$	[1]	translational y correction of deviation
$z$	[1]	z coordinate of point of object
$z'$	[1]	z coordinate of vector of projection
CAD	[1]	computer aided design
CCD	[1]	charged coupled device
CMOS	[1]	complementary metal oxide semiconductor
$D_f 1$	[mm]	distance between sensor and object case 1
$D_f 2$	[mm]	distance between sensor and object case 1
$D_f 1^*$	[mm]	distance between sensor and object case 2
$D_f 2^*$	[mm]	distance between sensor and object case 2
$E$	[V/m <sup>2</sup> ]	electrical field strength
$E_0$	[V/m <sup>2</sup> ]	amplitude of electrical field strength
FPGA	[1]	field programmable gate arrays
$H$	[A/m <sup>2</sup> ]	magnetic field strength
$H'$	[1]	centre of projection
$H_0$	[A/m <sup>2</sup> ]	amplitude of magnetic field strength
$I_{\text{Gauß}}$	[W/m <sup>2</sup> ]	intensity of laser beam after Gauß model
$I_{\text{max}}$	[W/m <sup>2</sup> ]	maximum intensity in row of sensor
$L$	[mm]	distance between centre of sphere and mechanical switch
LD	[1]	laser diode
$M'$	[1]	centre of projection plane
$O'$	[1]	projection centre
$P$	[1]	point of object
$P'$	[1]	projected point of object
$P_{\text{max}}$	[1]	position of maximum intensity
$P_{\text{spring}}$	[N]	force for position of rest added by spring
PSD	[1]	photo sensing device
$R$	[1]	rotational matrix
TTL	[V]	signal for sensor trigger

---

$X_0$	[1]	vector to the centre of projection
$X^*$	[1]	vector between centre of projection and point of object
$X'$	[1]	vector of projection
$Z$	[1]	propagation direction of laser



## 1. Introduction to current quality strategy

Modern automotive industry is facing an increasing demand for customer personalized vehicles (mass customization). Manufacturers are increasing the criteria of dimensional tolerances in order to fulfil customer's quality requirements. Furthermore the amount of parts and components existing in vehicles are constantly rising.

In order to ensure a constant series production which fulfils the quality demands, every single part in every single process during the production has to be placed in the correct location at the exact time. This will ensure the quality of sub assembled components and in the end of the production chain will lead to a manufactured product within quality requirements. Therefore defective parts and components have to be eliminated in the earliest possible stage of production.

Present quality assurance procedures take place via complex measurements. The received data of the respective vehicle parts and components are aligned and compared to recorded data of the design. Errors can be detected in position, direction and size.

Recently inline measurements were realized at certain points of interest within the production process, e.g. directly after welding processes, but not after every process. Therefore errors are only detectable after a defined amount of processes. This strategy of inline measurements tolerates a certain amount of defective parts and components. It increases the effort for a backward error analysis. The error is detected on the part or component and not identified on the tool itself. If there are identical tools for identical processes within the production line it is necessary to identify first the process causing the error before identifying the tool causing the defect. This may lead to large delays in production which are very cost-intensive and may incur loss of material.

In the main plant of the Volkswagen Golf production in Wolfsburg, for example, the welding procedures of the side panel involve various tooling, including industrial robots and assembling stations with several kinds of welding and bonding procedures. The quality assurance for each side individually takes place after the complete assembling of the side panel. The points of interest are measured directly and punctually on the

side panel. If an error occurs up to 90 faulty panels still may be within the production process. Furthermore there exist up to 256 different tool paths an individual side panel might have passed during its assembly processes.

The inline measurements are additionally correlated to a coordinate measurement machine in order to minimize measurement errors. If errors occur in the inline measurements, the results will be first approved by tactile measurement before changes will take place.

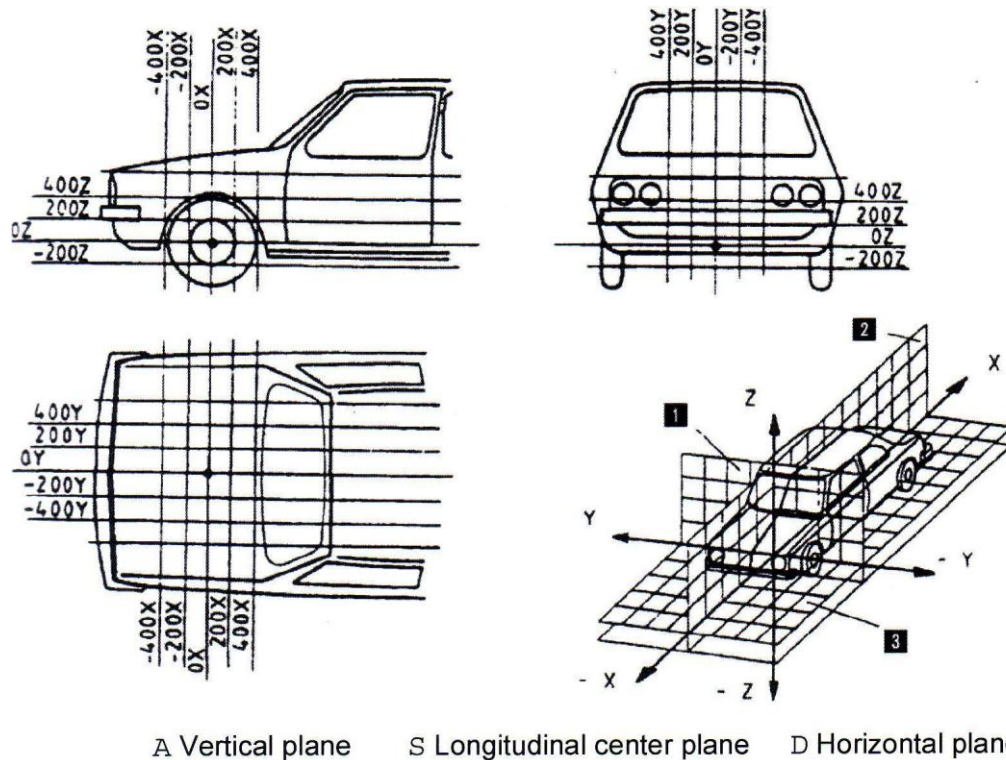
In order to keep consistency throughout the manufacturing and inspecting processes products, parts and the tooling are set up in the vehicle coordinate system. Measurement data is aligned confirming the Volkswagen RPS guideline. The RPS guideline is the platform of every measurement result and manufacturing process. The RPS guideline links via the RPS points every part to its three dimensional position to the vehicle orientated coordinate system.

The central focus is to minimize the quality control loop with an innovative inline measurement method confirming the Volkswagen guidelines. In the following the fundamentals of the Volkswagen Reference Point System guideline will be explained in detail. Furthermore the present measurement tools within the production processes will be identified.

### **1.1. RPS standard of Volkswagen**

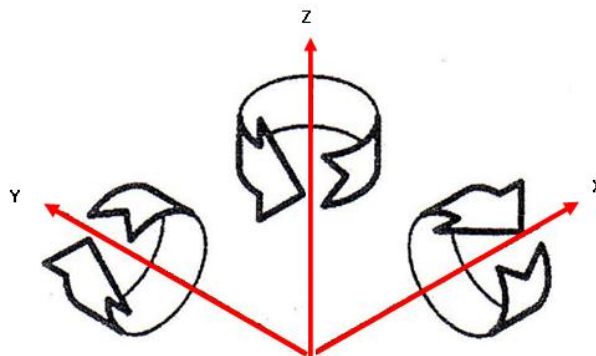
The Volkswagen RPS standard 01055 defines the principles of the component-oriented reference system. The Reference Point System standard applies to dimensioning and to manufacturing and inspecting single parts or assemblies in any phase of a product for uniform positioning throughout the manufacturing and inspection areas as well the assurance of identical dimensional references (Volkswagen AG 1996).

A vehicle is dimensioned by means of a global coordinate system with the origin in the centre at the level of the front axle. From the centre of this coordinate system grid lines spread out parallel to the axes. The grid lines are spaced 100 mm apart and theoretically penetrate the vehicle which is shown in detail in Figure 1.1. These grid lines enable the determination of the position of any vehicle component.



**Figure 1.1: Vehicle coordinate system (Volkswagen AG 1996)**

The reference point system is based on a component-orientated reference system. Every rigid body possesses six degrees of freedom in the three-dimensional space: three translational degrees parallel to the axes of a reference system and three rotatory degrees around the axes. These six degrees of freedom are shown in Figure 1.2.



**Figure 1.2: Degrees of freedom**

In order to support a non-rotationally-symmetric component uniquely in its three-dimensional orientation and position in the vehicle without ambiguity, it must be fixed in all six possible directions of movement. The 3-2-1 rule provides such unique fixing by determining the main-mounting distribution as illustrated in Table 1:

**Table 1: 3-2-1 rule**

No. of Mountings	Direction in 3D space
3	Z
2	Y
1	X

Implemented on a component this means by restricting it three times in Z direction, two times in Y direction and once in X direction it is explicitly defined in three-dimensional space. This rule can be applied to any rigid body. For non-rigid bodies additional support points might be necessary. Furthermore this rule is not only applied for quality assurance purposes it is also the basis for tool fittings in production processes. The specification of reference points, their declaration and tolerance can be found in Appendix A.

## **1.2. Quality assurance in production**

The following subsections give a description of the present quality insurance correlates to the body in white production of the Golf 5 model in the Volkswagen AG plant in Wolfsburg. It will identify the measuring procedures as well the quality loop of the side panel production.

### **1.2.1. Product path**

The side panel of the Golf 5 model consists of three parts. These are the outer panel, which is visible to the customer, and two inner sub assemblies, the inner rear and inner front assembly, which are invisible to the customer. The product path of the right side panel is shown in detail in Figure 1.3. At point one all required components for sub-assembly one are integrated into the manufacturing process. All components necessary for sub-assembly two are supplied to production at point two at the same time. Furthermore the third component is being integrated and prepared for manufacturing at point three. All the components and sub assemblies go through various process operations before being joined at point four. Before assembling all three parts no quality assurance technique is integrated in the process. Hence, if any errors occur in the previous individual operations there is no chance of detection (Baumert 2009). At point four in Figure 1.3 the three individual components and sub assemblies are joined to the product side panel. This can be realised by spot welding with four geometrical identical tools. From this point onwards each product, for the two door and four door model,

takes an individual path of processing. There are five (sixth drum in the installation process) horizontal drums, each equipped with four tools, which provide geometrical welding processes. On every drum two tools for two door models and two tools for four door models are installed. The path of the product does not follow any regularity. It depends on process capacity of the tooling. As detailed shown in Figure 1.3, product path unites after the geometrical welding in the drums. After passing further processes the parts finally reach point five. At this stage the sub-assembly side panel is completed and first quality assurance actions can take place. These processes take place simultaneously for the left and the right side of the vehicle.

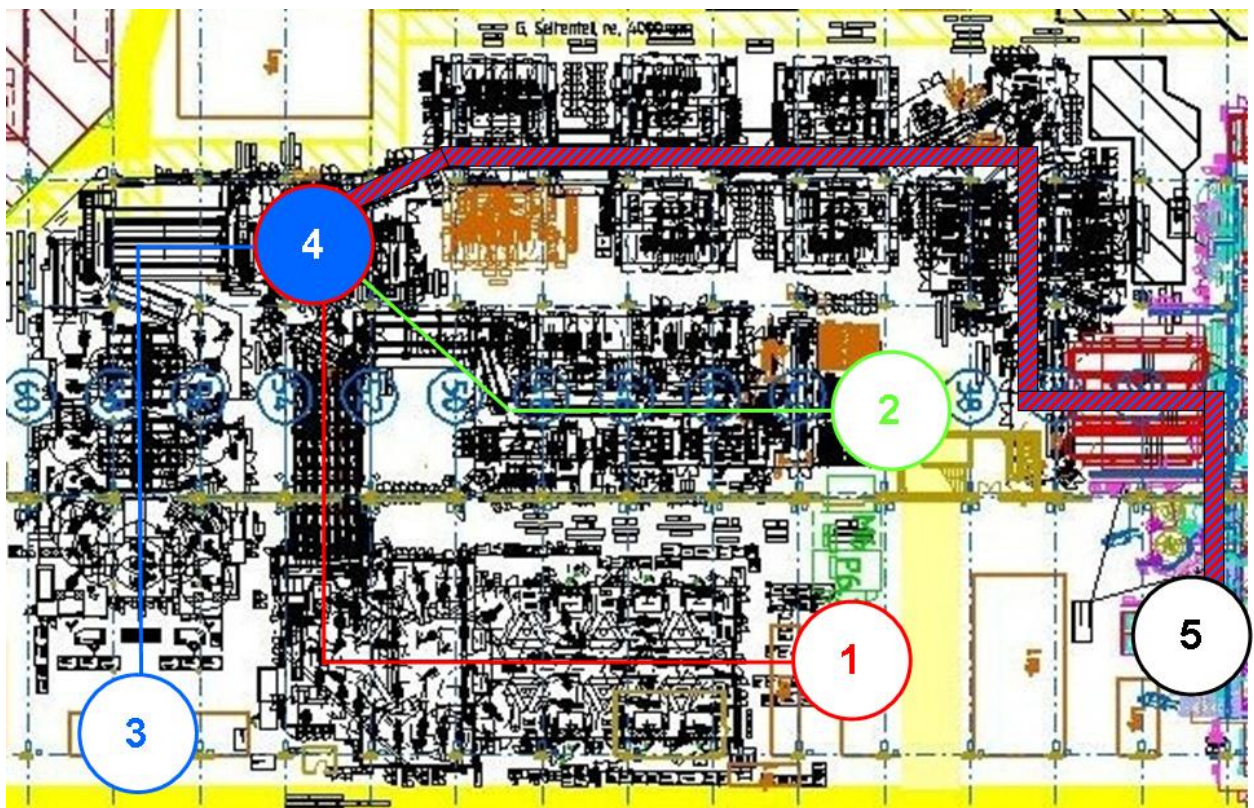


Figure 1.3: Product path side panel (Barthen 2009)

A Perceptron inline measurement system is installed into the process. Before leaving the sub-assembly every product is measured at defined dimensional points of interest. The product is placed into a fixture and aligned in the vehicle coordinate system by its RPS points. The Perceptron system transmits the actual data to intelligent Process Network software (Ipnet). The Ipnet software compares the received data to numerical data and analysis the results. If the results are within tolerances of the product no action will be taken. If the data is not as recommended three different steps of reaction are possible.

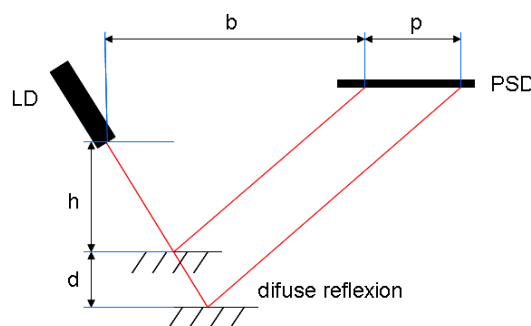


### 1.2.2. Measurement tools

The measuring procedures depend basically on three elements. There are two different measuring systems which do measurements in correlation to each other. Furthermore there is a software tool for data analysis. The two systems used are on the one hand the Perceptron inline measurement tool and on the other hand the tactile DEA coordinate measuring machine. Every four weeks correlation measurements take place in order to compare the results and if necessary recalibrate the Perceptron inline system (Barthen 2009). Both measurement principles and the software tools will be explained in the following subsections.

#### 1.2.2.1. Perceptron inline measurement

The Perceptron tool determines actual coordinates of points of interest on the product within the production line. The measuring method is based on a laser triangulation (Perceptron 2010). Laser triangulation is a technique which depends on the interaction between laser and the measuring object. Laser light is projected onto the surface of the object of interest. The light beam can be punctual, line shaped or more complex structured. Reflexions will occur at the point of impact between laser light and object. The type of reflections may vary on different surface materials (Donges, Noll 1993). The reflection is detected with a light sensitive sensor. The principle function is shown in Figure 1.4.



**Figure 1.4: Laser triangulation principle**

The principle is based on the assumption that incoming and outgoing angles of the light are identical. If geometric conditions change between sensor and object the geometrical values in the triangle will change. These geometrical changes can be detected and analysed. If the distance between the object changes the position of light impact on the sensor will change. The ratio of height to width will stay in every triangle equal. The mathematical relation is shown in detail in Equation 1:1.

$$\frac{h}{b} = c = \text{constant}$$

**Equation 1:1: geometricel relation (Schießle 1991:96)**

The sensor generates a spatial proportional signal. This signal is metrological detectable. The change of distance between object and sensor and the change on the sensor itself are proportional to each other.

$$\frac{d}{p} = \frac{h}{b}$$

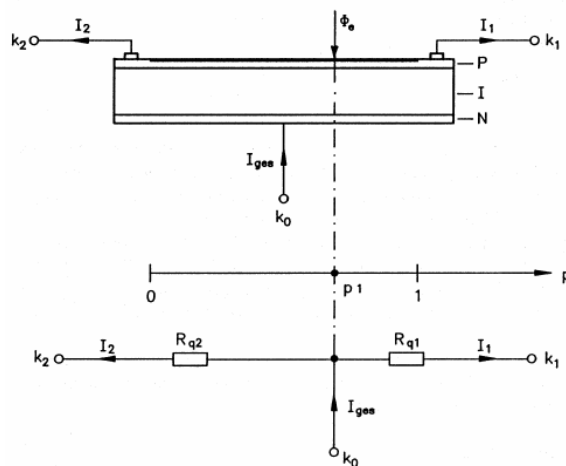
**Equation 1:2: Isosceles triangle (Schießle 1991: 97)**

Equation 1:1 and Equation 1:2 lead to:

$$d = \frac{h}{b} \cdot p = \text{constant} \cdot p$$

**Equation 1:3: Determination of distance (Schießle 1991:98)**

The detection of the position of light is realised with a position sensitive detector (PSD). This type of sensor functions with the photo electrical effect which is explained in detail in chapter 3.1.1. The analysis concentrates on the position of the incoming light and is independent from light intensity.



**Figure 1.5: PSD element (Schnell 1998)**

If light impacts on the sensor charge will be emitted and a current flow to both electrodes is occurring. The not illuminated elements of the PSD act as resistors, therefore the occurring current at the electrodes depends directly from the position of illumination and neglects the amount of illumination. Figure 1.5 shows a PSD element in

detail and highlights principles of the electrical circuit. The given example leads to the mathematical equation four

$$R_{q2} = p_1 \cdot R_q \text{ and } R_{q1} = (1 - p_1) \cdot R_q$$
$$p_1 = \frac{I_{\text{PSD1}}}{I_{\text{PSD1}} + I_{\text{PSD2}}}$$

**Equation 1:4: Calculation of position (Schnell 1998)**

In the current Perceptron system every sensor is installed into housing combined with a laser light to a measuring unit. Furthermore the Perceptron system consists of numerous sensors. A Perceptron system is shown in Figure 1.6. Every single sensor unit is responsible mainly for a measuring result at a certain area of interest. The total of the individual measurements result in the validation of the part.



**Figure 1.6: Perceptron (Perceptron 2010)**

If there are various points of interest on a product then either the installation of numerous sensors is required or additionally robots have to be installed. The Perceptron inline measurement system is an independent station integrated in the production process. Measurements take place within the tact time of production.

#### **1.2.2.2. Coordinate measuring machine**

The coordinate measuring machine is working with a tactile measurement method. The basic of the coordinate measuring machine is the three dimensional coordinate system. The measuring machine basically emulates the translational movement (Neumann 1990). The movement of the machine along the axes is registered by odometers. Additionally equipped with a rotary sensing device the coordinate measuring machine is

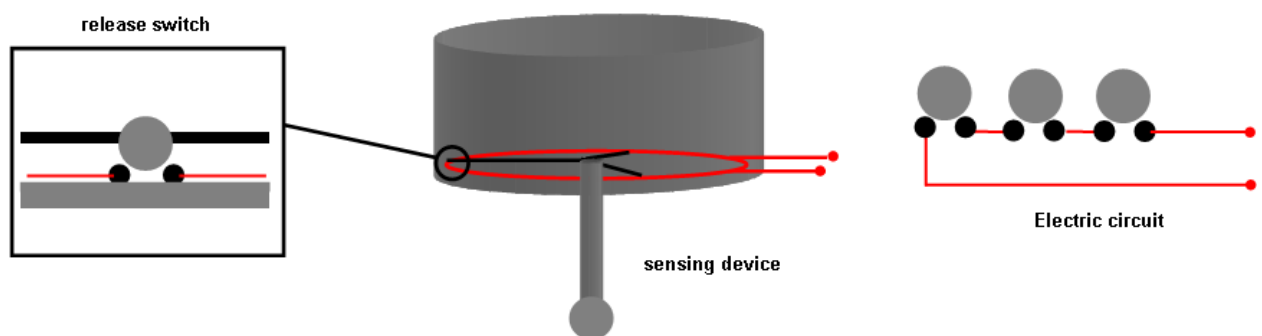


able to reach any point in the three dimensional space within its range. Instead of a tactile device an optical device can be installed at the rotary axis (Wäldele 1988). In order to receive data of the actual coordinates the sensor device has to release a signal if contact to the object surface is given (touch trigger). The simplest sensing device is a mechanically switching device. In majority of the applications the contact element between object and measuring machine is a sphere. Mathematically the distance between the centre of the sphere and any point of the surface is identical (Papula 2003).

$$\text{distance cp} = \text{radius} = \text{const.}$$

**Equation 1:5: Sphere (Papula 2003)**

The sphere is fixed on a sensing arm which is installed on a tripod. The position of rest is held by a spring. Figure 1.7 shows the principal design of a tactile sensing device with mechanical trigger.



**Figure 1.7: Tactile sensing mechanism**

All three contact surfaces of the tripod are switches (Neumann 2005). If the sphere is contacted by any direction at least one switch will be released and a signal is generated. The registered coordinates refer to the centre of the sensing device. If different directions of contact occur the results may vary. Based on the lever principle the required force for switch release differs. Figure 1.8 shows the mechanical proportions in detail. Two cases are demonstrated in which the required forces for switch release differ by a factor of two. The different forces are an outcome from the different lever conditions. In Figure 1.8 case two the required force results from:

$$F \cdot L = P_{\text{spring}} \cdot \frac{r}{2}$$

$$F = P_{\text{spring}} \frac{r}{2L}$$

**Equation 1:6: Lever equation case 2 (Papke 2010)**

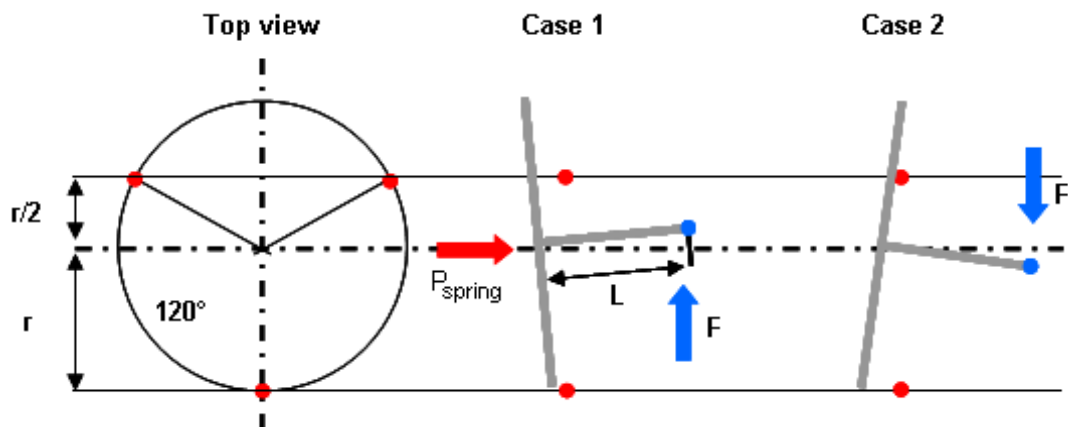
The same equation leads in the first case to a different required force:

$$F \cdot L = P_{\text{spring}} \cdot r$$

$$F_{\text{double}} = P_{\text{spring}} \frac{r}{L}$$

**Equation 1:7: Lever equation case 1 (Papke 2010)**

The required force varies with geometrical conditions of the tripod and the direction of contact. In the worst case the lever is reduced by a factor of two, therefore the force has to be doubled in order to achieve equilibrium.



**Figure 1.8: Mechanical trigger device**

The different forces lead to different switch points. The difference is not reproducible and therefore difficult to calibrate (Neumann 2005). In order to minimize this effect further sensor can be installed additionally.

Nevertheless tactile measurement machines reach the most accurate and most reproducible result in 3D measurements. Standard machines are able to achieve repeatable accuracies up to 1.5  $\mu\text{m}$  (Hexagon Metrology 2008).

### 1.2.2.3. Software analysis

In order to minimize human impact on the measuring results software tools analyse the generated data. There are two stages of data analysis. The first reports are generated at the machine itself. The results can be immediately displayed at the machine. Furthermore the reports are centralised and unified in a superior Volkswagen Qualitäts- und Informations- Rohbauleitsystem software tool (Quirl). The data gathered in the Quirl database can be accessed anytime from any computer, if authorized.

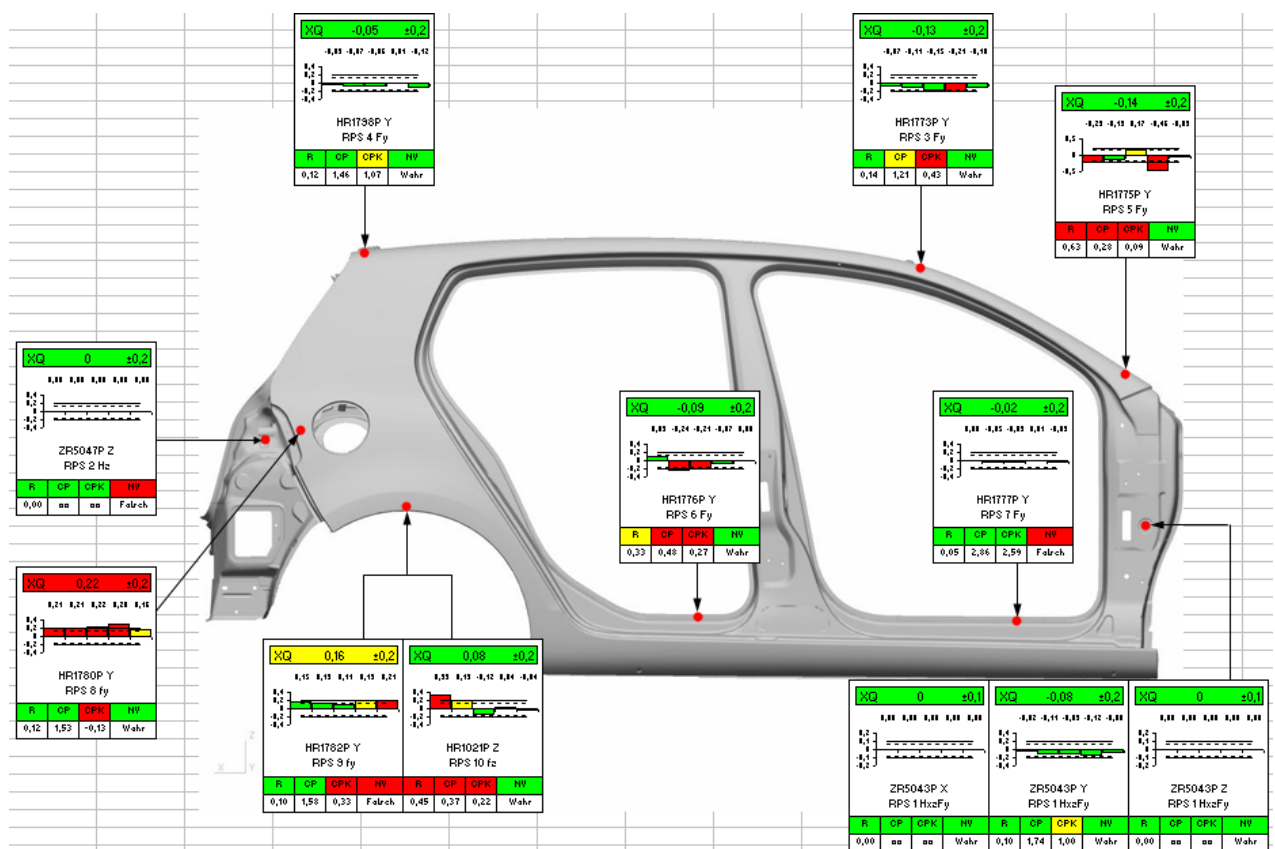


Figure 1.9: Quirl report (Hoffmann 2009)

There are four different types of data representations which depend on the users. All four types contain the same information (Schulz 2007). Figure 1.9 shows a Quirl report of the Golf A5 side panel in detail.

The Quirl software is able to identify results of a single measurement as well a trend analysis of one specific product or a point of interest over a defined period of time. Quirl displays numerical information of a measurement point as well coloured information. Figure 1.10 shows coloured information of a single measurement point in detail.

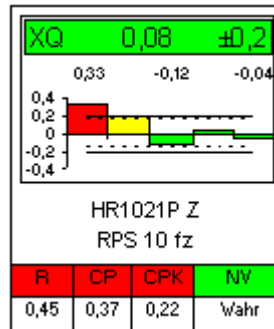


Figure 1.10: Quirl colour plot (Hoffmann 2009)

There are three colours for information, green, red and yellow. Actual data can be identified with its tolerances by colours. If the actual data is within tolerance the data will be displayed in green. If the data is still in tolerance but above 75 percent of the tolerance value it is displayed yellow. If the data is out of tolerance it will be marked red, as shown in Figure 1.10.

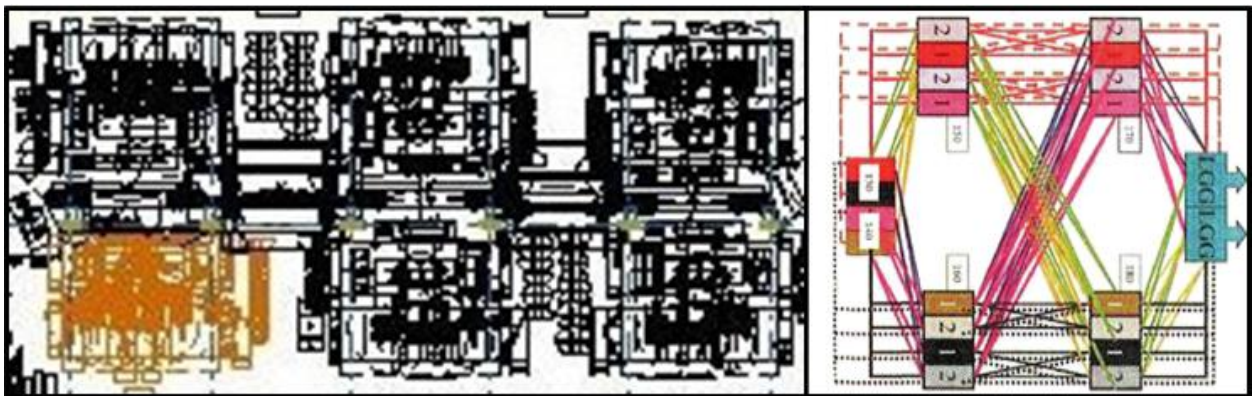
The machine reports are displayed similarly. The following description refers to the Ipnet software from Perceptron. The Ipnet software is able to display reports, trend analysis or focus on points of interest. Furthermore there are four different stages of tolerances each with different reaction to the process chain. If the actual data is within tolerance results will be displayed green and no reaction will take place. If the data of three consecutive measurements is in tolerance but above 75 percent of tolerance level it will be marked yellow. Furthermore a trend alarm will be activated. If three consecutive measurements are above tolerance results will be displayed red and a tolerance alarm will occur. Additionally there will be a production stop and a notification will be send to the person in charge. The last level of notification is pink. This type of error occurs if one measurement is high above tolerance. Similar to the red alert the production will be stopped furthermore the affected part will be taken out of production processes. If the following result is within tolerance production will keep running. If the next value is out of tolerance process keep stopped until error is identified and corrected.

### 1.2.3. Control loop and error detection

A control loop is a closed production system including machinery and workers. Within this circuit diagnosis of the processes and products takes place independently. The side panel production and its sub assemblies represent one of three control loops in the body in white production. The product path is explained in detail in chapter 1.2.1.

Quality assurance takes place at the end of the production chain. If an error is identified the control mechanism occurs. If a single error occurs the part will be checked and reconditioned. If a systematic error occurs it will be necessary to localize the error in the machinery and intervene. Depending on the size of the quality loop numerous machines have to be inspected. In the side panel production the error can only be identified at the end of the process, therefore every previous tool since the last quality assurance can cause the defect. While one part is analysed 90 further parts are already in production within the quality control loop (Baumert 2009). If the defective tool is localized in the first production process every product within the control loop will be affected.

The product path can not be identified, which leads to further difficulties. Even if the process causing the defect is localized there might be tools with identical geometry for identical processes. There are five drums with identical tools ("Wilder Mix") installed in the product path of the side panel. The drums are shown in Figure 1.11.



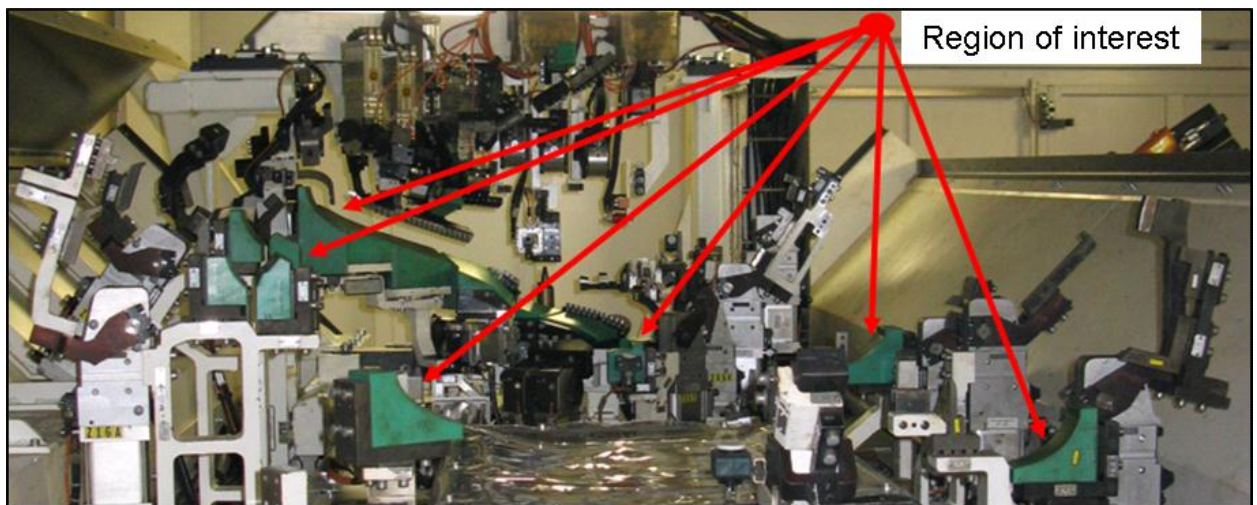
**Figure 1.11: Geometrical welding drums "Wilder Mix "**

This part of assembling, shown in Figure 1.11, gives 256 possible paths for an identical product. (Schulz 2007). If the defective tool is identified the element within the tool causing the error has to be spotted. Mechanics will fulfil necessary corrections and production is able to restart. Product analysis will give information if the reconditioning of the tool was successful or if further corrections are required.

#### **1.2.4. Error elimination**

Error identification is product based in the current quality assurance of the body in white production. Therefore no numerical value is directly linked to geometrical changes in the tool. It is the mechanics responsibility and experience to link the deformation of the product to required tool changes. There are two categories and five different types of defects occurring in the production. These two categories are fractures and

displacements. Fractures are most of the time located without ambiguity. Fractures differ in total or local appearance.



**Figure 1.12: Geometry elements of tool**

Displacements are more critical to identify. Minimal changes can have enormous impact on product quality. Displacements can occur in lateral, rotary or combined manner. Neither is it always possible to identify the element shown in detail in Figure 1.12 in the tool causing the defect (error position) nor is it possible to identify direction and size of the tool deformation immediately. Furthermore it does not have to be a single element it also might be a group of elements causing the defect.

If settings are changed there will always be a co-relational measurement required to confirm that the enforced changes in tool settings lead to a product within tolerance. Another error occurring especially in welding processes is deposits on contact surfaces. They can have either an impact on product surface or product geometrical conditions. Deposits can be identified by visual checks and simply be removed.

### **1.3. Disadvantages of current strategy**

The current strategy contains approved methods to identify errors in production. Nevertheless there are disadvantages linked to the strategy. First to mention is the actual size of the control loop. If there is a defect in the first process damaging the product, 90 more defective parts will be produced before there is a chance to identify the damage. Therefore at least 90 additional parts will be damaged in the same manner. This leads to massive reconditioning or numerous irreparably parts. Either result will end in enormous costs. The huge control loop leads to complex and time



intense backtracking strategies. Before deformation within the tools can be put down the tools causing the defect has to be identified clearly. In some cases product defects might give a hint which process is damaging the product. On account of the marginal tact time several processes are held in identical tools with identical geometries. Therefore the tool in the process has to be identified.

Current quality standards refer to product condition meanwhile there are no standards of tool conditions in production. Production will run until product damage is identified. Furthermore the deformation of the product is registered, not the deformation of the tool. Product deformation is a result of tool deformation. Tool defects are not clearly identified neither in position nor in direction and size.

Tool changes cannot be immediately be compared to nominal data. Setting changes have to be approved with the next product based measurement report. Tool changes will occur and be approved until the product is within tolerance.

## **2. Innovative quality strategy**

In consideration of the disadvantages of the current strategy an additional quality assurance tool is necessary in order to compensate the lack of information. Current quality strategy only applies to product data. For production site the link to geometrical conditions of the tools is a matter of particular interest. The innovative strategy needs to run fully automated in order to minimize human impact on measuring results. In financial aspects a system with a minimized control loop will be interesting for reducing recondition works and therewith minimize costs. Furthermore creeping processes of unintentional tool changes can not be neglected. On the hand the strategy shall provide information for tool changes to mechanics and on the other hand it shall record the changes of parameters made by the mechanics.

In order to detect defects of tools the system has to be integrated into the production cells. Production conditions differ from laboratory conditions. Therefore the strategy has to be optimized for the ambient conditions of the production facilities. Finally the interface for data providing has to be as intuitively as possible and suit Volkswagen regulations.

The majority of fixtures, tools and jigs are orientated in the vehicle coordinate system by RPS registration. Therefore the numerical information supplied by the innovative strategy has to conform to the RPS standard of Volkswagen.

The current quality considers only the data analysis of the product. It assumes as long the actual data of the product is within tolerance no changes in tool settings are required. Therefore the strategy suggests that as long the product is within tolerance the tool is intact.

The innovative strategy is based on the converse argument. As long as the tools are within tolerance the manufactured product will be within tolerance as well. Therefore the geometrical conditions of the tools are of particular interest. The additional continuous monitoring of the process tools will increase the capability of detecting errors in production processes. The optimum will be the detection of geometrical changes above tolerance before the first defect product is manufactured.



Of particular interest for the strategy are the parts of the tool which bring the product into the registered position and fix it during the process. A tool in the body in white production contains different parts and different materials which clamp the product in process position as shown in Figure 1.12. Geometry elements are centring pins, contour surfaces and clamps and its contrary surfaces. The material varies depending on the type of element and their position. Every element contacting visible surfaces of the product consists of synthetic material, while centring pins and clamping elements in majority consist of metal (Warnecke 2009).

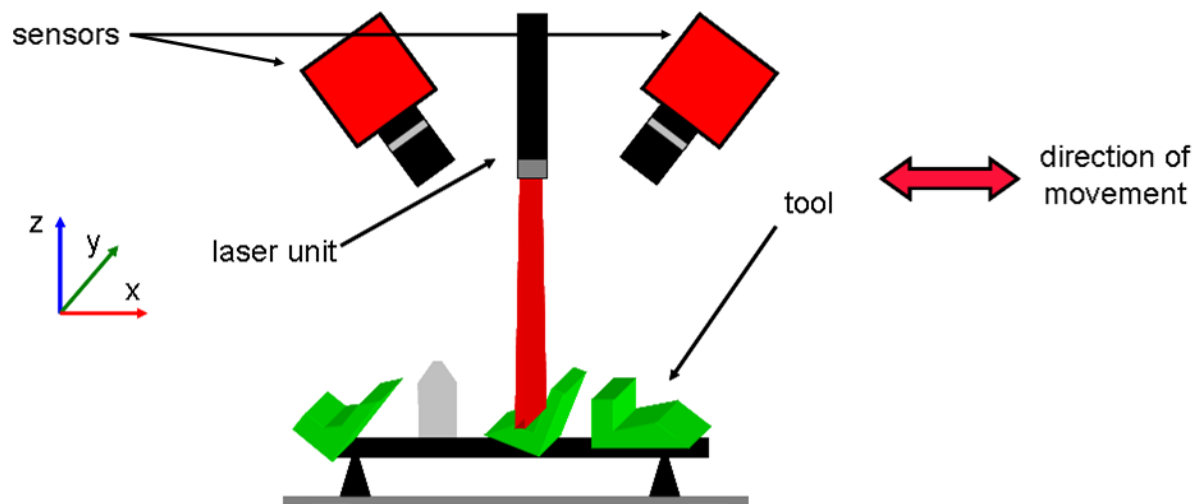
The above mentioned details lead to following requirements for the system realizing the innovative strategy shown in detail in Table 2.

**Table 2: Requirements for innovative system**

System requirements		
fact	necessary	optional
contact free	X	
compact	X	
fast	X	
stabil	X	
easy operating		X
various surfaces	X	
affordable		X

## 2.1. Measurement principle of innovative strategy

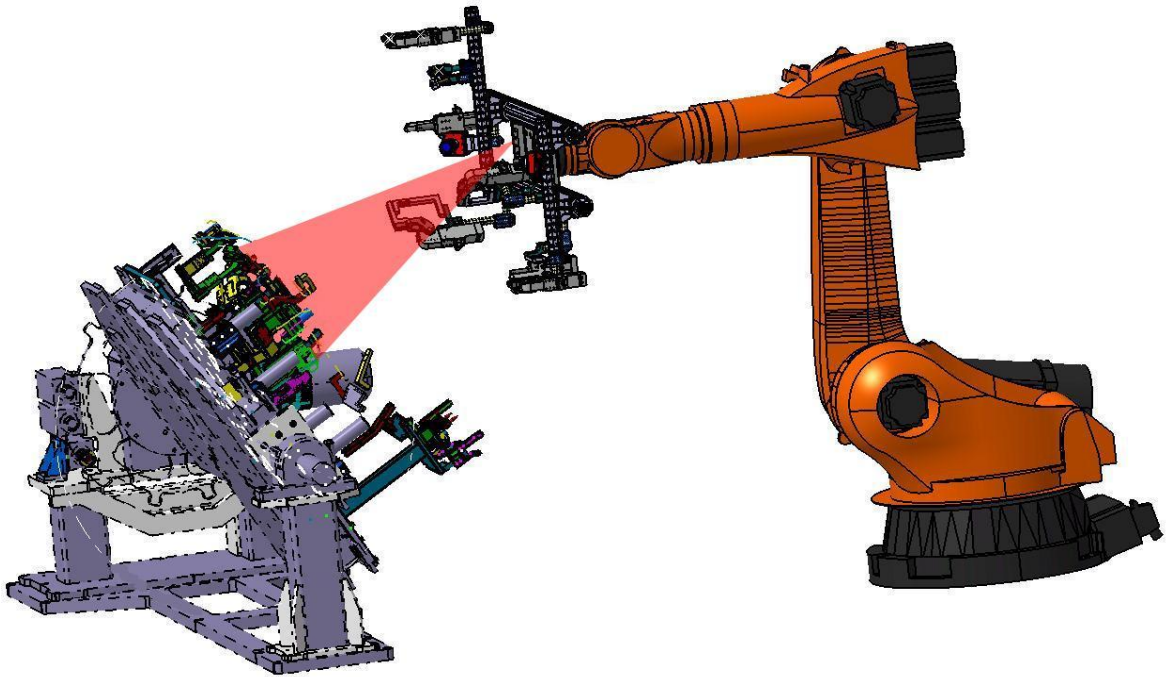
In order to fulfil the requirements optimal a value benefit analysis was carried out. Result of the analysis was that the ideal principle of measurement is a combination of photogrammetry and laser triangulation (Viol 2009). A laser line is projected onto the surfaces of interest within the tools. Image sensors detect the laser line and generate a profile of temporary two dimensional conditions. Figure 2.1 shows the principle in detail. By adding a relative movement between the object of interest and the sensor further temporary conditions will be registered and the third dimension is added to the process.



**Figure 2.1: Principle of measurement**

In order to receive a three dimensional result with numerical values components need to interact with each other.

Furthermore the system is supposed to be installed into the production cells itself. No additional process tact should be installed in the production chain. Therefore the space for units for required movement is limited. In ideal scenarios the already installed equipment for automation such as robots, turn tables and linear units can be used for the innovative measurement strategy. Figure 2.2 shows a possible installation of the system hardware in the handling tool of a common industrial robot.



**Figure 2.2: Robot installation**

In the in Figure 2.2 shown example of installation no additional space and no additional handling tool is required. In this installation example a stationary tool and a handling robot are shown. The innovative system is installed into the grab of the robot. The measurement procedure and the required linear movement can be realised with the robot. Furthermore the same strategy can be realised in a vice versa scenario. If it is required to measure the geometrical conditions of the grab of the robot the innovative system will be installed on a fix place in the production cell. The robot will pass by the measuring system in a linear movement while the sensor generates three- dimensional data of the grab.

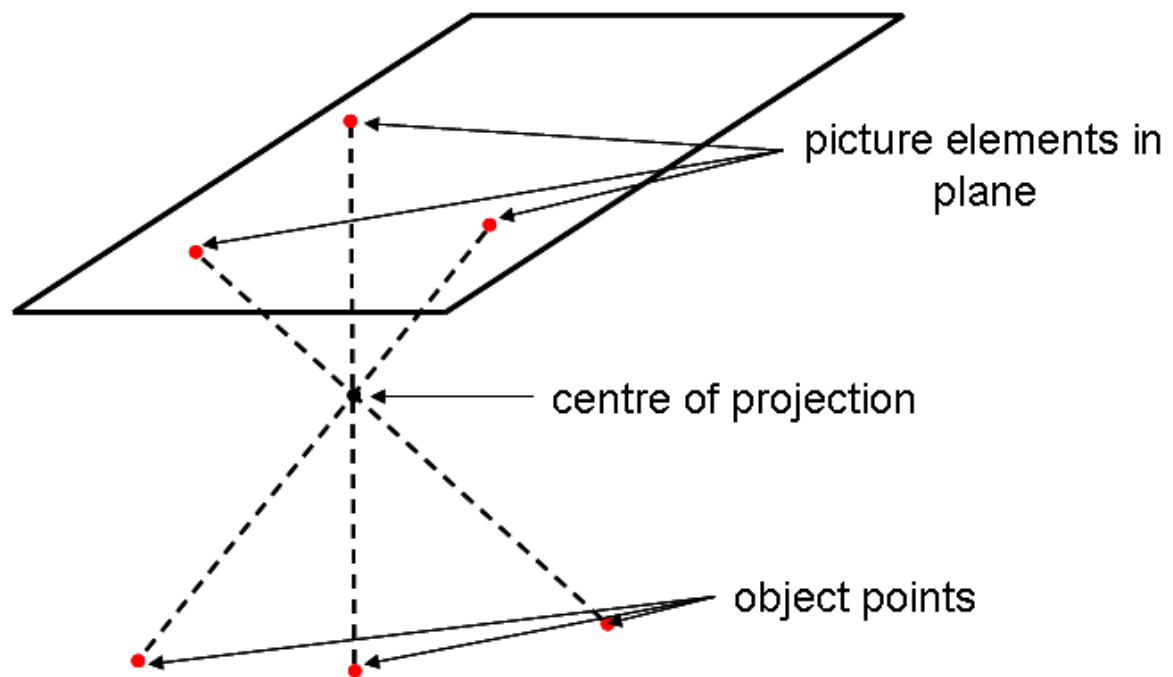
## **2.2. Principle laser triangulation**

The principle of the laser triangulation is based on the identical mathematical equations explained in chapter 1.2.2.1. In order to generate three- dimensional surface information an additional translational movement is required.

## **2.3. Principle of photogrammetry**

The photogrammetry is a tool for detecting position and shape of an object within the three- dimensional space. If two dimensional information from an object is required at

least one photo has to be taken. In an optimal case it is taken orthogonal to the object of interest. If three-dimensional information from an object is required at least two photos have to be taken. These two photos from the object have to be taken from two different perspectives (Michels 2006). In order to describe an object in its three-dimensional dimensions the bundle of rays has to be recalculated. The calculation is based on the principle of the central projection.

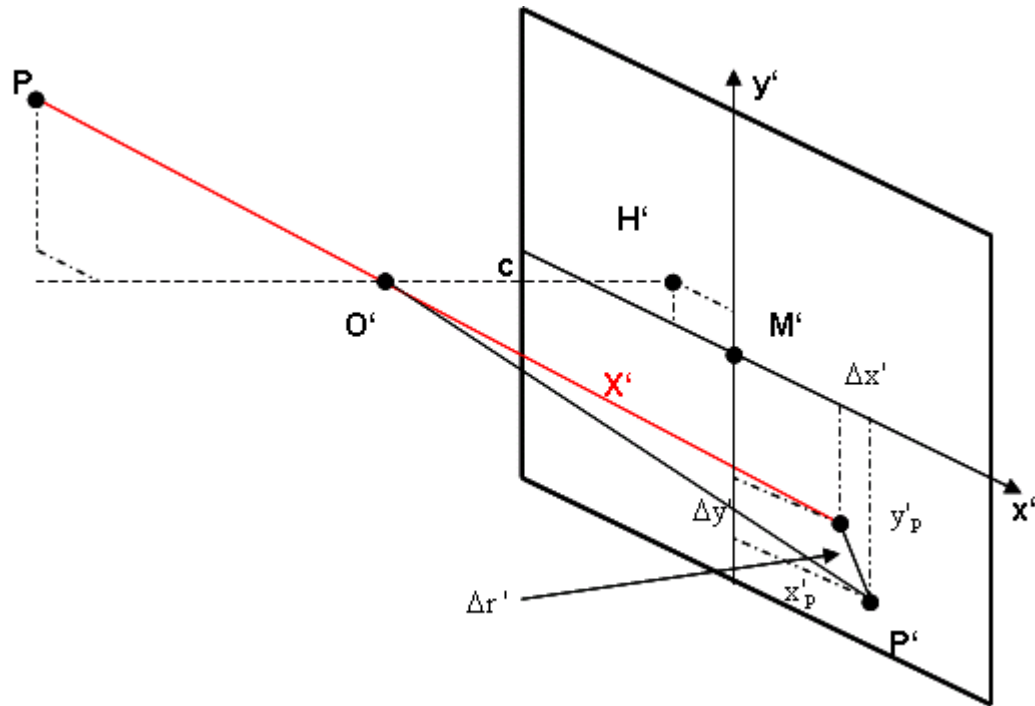


**Figure 2.3: Central projection**

Figure 2.3 shows three points in the three-dimensional space and their projection on a plane through a common centre of projection. Further it is obvious that the points in the three-dimensional space and their projections on the plane do not share a coordinate system. In the photogrammetry exist two standard orientations, the inner orientation represented by the camera parameters and the superior outer coordinate system.

The parameters of the inner orientation describe mathematically the position of the centre of projection in the projection plane coordinate system, the orthogonal distance between projection centre and projection plane as well the deviation from the ideal mathematical condition of the central projection. Figure 2.4 shows the schematic process of a projection within a camera. Within the calculations the system is considered to be three-dimensional. The system consists out of the projection plane and the lens. The position and the distance of the centre of projection is described on

the by reference points defined projection plane coordinate system as well the deviations from the ideal central projection.



**Figure 2.4: Point projection**

With knowledge of the in Figure 2.4 shown parameters of the distance  $c$ , the projection plane centre  $H'$  and the deviation  $\Delta r'$  the corrected projection vector  $x'$  can be calculated with Equation 2:1.

$$X' = \begin{bmatrix} x' \\ y' \\ z' \end{bmatrix} = \begin{bmatrix} x'_P - x'_0 - \Delta x' \\ y'_P - y'_0 - \Delta y' \\ -c \end{bmatrix}$$

**Equation 2:1: Inner Orientation (Luhmann 2003)**

In which  $x'_P$ ,  $y'_P$  are the measured coordinates of the projection point  $P'$ ,  $x'_0$ ,  $y'_0$  are the coordinates of the centre of the projection plane  $H'$  and  $\Delta x'$   $\Delta y'$  are the translational correction of deviations. By calculating the inner orientation camera systems can be calibrated (Luhmann 2003).

The connection between the inner and the superior outer orientation can be mathematically described. Six parameters describe the position and orientation of the

three- dimensional projection system in the superior object coordinate system. The calculations base on the collinearity equations. These equations describe the three-dimensional position of an object point. Figure 2.5 shows the constellation in detail.

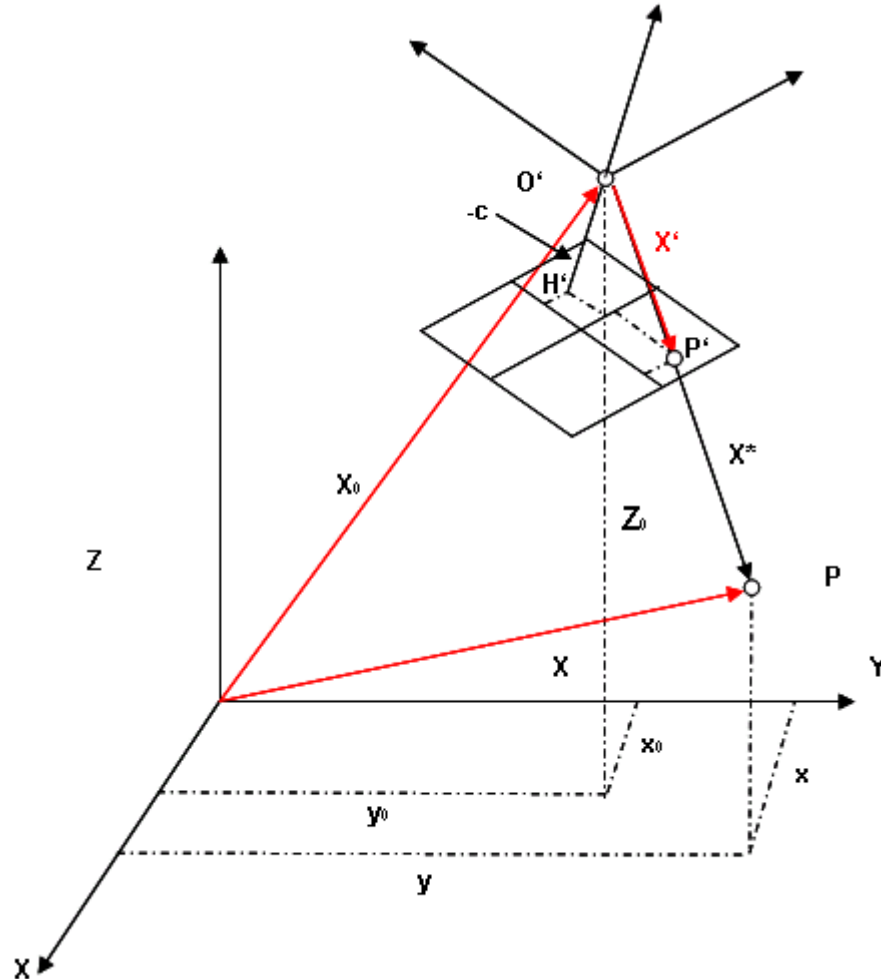


Figure 2.5: Collinearity condition

The coordinates of the object point can be deduced by the space vector  $X_0$  to the centre of projection  $O'$  and the vector  $X^*$  between the centre of projection  $O'$  and the object point  $P$ . This is shown in Equation 2:2.

$$X = X_0 + X^*$$

Equation 2:2: Point of object (Luhmann 2003)

The vector between the centre of projection and the point of the object can not be directly ascertained. Therefore the known vector of projection  $X'$  substitutes the in same direction pointing vector  $X^*$ . For substitution the vector  $X'$  has to be transferred into the space of object by a rotational matrix  $R$  and a scale factor  $m$ , shown in Equation 2:3.

$$X^* = m \cdot R \cdot x'$$

**Equation 2:3: Substitution (Lumann 2003)**

This substitution leads to Equation 2:4 which describes the reproduction of a projected point in the superior object system.

$$X = X_0 + m \cdot R \cdot x'$$

$$\begin{bmatrix} X \\ Y \\ Z \end{bmatrix} = \begin{bmatrix} X_0 \\ Y_0 \\ Z_0 \end{bmatrix} + m \cdot \begin{bmatrix} r_{11} & r_{12} & r_{13} \\ r_{21} & r_{22} & r_{23} \\ r_{31} & r_{32} & r_{33} \end{bmatrix} \cdot \begin{bmatrix} x' \\ y' \\ z' \end{bmatrix}$$

**Equation 2:4: Reproduction (Luhmann 2003)**

The addition of the projection centre and the factors of deviation finally lead to the equations of collinearity. Equation 2:5 shows the detailed formulas of the collinearity condition.

$$x' = x'_0 + z' \cdot \frac{r_{11} \cdot (X - X_0) + r_{21} \cdot (Y - Y_0) + r_{31} \cdot (Z - Z_0)}{r_{13} \cdot (X - X_0) + r_{23} \cdot (Y - Y_0) + r_{33} \cdot (Z - Z_0)} + \Delta x'$$

$$y' = y'_0 + z' \cdot \frac{r_{12} \cdot (X - X_0) + r_{22} \cdot (Y - Y_0) + r_{32} \cdot (Z - Z_0)}{r_{13} \cdot (X - X_0) + r_{23} \cdot (Y - Y_0) + r_{33} \cdot (Z - Z_0)} + \Delta y'$$

**Equation 2:5: Collinearity condition (Luhmann 2003)**

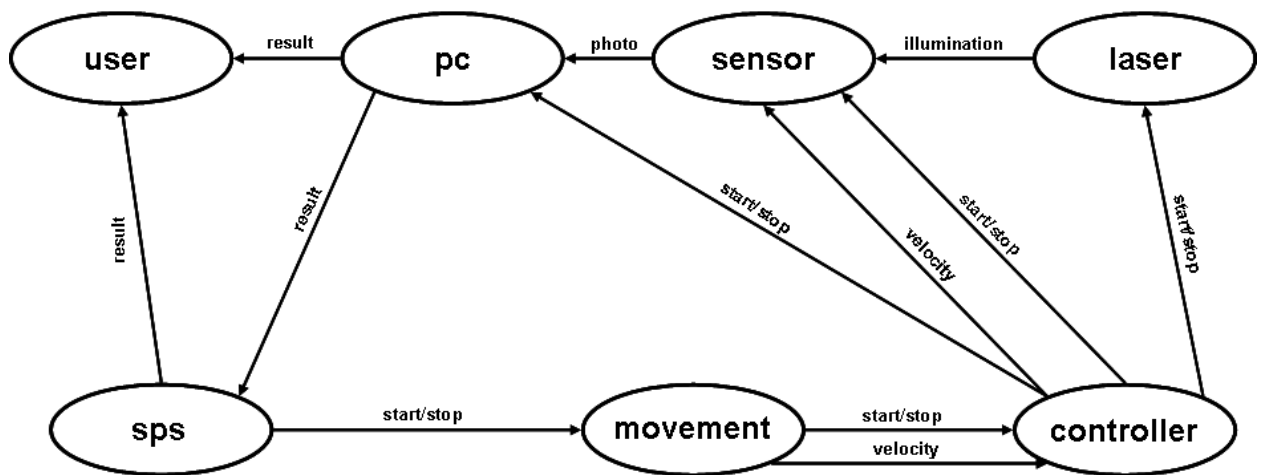
These equations describe the transformation of a point of an object (X, Y, Z) into a projected point (x'<sub>P</sub>, y'<sub>P</sub>) in consideration of the inner and outer orientation of the projection.

## 2.4. Measurement method

The innovative system will be installed into production cells. Therefore the space for installation is limited. Furthermore the chance of a complex calibrating procedure is not given.

The system will include different components with different tasks. A laser unit is required for projection of an adequate line onto the objects of interest. Under a certain angle a sensor is installed for detection of the projected laser line. Depending on the required information more than one sensor has to be installed. This will reduce the lack of

information due to indentation. For the required movement between sensor and object either a linear unit or an industrial robot can be used.



**Figure 2.6: System setup**

Figure 2.6 shows all required components and their communication. The circuit starts in the programmable logic control of the production cell (PLC). The control will give the robot the signal to execute a measurement. If the robot has reached the position of measurement it will share this information with the sensors. Furthermore the sensor needs information of how fast is the actual velocity between the object and the sensors. In order to achieve a constant density of object information the velocity and the pictures taken by the sensor need to be constantly synchronised. Therefore a controller is installed in between. It will generate the required information for the sensor. For safety reasons the laser module will not be switched on continuously, it will be activated by the controller if necessary. If activated, sensors will detect the projected laser line and give their pixelated information to a central computer. The central computer is able to gather the information and calculate the result of the measurement. The result has to receivers, on the one hand the machine operator requires information of machine conditions and on the other hand the PLC needs information about machine condition.

## **2.5. Advantages & Disadvantages of measurement method**

The use of a combination of photogrammetry and laser triangulation holds a lot of advantages to the process but there are also disadvantages.

On the one hand this measurement method principally can be used for any measuring dimension but on the other hand maximum accuracy will depend on the physical



resolution of the sensors. Furthermore the object of interest has to be discoverable by the laser projection and the photo sensor.

The measurement method allows high frequencies of measurements and the generated data will be available at a later date. It will give the opportunity of a complete documentation of tool condition in the production process.

Furthermore it is a non contact measurement, which allows a distance to the object of interest. The ideal system setup can be realised with a lens.

**Table 3: Advantages and limits**

<b>System advantages and limits</b>	
<b>advantages</b>	<b>limits</b>
<b>contact free</b>	<b>contact free</b>
<b>measurement volume</b>	<b>physical resolution of sensor</b>
<b>operator independent</b>	<b>additional illumination</b>
<b>independent from ambient light conditions</b>	<b>depth of field</b>
<b>high measurement frequencies</b>	<b>visibilty of objects required</b>
<b>continuous documentation</b>	

### 3. State of Technology

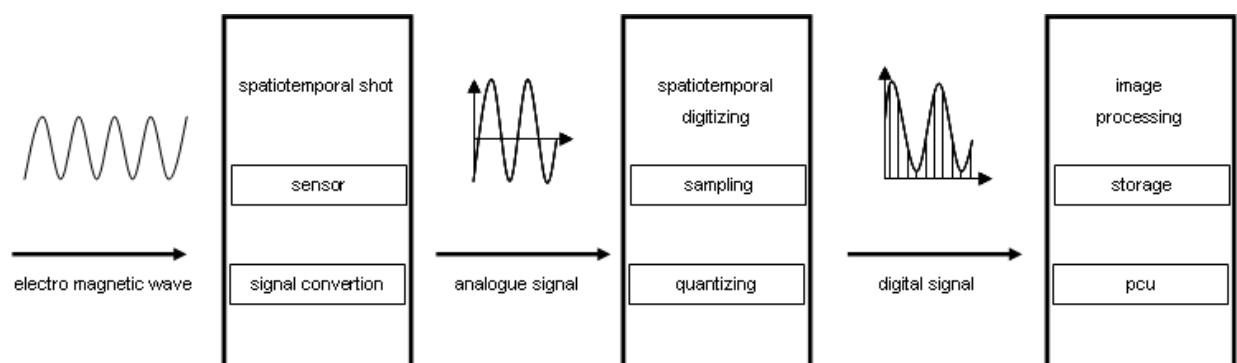
This Chapter will give in the following subsections an overview of the state of required technology for the innovative measurement method. Necessary components will be pointed out and their principle mode of operation will be highlighted and explained in detail. Furthermore the sub sections will define the required interfaces for system communication as well the software requirements for the innovative measurement method.

#### 3.1. Components

Automation and optical measurements are used in many parts of industry, therefore a lot of components which will fulfil the innovative measurement system needs are already acquirable.

##### 3.1.1. Optical sensors

Electro-optical sensors have the capability to detect electro magnetic waves from an object in a spatiotemporal way. They accumulate signal charge in each pixel proportional to the local illumination intensity, serving a spatial sampling function (Litwiller 2001). A digital gray scale value image is compiled by digitising and quantizing the analogue signal. Electro- optical sensors are able to convert natural light as well as laser light.



**Figure 3.1: Digital image processing**

Electro- optical sensors differ in assembly and technique. There are couple charged device sensors (CCD) and complementary metal oxide semiconductor sensors (CMOS) either column based or area based. The two techniques vary in the way they read out signals. If an exposure is completed, a CCD sensor will transfer each pixel's charge

packet sequentially to a common output structure. There the conversion from charge- to- voltage takes place, will be buffered and then send off chip. A CMOS imager converts the charge- to- voltage in each pixel separately. This difference in readout techniques has significant implications for sensor architecture, capabilities and limitations.

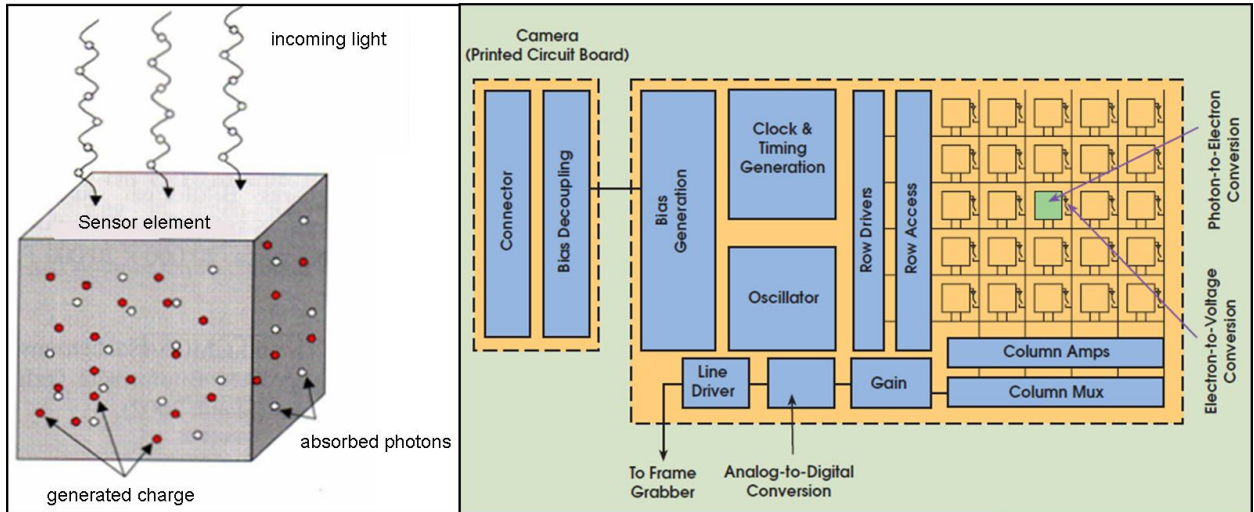
### 3.1.1.1. CMOS sensor

A CMOS image sensor is a pixelated metal oxide semiconductor. There are two major configurations of elements on the sensor. On the one hand there exist a column wise configuration and on the other hand the matrix configuration of elements. The functionality is identical. Every single sensor element has the capability to convert incoming light into charge. The semiconductor absorbs incoming light (photons) and forms electron-hole pairs. Every single element in the sensor is able to generate a specific amount  $n_e$  of charge from a defined amount of incoming photons  $n_p$ . The degree of efficiency  $\eta_{\text{ext}}$  relies on the one hand on the material of the sensor element used and on the other hand on the wave length of the incoming light.

$$\eta_{\text{ext}} = \frac{n_e}{n_p}$$

**Equation 3:1: Quantum efficiency (Luhmann 2003)**

Figure 3.2 shows the transformation from incoming light to charge. The incoming photon is absorbed in the semiconductor layer of the sensor element. The element generates a negative charge. The charge is attracted by a positive electrode and causes an accumulation proportional to the illumination intensity. This process can maximum take place until saturation of the element occurs. The positive electrical field of the electrode is generated by a potential step (Luhmann 2003).



**Figure 3.2: Photon- to- electron conversion**

Only about thirty percent of the area of a CMOS sensor is light sensing pixel area. The majority of the area is filled with on board circuits. These circuits facilitate each pixel individually to convert their potential step to a voltage. The voltage is delivered to an analogue- digital- transmitter which converts the signal and provides it to further processes. The on board circuitry allows the exceptional function of windowing. Means, it is possible to activate or deactivate pixels explicitly in their function from external control. Especially in cases in which not every pixels information is required this option reduces generated data. The amount of data and the maximum frame rate is inverse proportional. By selecting fields of interests on the sensor and decreasing data amount it is possible to increase the frame rate and process speed.

### 3.1.1.2. 2D and 3D sensors

Optical CMOS sensors differ in design and functionality. There are 2D CMOS sensors and 3D CMOS sensors. Both types generate pixelated information as described in detail in chapter 3.1.1. The two sensor types differ in data output. The 2D sensor will transfer the full generated picture information to a superior computer for further processing. The 2D sensor generates a two dimensional gray scale value image. The appearing data amount is proportional to the number of pixels generating the information. The data amount per second can be calculated with Equation 3:2.

$$\frac{\text{bit} \cdot \text{pixel}}{8} \cdot \frac{\text{profiles}}{\text{sec}} = \frac{\text{bytes}}{\text{sec}}$$

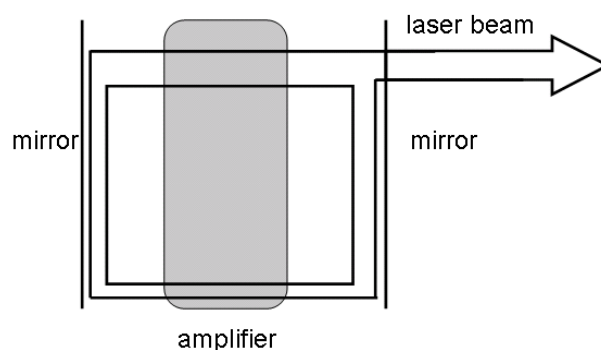
**Equation 3:2: Data amount (Schlitter 2010)**

Conventional 2D sensors are equipped with at least one camera link port. There are three different standard configurations: base, medium and full.

On the other hand there are 3D sensors. In contrast to 2D sensors they are equipped with field programmable gate arrays (FPGA) chips. This difference enables a pre-processing of the generated gray scale value image. The picture information can be reduced to the minimum of required information. Data transfer is minimized, therefore most 3D sensors can be operated with standard network cable. In addition a control connection has to be supplied to the sensor. The superior computer and the sensor can be located in a range of 100 meters without any restrictions in operation. Furthermore 3D sensors can also be equipped with camera link cables.

### 3.1.2. Laser

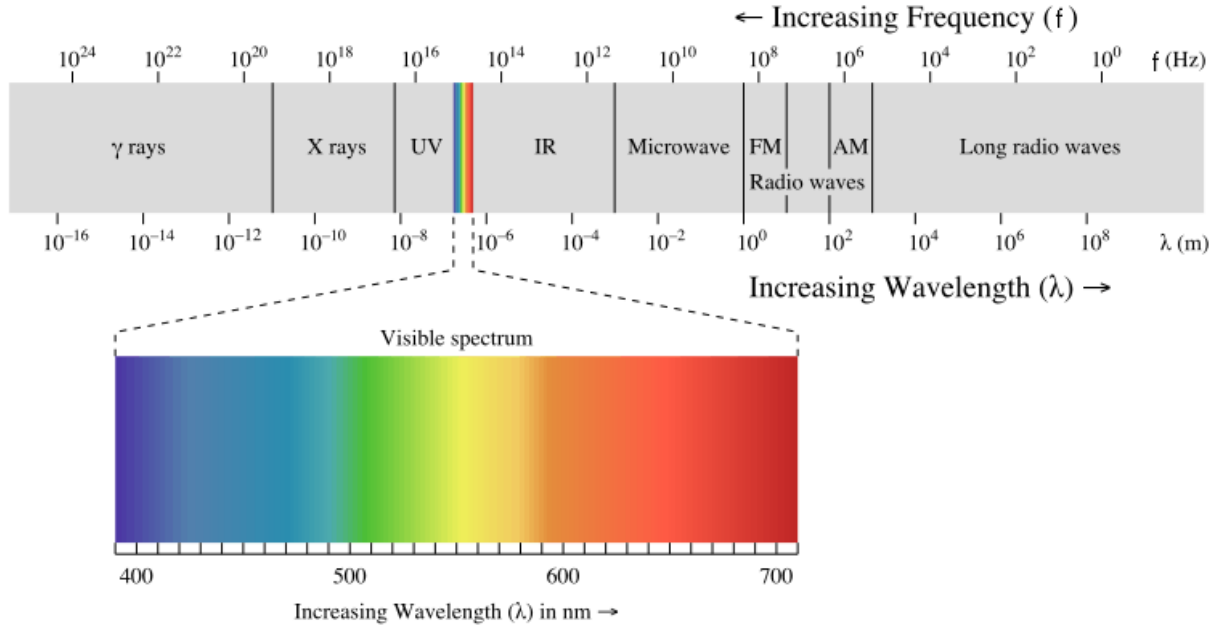
Light amplification by stimulated emission (Laser) and thermic light are based on different principles of light creation. In a thermic light spontaneous emission is the major process which generates light, a laser generates light by stimulated emission. Figure 3.3 shows the schematic structure of a laser module. The most important part is the optical amplifier. It is capable of amplifying a light wave without phase displacement. Within the amplifier numerous stimulated atoms are located which amplify incoming light by induced emissions. As shown in Figure 3.3 mirrors are located on both sides of the amplifier. This is the optical resonator of the laser module. Only a part of the light which passed the amplifier leaves the laser module. The other part will stay in the module and run through the cycle again. A laser module will only start if the light wave in the resonator superimposes itself in phase (Donges, Noll 1993).



**Figure 3.3: Principle function of laser**

The significant difference between thermic light and laser light is the coherence of the laser (Bauer 1991). In a coherent light are the electrical and the magnetic field strength

at two individual spatiotemporal points in a defined mathematical correlation to each other (Donges, Noll 1993). Laser is a small spectrum of the bandwidth of light as shown in detail in Figure 3.4. The wave length of laser light varies from  $\lambda \sim 0.1 - 10 \mu\text{m}$ .



**Figure 3.4: Wave length (Sipex 2007)**

The mathematical base for calculations of laser parameter is the harmonic wave. A laser can be mathematically described with Equation 3:3:

$$E = E_0 \cdot \cos(\omega t - kz - \phi_0)$$

$$H = H_0 \cdot \cos(\omega t - kz - \phi_0)$$

**Equation 3:3: Harmonic wave (Donges, Noll 1993)**

The electrical field strength  $E$  can be calculated with the amplitude of the electrical field strength  $E_0$  and the cosine of the difference of the circular frequency the number of waves and the phase. The same can be made for the magnetic field strength  $H$  as shown in Equation 3:3. The circular frequency and the frequency are defined as:

$$\omega = 2\pi f$$

**Equation 3:4: Circular frequency (Donges, Noll 1993)**

The mathematical contiguity between the number of waves and the wave length is shown in Equation 3:5:

$$k = \frac{2\pi}{\lambda}$$

**Equation 3:5: Number of waves (Donges, Noll 1993)**

Furthermore are the circular frequency and number of waves as well the frequency and the wave length described in the dispersions relation in Equation 3:6.

$$\frac{\omega}{k} = c_w = \frac{c_0}{n}$$

$$f\lambda = c_w = \frac{c_0}{n}$$

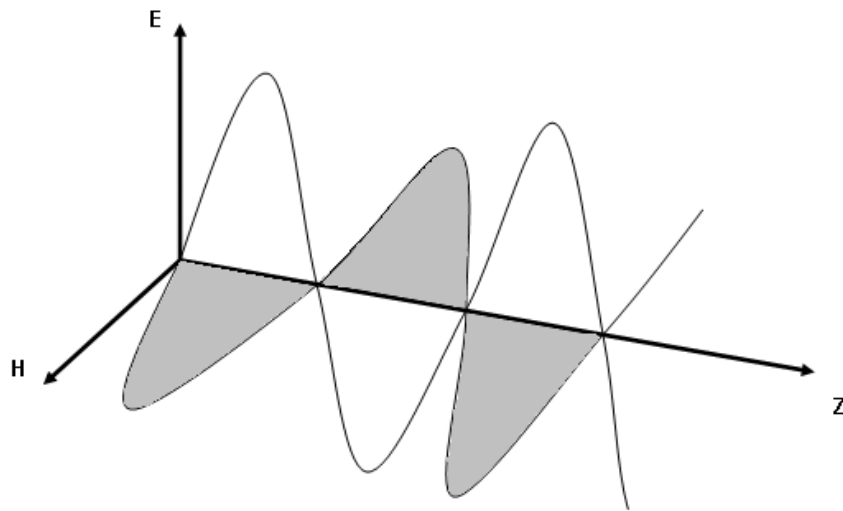
**Equation 3:6: Dispersions relation (Donges, Noll 1993)**

The dispersion relation refers to the speed of light in vacuum and the reflective index of the medium in which the laser is operating. The electrical field strength and the magnetic field strength are proportional. A laser wave transports energy, it's intensity is proportional to the square of the amplitude and can be calculated with

$$I_w \sim E_0^2$$

**Equation 3:7: Wave intensity (Donges, Noll 1993)**

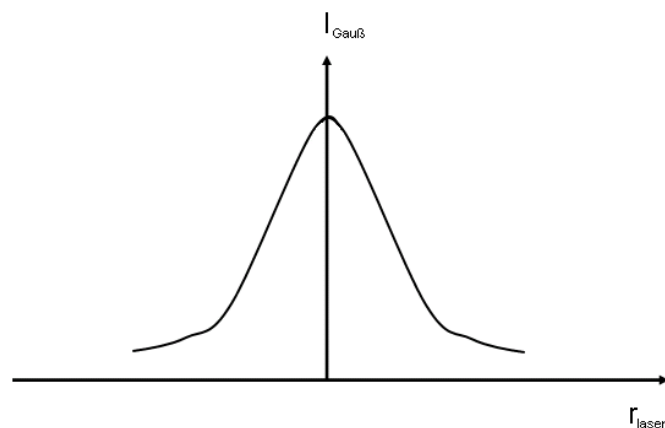
Laser waves are transversal waves, means that the magnetic field strength, the electrical field strength and the propagation direction Z are perpendicular to each other. The model of a transversal wave is shown in Figure 3.5.



**Figure 3.5: Harmonic wave**

A laser can be non-ambiguously described by five parameters: Intensity, phase, propagation direction, wave length and polarisation.

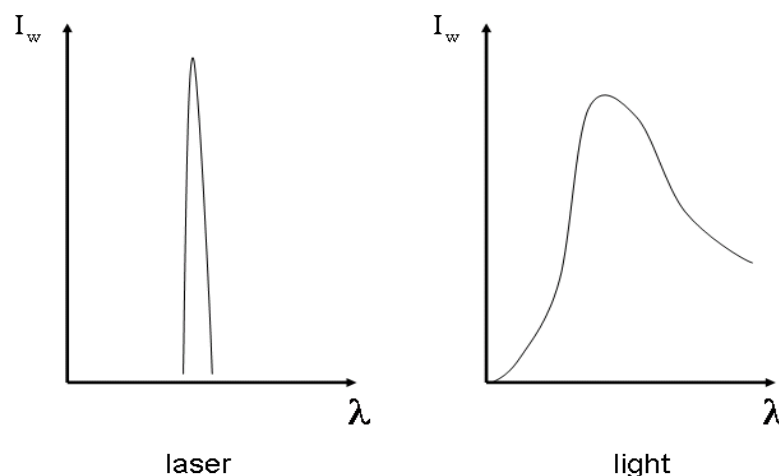
Whether laser light is mathematically based on the harmonic wave the real intensity of a laser light is not constant through the radius. There are different models of allocation of intensity within the laser beam. The most common is the Gauß model. In the Gauß model the laser beam is a rotary symmetric beam. Figure 3.6 shows the allocation of intensity within the radius of a laser beam in detail.



**Figure 3.6: Gauß model of intensity**

The highest intensity of the laser beam is concentrated in the centre. The intensity decreases outwards the radius of the beam.

Laser does have a minimum divergence of ray and a minimum spectral bandwidth. Figure 3.7 shows exemplarily the spectral bandwidth of a laser and a normal light in comparison.



**Figure 3.7: Spectral bandwidth of laser and of light**



This monochromatic laser light can be filtered with a pass filter. The laser light will almost completely permeate the filter whilst the broadband daylight almost completely will be absorbed or reflected from the filter. This phenomenon allows the concentration on the reflection of the laser light and neglecting reflections of daylight.

### 3.1.3. Industrial robots

Industrial robots are designed for different tasks in different parts of the industry. The majority of robots are installed in the automotive industry. Main tasks of industrial robot within the automotive industry are welding applications, handling and glue applications (Knoll, Christaller 2003).

Robots are multiple capable automates for motion equipped with multiple axes. The movement and sequence of movement is in angle and distance without mechanical interference free programmable (Weber 2009).

Robots are designed with several axes and joint. Figure 3.8 shows on the one hand a picture of a common industrial robot and on the other hand the schematic model of a robot. The tool centre point of the robot is located at the end of the last axis. In order to determine the exact position of the tool centre point of a robot within the three-dimensional space a coordinate system is required. By using a position vector the position can be described indisputable. In Figure 3.8 a schematic robot with its sub coordinate systems of the joints and axes is shown in detail.

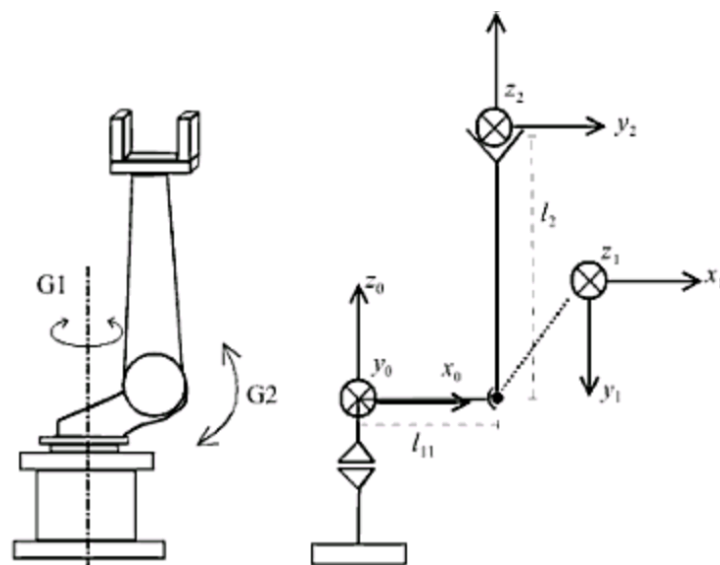
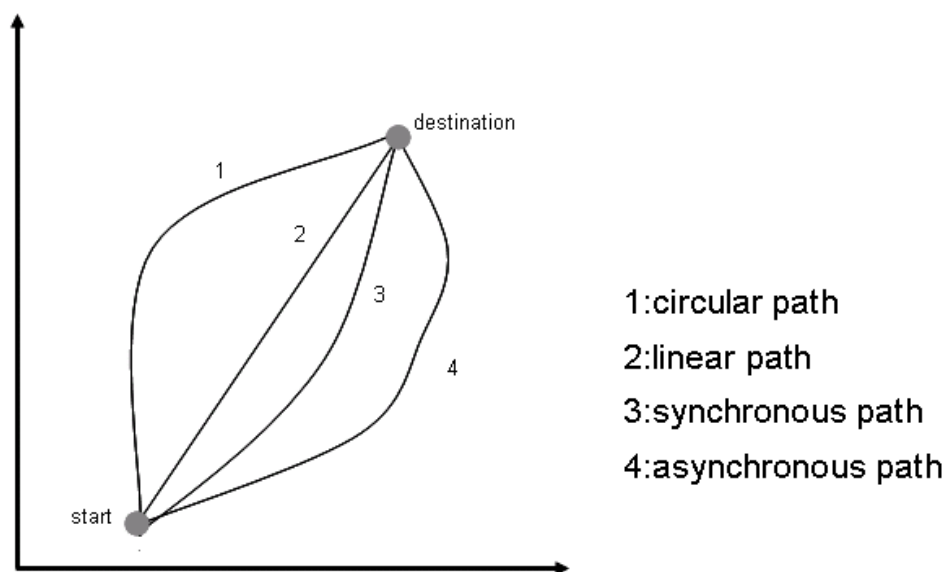


Figure 3.8: Industrial robot

The position and orientation of the tool centre point of a robot is described by the joint coordinates. The joint coordinates are the angles of the joints. The joint coordinates may vary if the operator programs a position (X/Y/Z) of the tool centre point in the world coordinate system. In order to describe the complete position of a robot in the three dimensional space the Denavit-Hartenberg-Konvention is used (Weber 2009).

In common cases three dimensional position and orientation of a point is described by six parameters. Details are shown in chapter 2.3. The Denavit-Hartenberg-Konvention describes the relative position of two adjoining coordinate systems by four parameters. In robot systems are three parameters fix only the fourth parameter, the joint position, is variable and can be determined with the Denavit-Hartenberg-Konvention (Weber 2009).

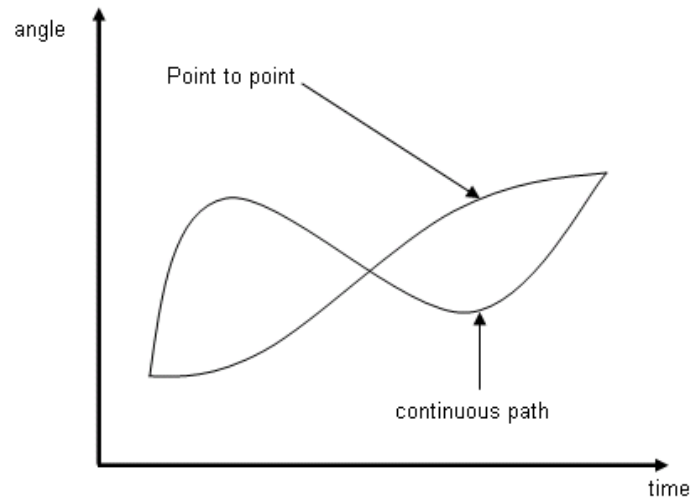
A robot has various options of movement. The three major controls are the point to point movement, the continuous path movement and the circular path movement. Figure 3.9 shows the different modes of movement in detail. The point to point control differs in synchronous and asynchronous movement. In the asynchronous mode every single axis reaches its final destination independent from the other axes. Therefore the axes will not stop at the same time. In the synchronous mode all axes movement depends from the axis with the longest time of operation. The other axis will be reduced in speed that all axes reach their destination at the same time.



**Figure 3.9: Modes of movement**

The majority continuous path control is operated with a linear movement. In this mode of operation, the robot will reach its destination by a linear path. The circular path is

defined by the starting point, an auxiliary point and the destination. The changes of angles in the joints differ in the different modes. The changes in the point to point mode can be minimal while the changes in the circular and the linear modes may be significant.



**Figure 3.10: Angle single axis during movement**

Figure 3.10 shows possible difference in angle of the same axis during operations. The starting point and the destination in the different modes are exactly the same but the interaction of the axis differs extremely. In the point to point mode the operation is guaranteed. In the continuous path modes operations can not be guaranteed because required movements may exceed the limits of angle movement of an individual axis (Weber 2009).

Furthermore is the velocity between two points not constant neither in the tool centre point of the robot nor in the individual axis of the robot. A movement of a robot can be split in three phases. One way of calculating parameters of movement of the robot is the ramp profile of movement. Figure 3.11 shows the profile of movement in detail. The Figure shows the period of acceleration and braking, the velocity of the robot over the time of movement and the travelled distance. The assumption is that a robot has at the starting as well at the end point a velocity of zero.

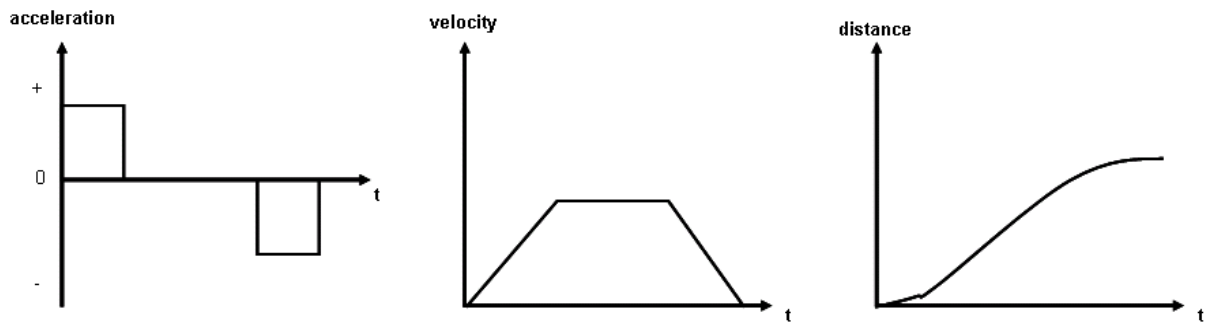


Figure 3.11: Robot parameters during movement

At the beginning there is a phase of acceleration. After reaching nominal speed the velocity stays constant. In order to have a velocity of zero at its destination the robot slows down before reaching its destination.

### 3.2. Software

Software requirements split in two topics. On the one hand a software tool for sensor information read out is required and on the other hand software for interaction with the operator and display of the measurement results is required. The market supplies neither one. But there are different algorithms available for sensor readout which can be implemented into free programmed software.

There are three different types of read out algorithms: the centre of gravity algorithm, the threshold algorithm and the maximum/peak algorithm. The different ways of calculation are visualized in Figure 3.12 and explained in detail in the following.

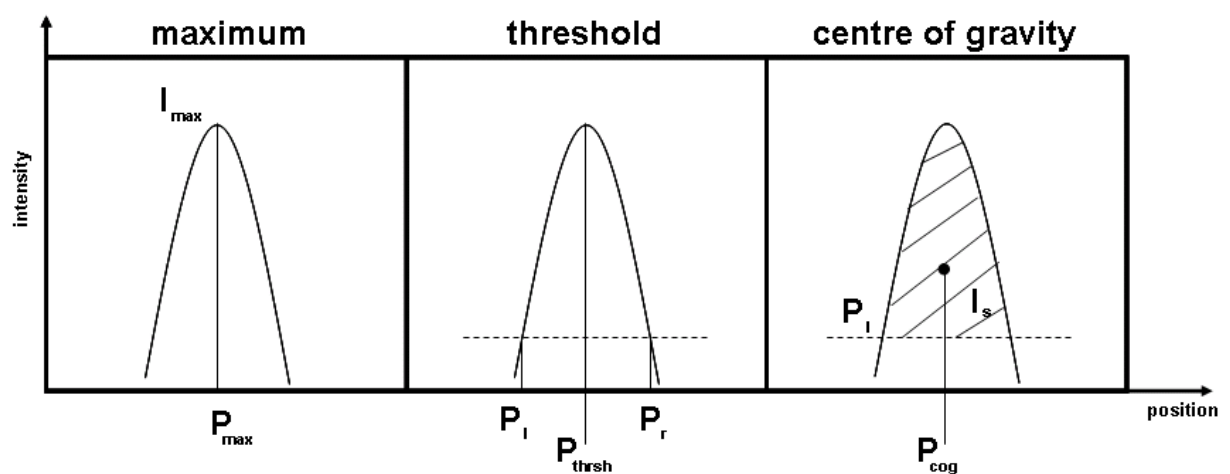


Figure 3.12: Sensor read out algorithm

In the maximum algorithm every single row of the sensor will be calculated individually. If the maximum intensity  $I_{\max}$  is detected the position  $P_{\max}$  can be determined. If there is more than one local maximum the first maximum will be calculated, starting from row zero.

In the threshold algorithm a minimum illumination is defined. The algorithm detects the two break through points of intensity. The position of the threshold position can be calculated with the left and right breakthrough points  $P_l$  and  $P_r$ . Equation 3:8 shows the formula in detail:

$$P_{\text{thrsh}} = \frac{(P_l + P_r)}{2}$$

**Equation 3:8: Threshold algorithm (Stemmer 2009)**

The centre of gravity considers the whole amount of incoming illumination. First the position of the left edge of the laser beam  $P_l$  for a given threshold is determined. Furthermore the sum of intensity  $I_s$  and the first order moment  $M_s$  are computed. The position value of the laser line (centre of gravity of the beam profile) is then obtained with Equation 3:9:

$$P_{\text{cog}} = P_l + \frac{M_s}{I_s}$$

**Equation 3:9: Position of centre of gravity**

Additionally there are software libraries which are able to merge pictures of the same object from different sensors. In order to receive metric information from the measured object a transformation from pixelated information to metric information is necessary. There is one software library which is capable transforming pixelated information to metric information. Both, the merging and the calibrating tools, are only software libraries, there is no such complete software which fulfils the requirements of this project.

The user interface and communication software of the innovative system has to be programmed completely since there has not been such task before.

### **3.3. Required interfaces**

This subsection identifies the required interfaces for communication between the components and further for the interaction between the software and the components. For the communication between the processing computer and the cameras either network interface cards or frame grabber card can be used, depending on the data output of the sensor.

#### **3.3.1. Framegrabber**

A frame grabber is the interface between the processing computer and the sensor. The communication between the sensor and the grabber card is bidirectional. On the one hand the frame grabber sends a predefined trigger signal to the sensors. On the other hand the sensors send their generated data to the frame grabber. The pictures are being pre-processed in the grabber and then provided for further processes and analysis in a superior software tool.

#### **3.3.2. Controller**

For the interaction between the computer and the production cell a specified controller is required. The controller is supposed to transfer an input signal into a trigger output signal. The calculation of the properties between input and output signal have to take place in the controller itself. Furthermore the controller is supposed to activate and deactivate the laser module if necessary. Since there is no similar system on the market, the controller will be designed specifically for this prototype system.

## 4. System implementation

This chapter will define the production cell in which the innovative measurement system will be implemented. Furthermore will the subsections point out the implementation of the hardware into the cell as well describe the development and structure of the required software.

### 4.1. Production cell

The prototype system will be integrated in the production in the body in white production. The cell manufactures the tailgate of Golf+ model. The layout of this production is shown in detail in Figure 4.1.

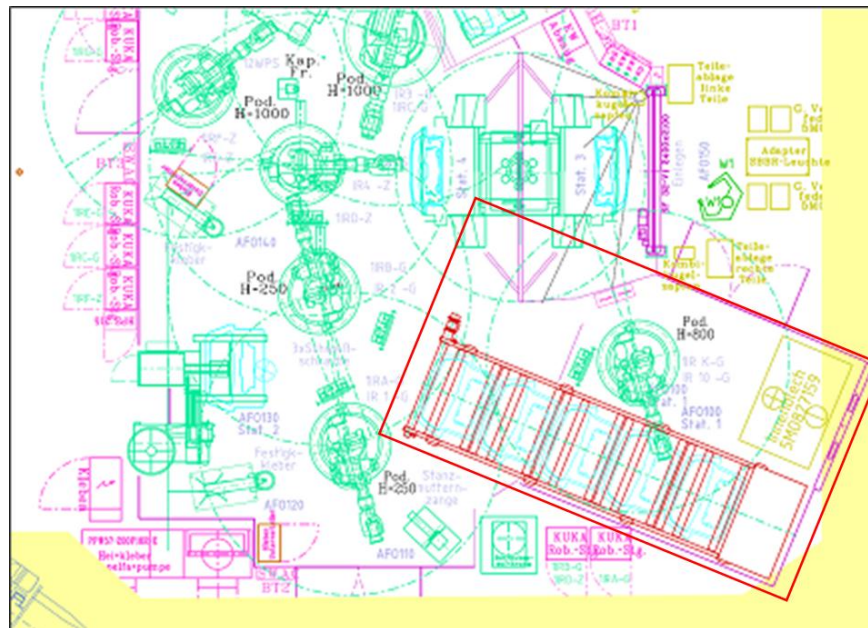
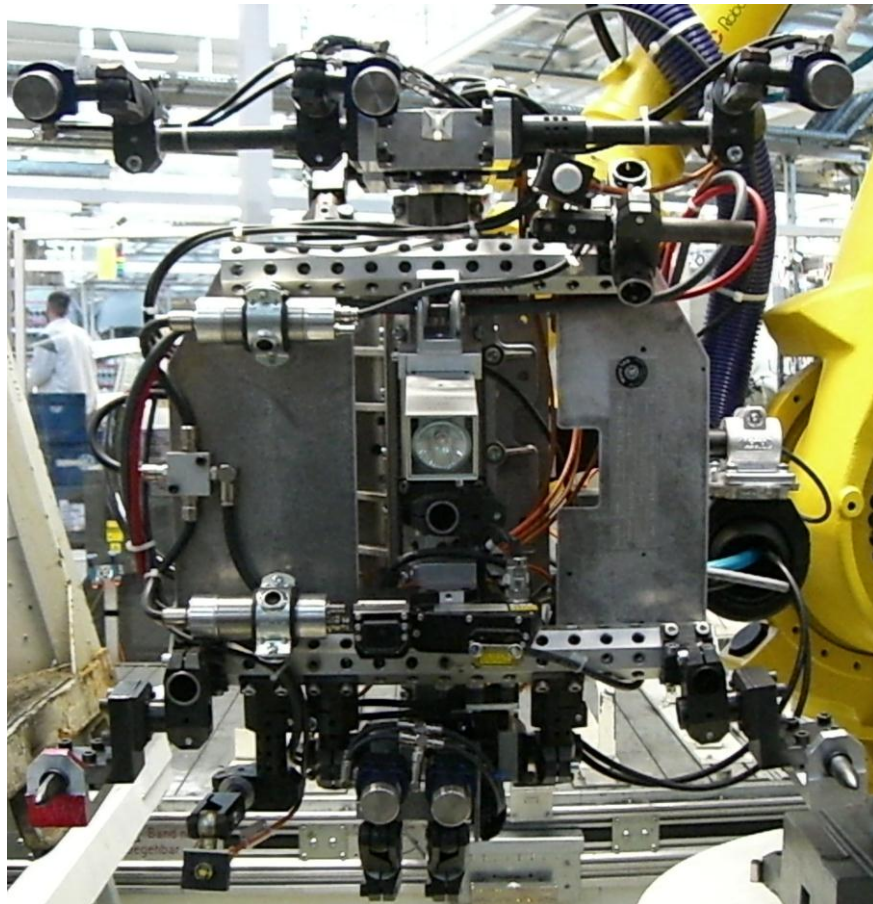


Figure 4.1: Layout tailgate Golf+ (Labahn 2010)

In this cell are one industrial robot and one conveyer installed and one box with parts for further processing is placed in the cell. In this part of the production cell only handling operations of the part is realised. The robot is equipped with a grab and a vision system. The robot will place its grab in front of the box in order to grab a part from the box. After picking the part the robot will handle it and place it onto the conveyer. The conveyer is equipped with five product fixtures. The robot will repeat its process until all five fixtures are loaded.



The point of interest in this production cell is the grab of the robot. It is equipped with two RPS pins and five magnetic holders. If the robot loads the part into the grab it extends the magnetic valves and dons them. By retracting the magnetic valve the part will be positioned with the RPS pins and clamped into its designated position. On the one hand the dimensional properties between the RPS pins are of interest. On the other hand the position of the magnetic valves to each other and the comparison of the positions of the pins and the valves to each other are of particular interest for the process.



**Figure 4.2: Robot grab in production cell**

Figure 4.2 shows the grab of the robot in detail. On the bottom are the two RPS pins located. Furthermore the five extendable magnetic valves, two at the bottom between the RPS pins and three on top of the grab, are clearly to identify.

The cell is not part of the main assembly lines of the Golf production. It is maximum two of three shifts in production process. The amount of manufactured tailgates per day is 450 (Labahn 2010).



These conditions make the cell ideal for a prototype implementation of the innovative measurement system into ambient conditions of the production.

## 4.2. Hardware

The first prototype was specified for the previous described production cell. Figure 4.3 gives an overview of the hardware components used for this prototype system. The system is the combination of an optical sensor, a frame grabber, a laser module and a common industrial computer. For the relative movement between the object of interest and the sensor the industrial robot, which is already installed in the production cell, is used. Additionally a controller for the communication between the robot and the other components has to be designed.

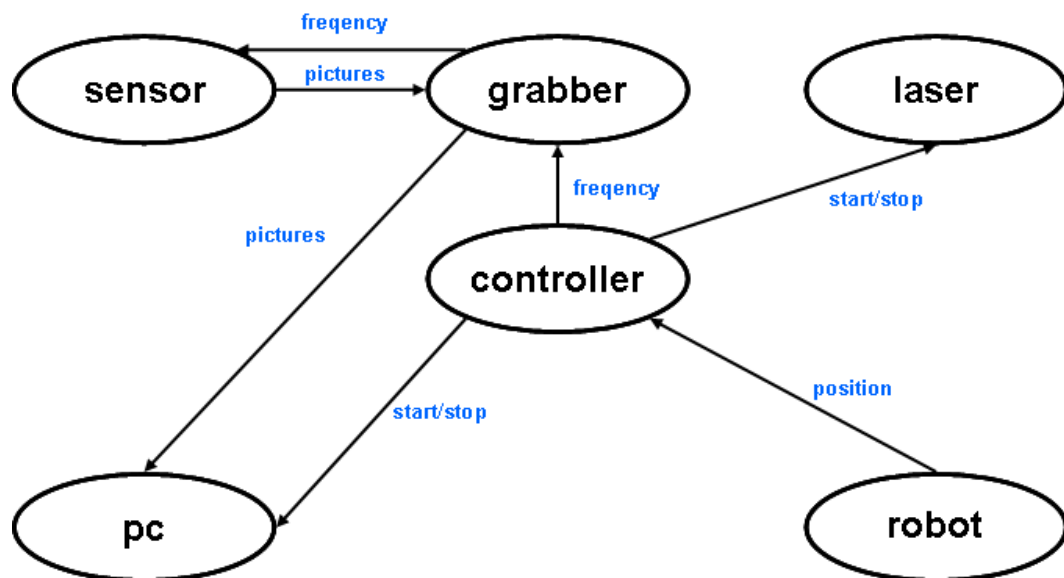
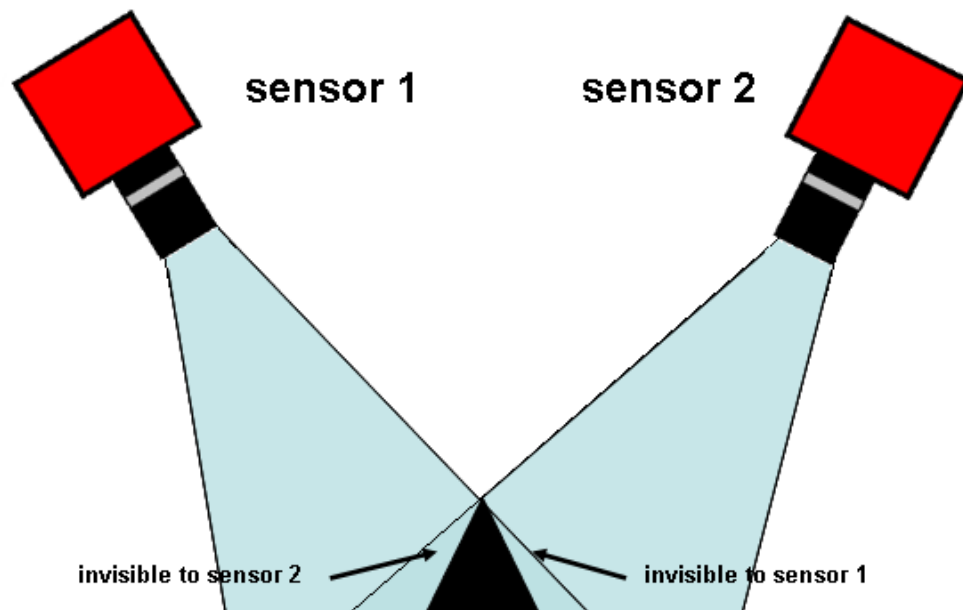


Figure 4.3: Hardware components

In order to generate complete three- dimensional information of the components of the grab a multi sensor system is required. Figure 4.4 shows the limitations of individual sensors in detail. The sensors are only able to generate pixelated information of a shape if it is able to detect illumination. If an illuminated shape is hidden from other parts of the object of interest no information can be generated. In some cases it is necessary to combine the generated information from different sensors with a different perspective of the object of interest. In the example shown in Figure 4.4 sensor 1 is able to generate full information of the left side of the pattern, but no information of the right side. On the other hand is sensor 2, which is able to generate full information of the right

side of the pattern. The combination of the generated data will complement the lack of information each sensor has individually.



**Figure 4.4: Sensor capabilities**

For the first test purposes in production conditions the prototype system is equipped with 2D CMOS sensors. Used are two Dalsa Falcon 4M60 sensors. These sensors have a resolution of four mega pixels. The resolution is 2352 pixels in width and 1728 pixels in height. In full resolution 62 pictures per second can be grabbed with each sensor. The sensors are each equipped with two camera link standard ports and possess a camera link medium data output. The sensors run with a global shutter and the frame rate can be increased by vertical windowing. Further details are listed in Appendix B (Dalsa 2010).

The sensors are equipped with optical lenses from Zeiss. Installed are the industrial versions Planar T 1,4/50 with a focal length of 50 mm. Used are lenses with a F mount connection system. Additionally a pass filter is used for each sensor.

The via camera link cable transmitted data of the sensor is processed in a standard computer. The computer is equipped with two frame grabbers from silicon software. The product details are shown in Appendix C. Additionally a trigger board is installed to the frame grabbers. The trigger board allows trigger signals from an external component. The board is designed for TTL signals.

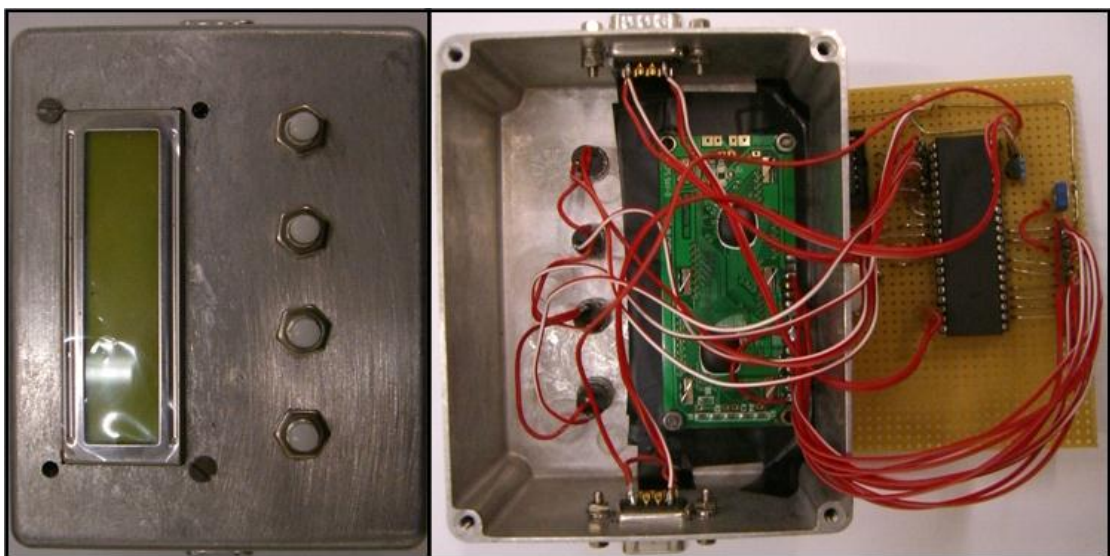
For the illumination of the components of interest a laser module from stocker yale is used. The laser module has an intensity of 35 milliwatts in punctual operation mode. The wave length of the module is 635 nm. This leads to a laser classification in class three. Additionally a linear module is installed at the front of the module. The opening angle of the linear module is 60 degrees. By spreading the punctual intensity in a line the punctual intensity can be reduced to laser class 2M. The laser module and the linear module are shown in detail Figure 4.5.



**Figure 4.5: Laser module**

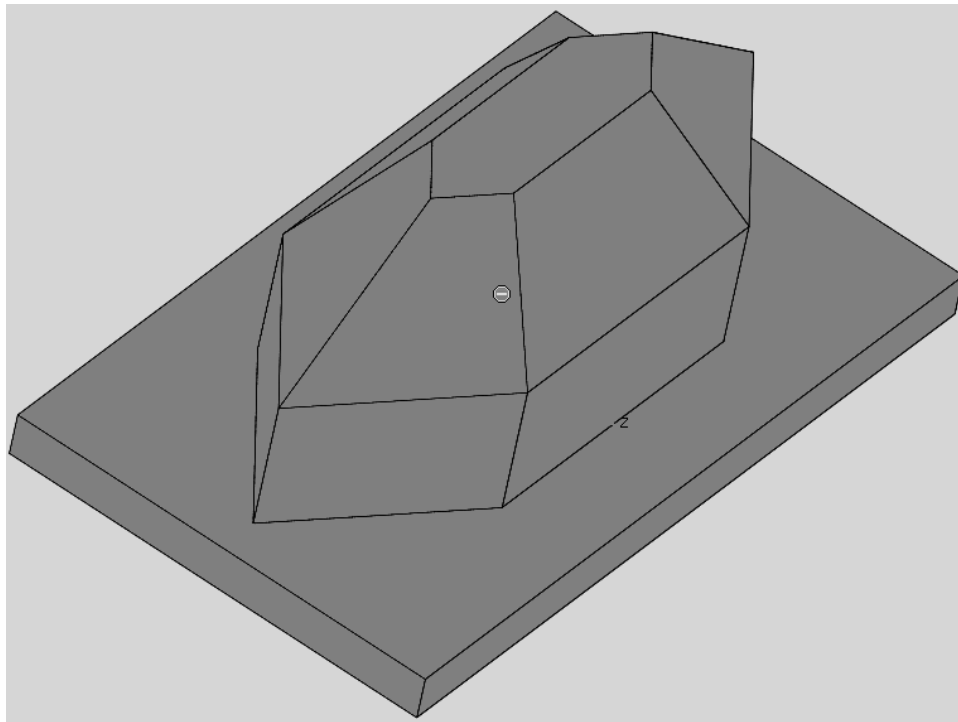
All laser classes and recommended precautions are explained in detail in Appendix D.

For communication between the industrial robot and the rest of the system a controller is designed. The controller consists of two ports, a free programmable atmel chip and a display for configurations. Figure 4.6 shows the circuit diagram and the controller itself in detail.



**Figure 4.6: Atmel controller**

Furthermore a pattern for system calibration is required. The pattern has to be installed within the operation range of the system. The calibration procedure requires the same relative movement between the sensor and the pattern as the measurements. The pattern is shown in detail in Figure 4.7. It is necessary that the direction of movement is along the longest axes. All installed sensors have to detect the projected laser line from the top of the pattern.



**Figure 4.7: Pattern**

Furthermore are cables for power supply of the single components and communication necessary for the system implementation. These will not be defined in detail.

### **4.3. Software**

The software contains different libraries with different tasks. The main components are the peakfinder library, the merger library, the metric library and the match library. Furthermore individual controller software is designed for this application. The controller software is specified for a controller board with a microcontroller. The libraries are available on the market as dynamic link libraries (.dll) and can be implemented in common source codes (Schlitter 2010). Their individual functions will be defined in the following. The interrelation of the individual libraries is shown in detail in Figure 4.8.

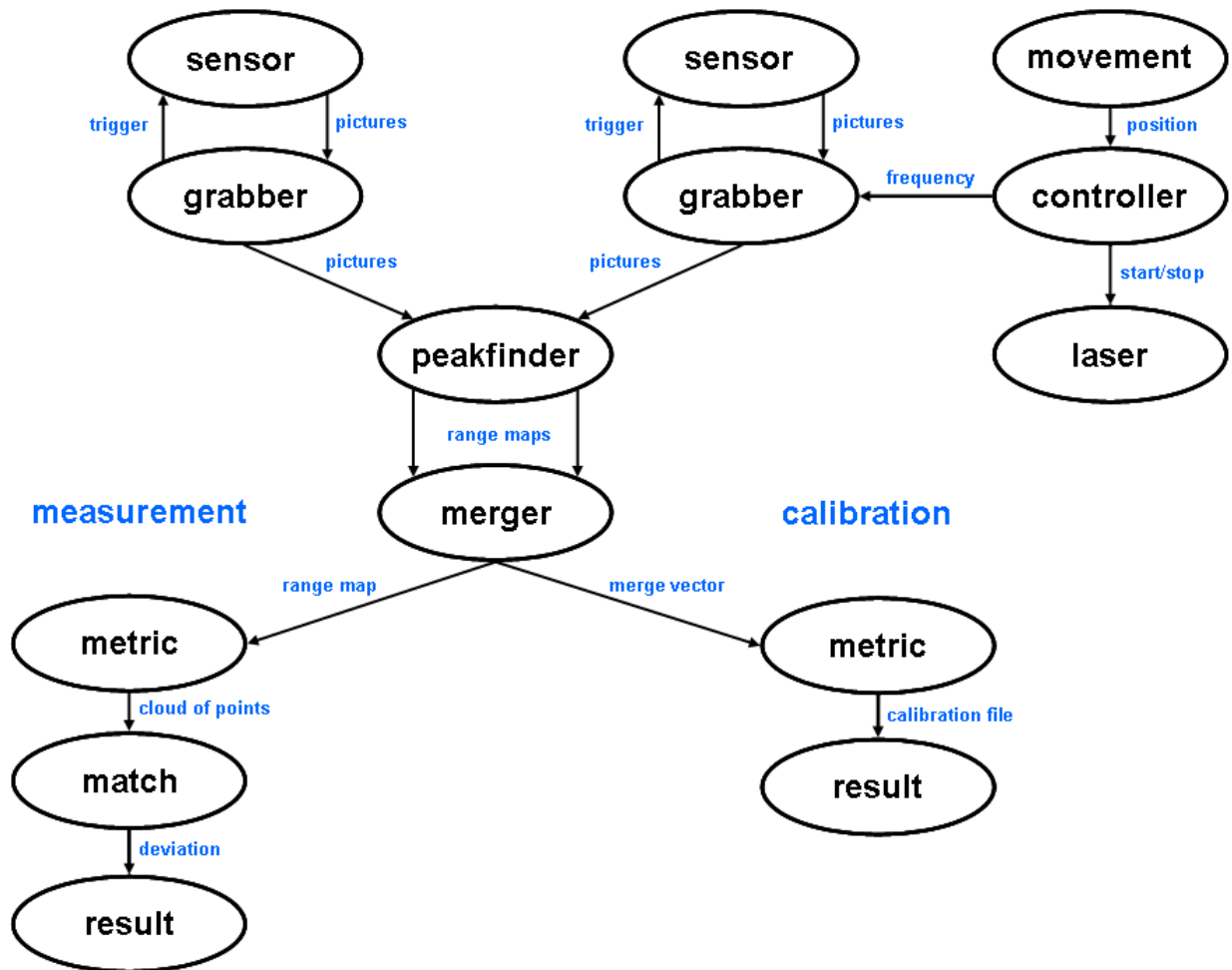


Figure 4.8: Software processes

For a measurement an actual position signal of the robot is delivered to the controller. The controller software transforms the robots information into a real time velocity signal. The data output of the controller is a velocity proportional frequency signal. The ratio parameters can be set individually by the operator. The frequency is transmitted to the trigger board of the frame grabber. Additionally the laser module will be activated if the robot delivers a signal. Furthermore the software is capable of transmitting information about the part which is being measured recently. This occurs in majority if one single system will be used for different measurement tasks.

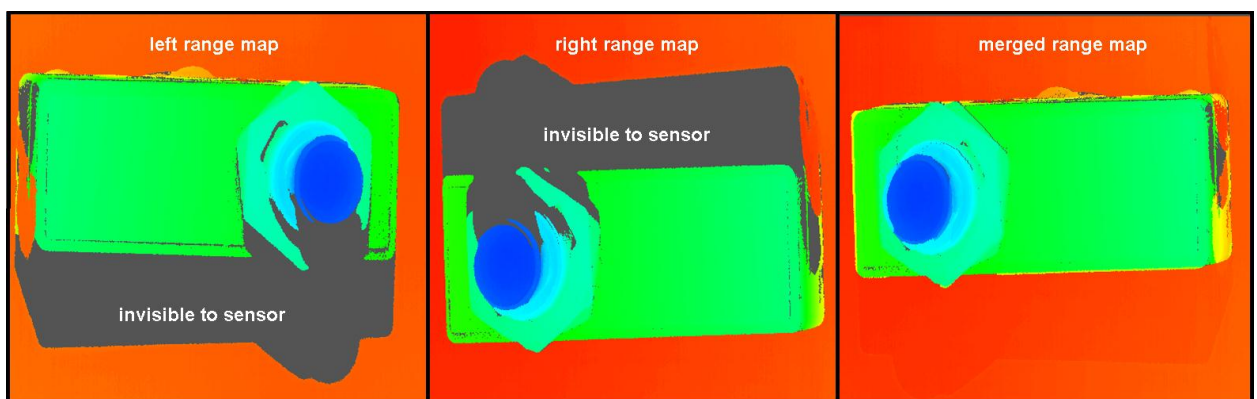
The software fetches the triggered and digitized gray scale value pictures from the frame grabbers. The software processing chain starts with the peakfinder library. The peakfinder library will calculate the peak illumination for every column of the picture individually. The library creates one profile of sensor illumination per picture. The sum of all consecutive profiles of one camera is formed to a spatiotemporal illumination model of the measured object. The process is highlighted in Figure 4.9. This process runs

parallel for every single sensor. The spatiotemporal illumination model is called range map (\*.arm).



**Figure 4.9: Peakfinder processing**

The next step in the process chain is the merging of the individual range maps to one combined range map. From this stage on processing may vary. Two paths are possible: the system calibrating and the processing of measurements. The calibrating mode is described in detail first, because system calibration is required for the actual measurement process. In the calibration mode the merger will displace the individual range maps until the maximum overlapping of information is reached. The displacement vector is identified and allows assumptions of the geometrical constellation of the sensors to each other. The displacement vector is saved in a separate file and provides displacement information for further computing of the following range maps. In the measurement processing mode the merger library will use the generated configuration file for displacement of the individual range maps in order to generate one range map including information of all sensors. Figure 4.10 shows the merger process in detail.

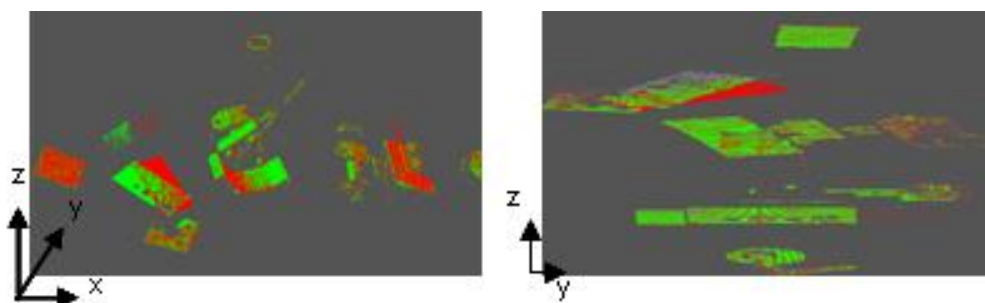


**Figure 4.10: Merge process of range maps**

The range map of the left sensor has a lack of information on the bottom of the object of interest. The range map of the right sensor has a lack of information on the top of the object. If the generated information of both individual range maps are added to each other, by merging them, the lack of information can be compensated.

The next step in processing is the transformation of pixelated information into metric information. Similarly to the merging at this stage two paths of processing are possible: In the calibration mode the pixelated information of the range map is transformed into metric information. For calibrating purpose a known pattern is scanned. The metric constellation of the pattern is saved in a calibrating file. The pixelated information is compared to the metric information and a proportional ratio is being calculated and saved in a separate metric configuration file. At this stage a calibrating accuracy and the system deviation is shown and the system is ready for measurement processing. In the further processing mode the metric configuration file is used for transformation of the pixelated range map information into metric information. The result after this process is a cloud of points in the three- dimensional space in the data format \*.cop.

The last step of the processing chain is the match library. The match library calculates the deviation of two cloud of points. Therefore the cloud of points are subtracted point by point from each other. Before the deviation can be determined the two models have to be aligned in the three- dimensional space. In the software are two different options of alignment implemented: the best fit algorithm and the RPS registration. The best fit algorithm calculates the best possible match of the whole cloud of points. The developed RPS registration differs in the alignment. It considers the in chapter 1.1 defined standard of Volkswagen. The RPS registration aligns the actual cloud of points at predefined objects with the nominal data. Figure 4.11 shows two cloud of points, the actual data and the nominal data, before alignment and after the best fit alignment.

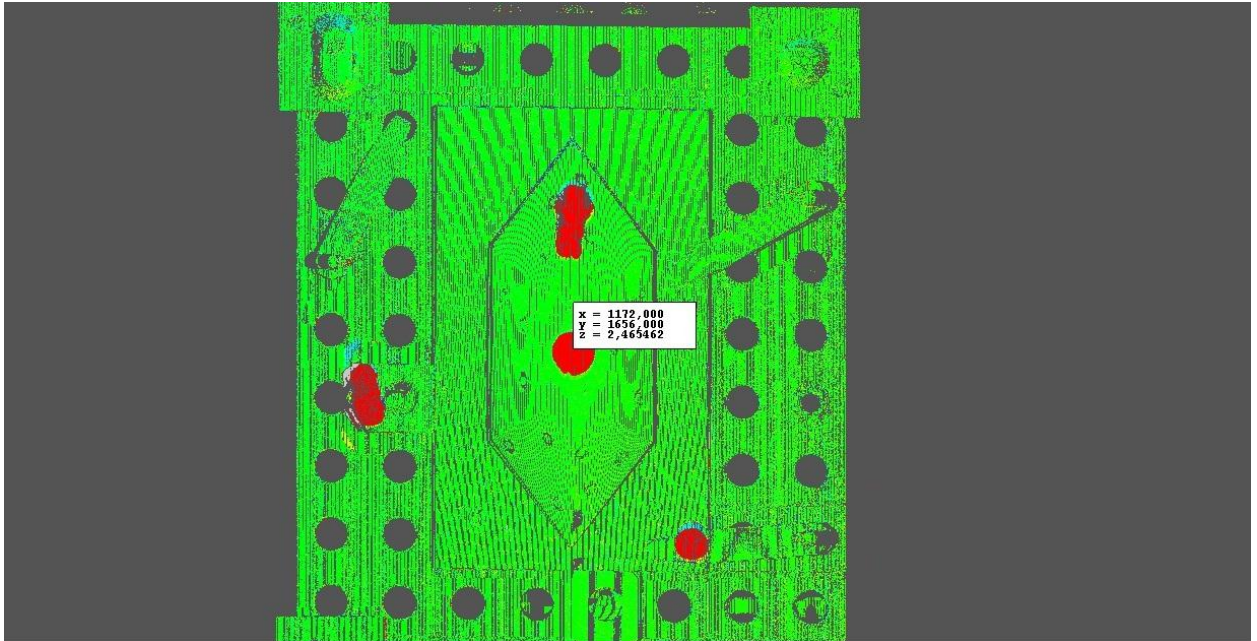


**Figure 4.11: Cloud of points**

The whole software parameters are illustrated in Appendix E. The scheme includes all described libraries and additionally the committed parameters.



The result of the deviation between the actual data and the nominal data is displayed in a personalized user interface. The deviations are displayed with a colour range map. Figure 4.12 shows a measurement result in detail.



**Figure 4.12: Display of a result**

The green coloured parts of the cloud of points are within tolerance. Areas which are outboard of tolerance are being displayed either in red or in blue. If the deviation is towards the measurement system it will be displayed red. If the deviation is away from the measurement system it will be displayed blue. Additionally are the deviations displayed in metric values with the cursor.

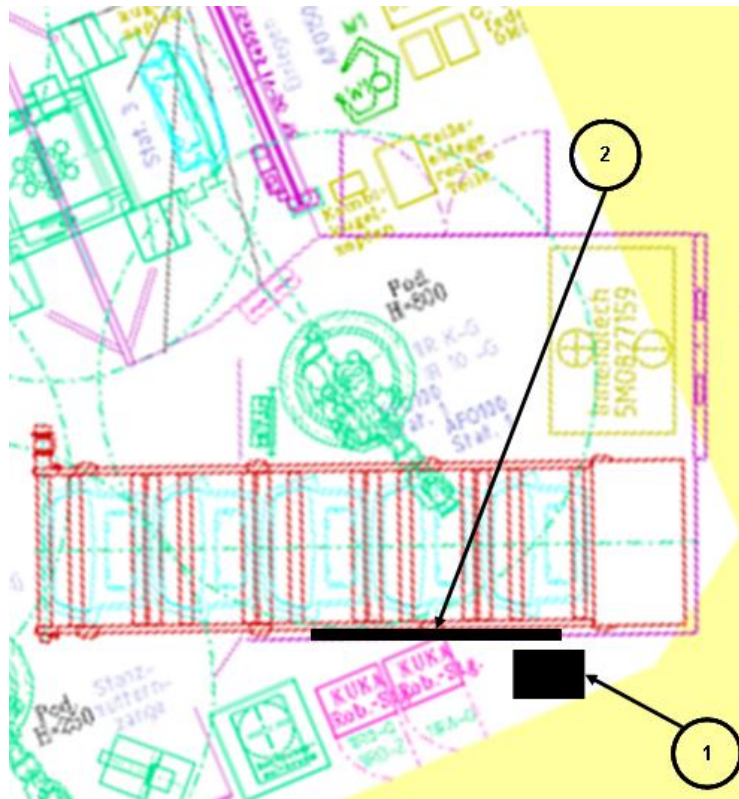
The design of the complete software is realised in a plug in system. Therefore a configuration menu is integrated into the software. This allows the usage of the same software for different measurement tasks. The operator is able to predefine the type of used sensors, the number of used sensors, the type used sensor interface, the definition of different values for the nominal data and finally the modus of registration.

#### **4.4. System setup**

The space for the installation of the innovative system is limited in the chosen production cell. The sensor and the laser module have to be installed in the operation radius of the robot while the computer and the controller can be placed outside the cell. Figure 4.13 shows the places for integration of the system hardware in detail. The



computer is placed next to the robot controls. Number 1 in Figure 4.13 shows the exact position of the computer.



**Figure 4.13: Hardware integration**

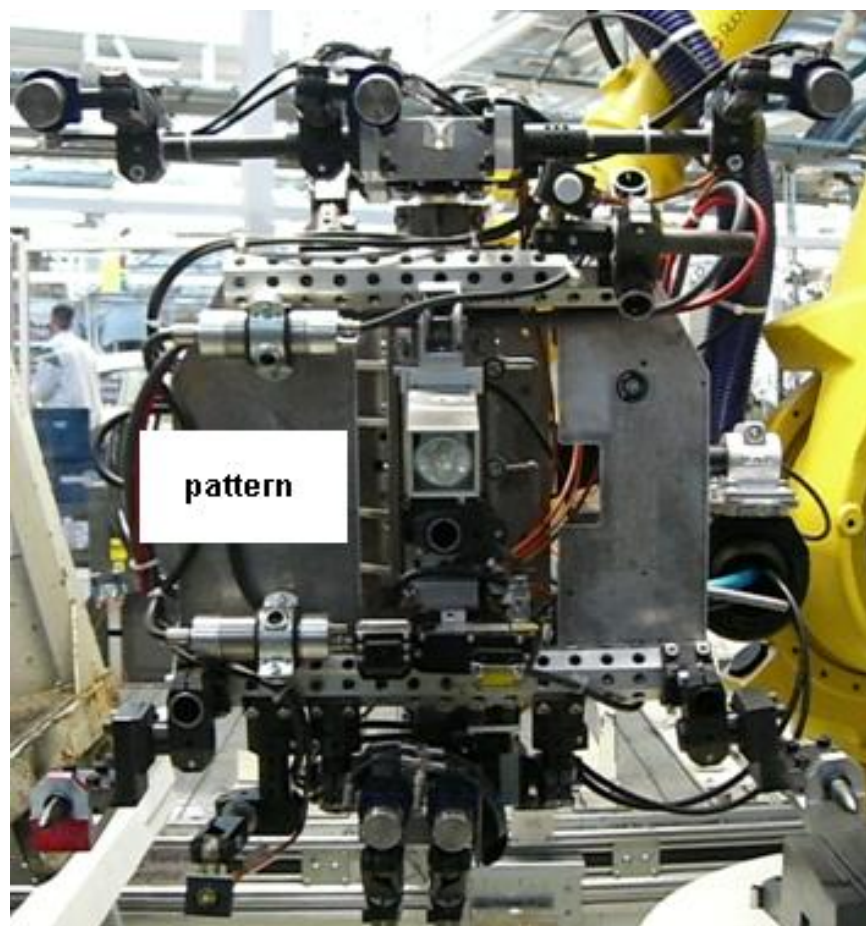
In this place no fork lifter will pass by and additionally it is placed behind a barrier. In this way the risk of accidental crashes is minimized.

The sensors and the laser module are installed in one unit into the cell. The unit is installed above the fencing around the production cell within the operation range of the industrial robot. Number 2 in Figure 4.13 shows the exact place of installation of the unit in the production cell. In order to fulfil laser safety requirements a housing for the laser module is installed additionally. In consideration of the ambient conditions in the production additional equipment has to be installed. Due to the high concentration of pollution in the air of the production hall the sensors are protected by metal housing on top. Figure 4.14 shows the implemented sensor unit in detail. The changing temperatures, especially the peak temperatures required a cooling for the sensors. The cooling is activated in dependence of the temperature of the sensors.



**Figure 4.14: Implemented sensor unit**

For the calibration of the system the calibration pattern has to be installed into the grab of the robot. Figure 4.15 shows the installation of the pattern onto the grab in detail.



**Figure 4.15: Robot grab with calibration pattern**

The pattern is placed in between the pneumatic valves of the measuring volume. This allows a calibration of the system with a path identical to the measurement path of the robot.

For the measurements additional measurement and calibration cycles have to be implemented in the path of the industrial robot. In consideration of the robot parameters explained in detail in chapter 3.1.3 a simulation of the future robot path was executed. Required is a continuous linear movement between the sensor and the object of interest. The simulation gives a conclusion about the starting and the end point of the linear movement in consideration of the ramp effect of the robot. The measurement speed of the system is 100 millimetres per second. The simulation considered that it is required to start the start at minimum 100 millimetres with the linear movement before the actual measurement or calibration can take place (Lange 2010).

## 5. Measurement with innovative system

The innovative measurement system differs in operation from other systems. This chapter with its subsections will give an overview how the system has to be configured, how it is calibrated and what possibilities of measurements and alignment are implemented in the innovative measurement tool.

### 5.1. General settings

For optimal functionality the system requires an accurate installation. The system is able to compensate minor deviations but the more accurate the installation occurs the more accurate will be the calibration and the later achieved measurement result. If more than one sensor is used for the system they should physically have the same distance and angle to the projected laser line. Figure 5.1 shows an optimal sensor constellation. In the side view the angle and the distance between the laser module as well the distance between the sensor and the object are highlighted. Furthermore should the point of intersection of the centre axis of the sensors meet exactly at the projected laser line. The top view in Figure 5.1 shows an example of two installed sensors in detail.

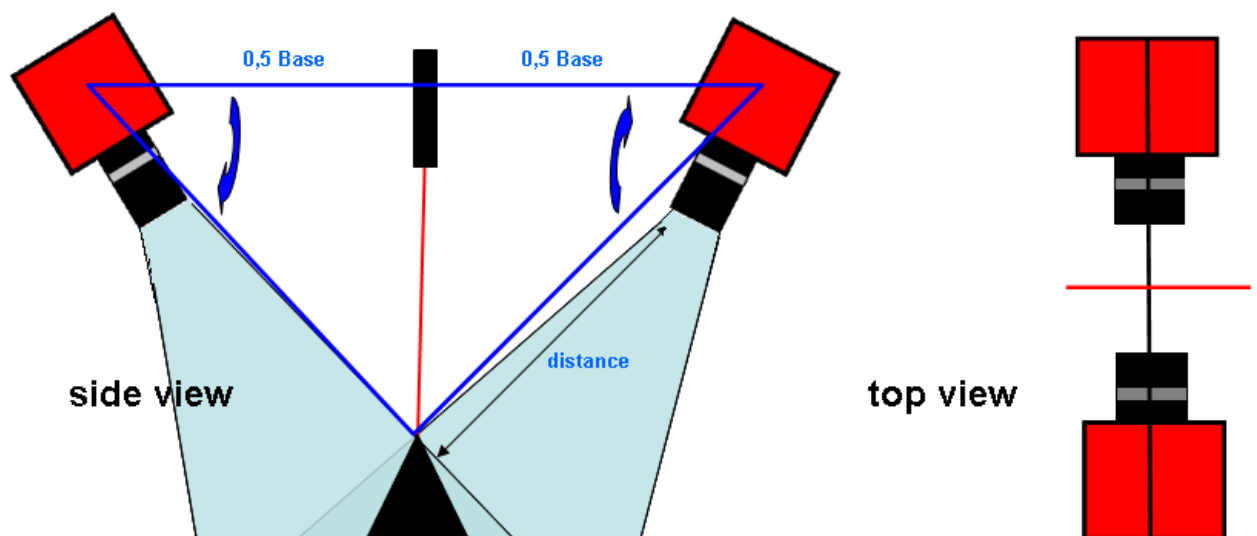


Figure 5.1: Optimal sensor constellation

In this case the centre axes of the two sensors form one line. Additionally is the axis of the sensor orthogonal to the projected laser line and the intersection divides the line in half.

If the measurement volume does not need the complete sensor resolution, like shown in position 4 in Figure 5.2 the resolution should be reduced. The reduction of the activated pixels in the sensor will reduce the generated data amount and will lead to an increased data processing.

The developed software is separated in different modes and is always structured in the same way. Figure 5.2 gives detail information about the graphical user interface structure of the designed software tool. The software is subdivided in seven major parts for operator information. Position 1 highlights the control area for the operator. The software provides a selection of the modes, a setting selection and a system information link. There are three different software modes: manual mode, automatic mode and calibration mode. The modes will be described in detail in the following subsections. The activated mode of the software tool is always shown on top in the centre of the software tool.

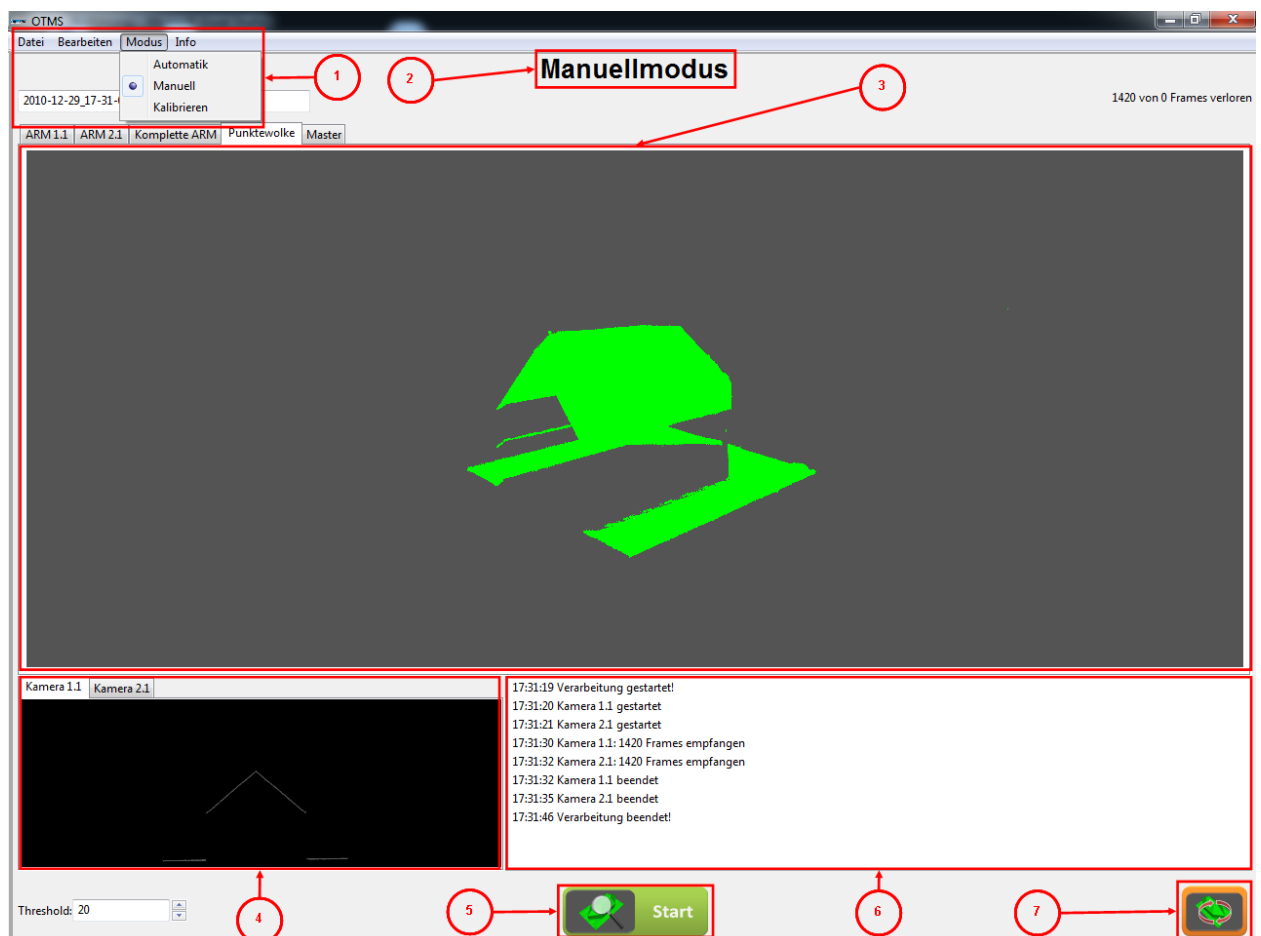


Figure 5.2: General software overview

The majority of the screen is filled with the actual measurement data generated by the system. Position 3 in Figure 5.2 shows parts of a calibration pattern scan. The data is displayed as a three- dimensional cloud of point and can be inspected from any angle and distance.

If the system operates in manual mode a constant live view is integrated in the graphical user interface. The system provides the live view from every single activated sensor of the system. The live view delivers information about how many pixels the measurement volume requires. Furthermore irregularities can be identified in the live view.

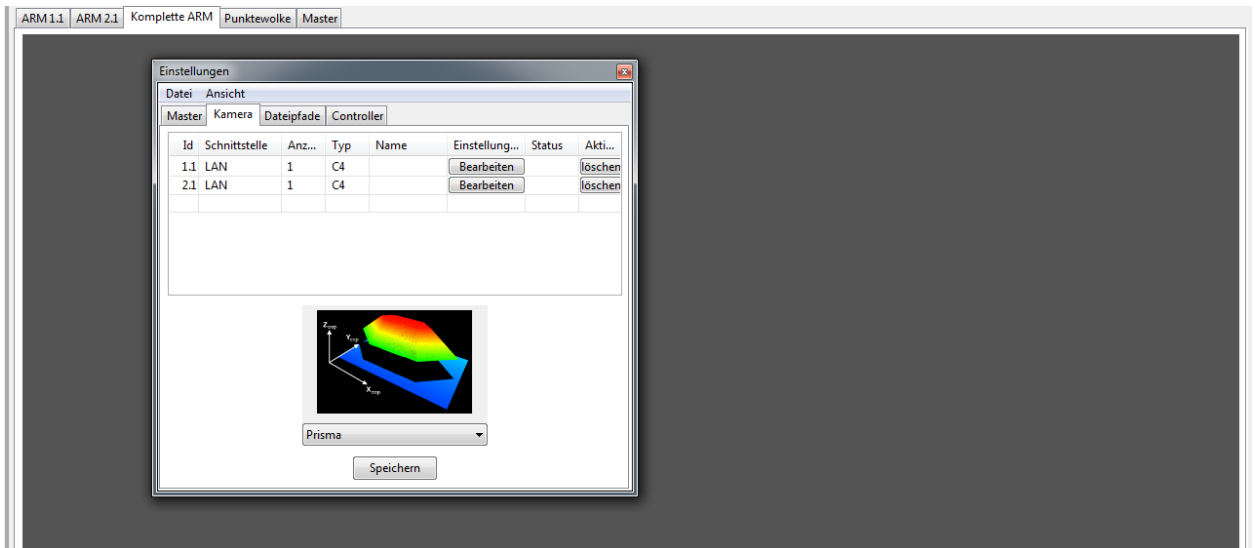
The activation or deactivation of the measurement system always occurs in the bottom centre of the screen. If the system is ready to be activated the button occurs green, like shown in Figure 5.2. If the software is in measurement processes the button will occur red and deactivates the actual measurement process, if activated.

Further information for the operator about sensor status, process status and data generated is displayed in the status window. Position 6 in Figure 5.2 points out the status window after a single measurement is completed.

The dialogue for the predefinition of nominal data starts with the highlighted position 7 in Figure 5.2. All software components will be explained in detail in the following sub sections.

## **5.2. System configuration**

The system is designed in a plug in principle. Therefore different parameters have to be defined before measurements can take place. The main parameters of the system are the type of sensor used, the interface used for communication with the sensor, nominal values of the calibration pattern and the type of controller.



**Figure 5.3: Setting dialogue**

Figure 5.3 shows the graphical user interface of the settings dialogue. In the sensor settings the operator defines first the number of sensors used in the application. The data received from sensors vary, therefore the type of sensor has to be defined. Furthermore each sensor has to be associated with an interface. Depending on the sensor this is either a frame grabber or a network card for each sensor. In some cases sensors may share one interface.

Depending on the size of the measurement volume the requirements for the calibration pattern vary. In order to generate an optimal result of calibration different pattern are manufactured and saved as files in the software tool. The pattern differ in their dimensions. If the system calculates with the wrong metric dimensions of the pattern the generated metric file will not be realistic. Therefore the software provides a selection of different calibration pattern.

Depending on the hardware used for the relative movement between the sensor and the object of interest different controller can be used. The software offers the definition of the implemented controller in the measurement tool as well the definition of the generated trigger signal.

Finally the operator can select an individual path for file saving. If these settings are finalized a settings file will be generated and saved.



### 5.3. Calibration of system

The system has to be calibrated in order to transfer the generated data from pixelated information to metric information. The software contains a calibration mode for system calibration. The calibration of the measurement system splits in two types of calibrations which run automatically one after another.

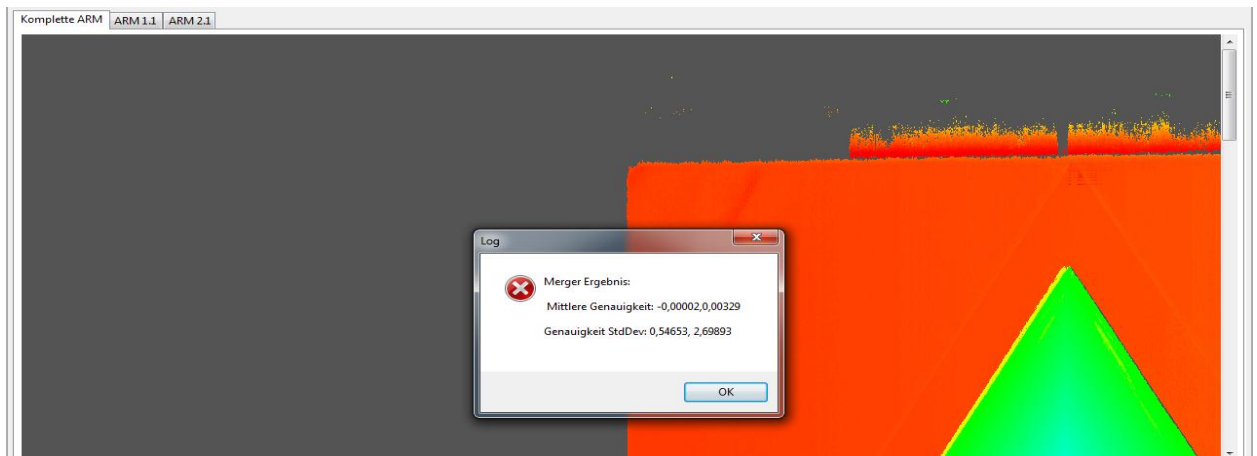
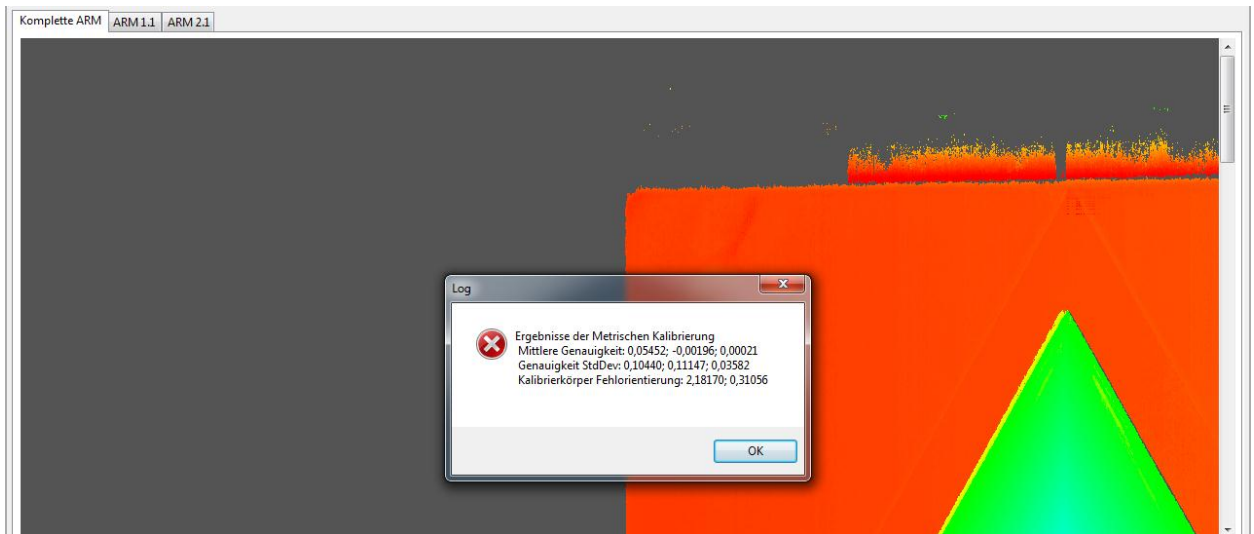


Figure 5.4: Result of merger calibration

First the system recalculates the constellation of the sensors to each other and their constellation to the laser module. This procedure is the merger calibration of the software. The software process is described in detail in chapter 4.3. The measurement software displays the result of the accuracy and the standard deviation of the merger calibration for the operator before calculating the metric calibration. Figure 5.4 shows the result of the merger calibration in the graphical user interface in detail. If an error occurs during the merger calibration the operator has the chance to view the generated range map from the individual sensors. This supports the detection of errors in the calibration mode. If the merger calibration fails the software will not continue with the metric calibration.

After a successful merger calibration the system will start automatically with the metric calibration. The metric calibration will transfer the generated measurement data from pixelated information to metric information. The software refers to the in the system configuration defined calibration pattern. The result of a metric calibration is displayed in the graphical user interface and is shown in detail in Figure 5.5.





**Figure 5.5: Result of metric calibration**

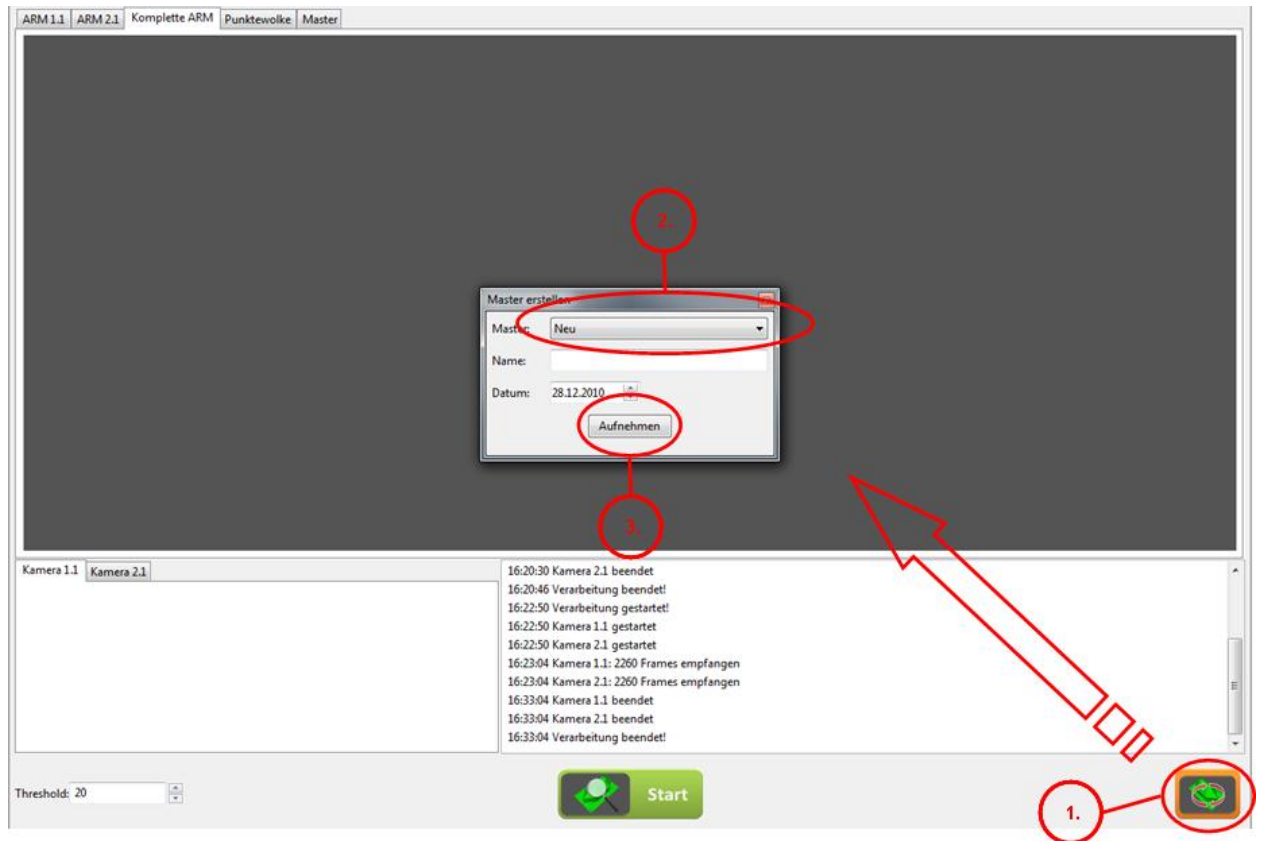
The result highlights three different parameters of the calibration. First it displays the average accuracy for each coordinate axis in detail. Second it identifies the standard deviation of the calibration. Details of calculation of the standard deviation are described in chapter 7.3. Finally the result points out the disorientation of the calibration pattern towards the axis of the linear movement. If the calibration is successful and the calibration accuracy fulfils quality requirements the system will be ready for measurements. The following measurements will consider the saved calibration files for their calculation of deviation.

## **5.4. Definition of nominal data**

In order to generate a measurement result a comparison of data has to occur. The actual data is generated during the measurement. The nominal values have to be predefined. The software of the innovative measurement system gives different options for predefinition of the nominal data.

Most parts or components have been designed in CAD software before being manufactured. If the actual data of the object is supposed to match the CAD data this data can be imported into the software and defined as nominal data.

In some cases the product has changed during processes and the earlier CAD data does not match to the actual dimensions of the product.



**Figure 5.6: Configuration of nominal data**

In this case the system is able to generate a cloud of points of the actual conditions of the product and predefine these geometrical parameters as nominal data. Figure 5.6 shows the graphical interface in detail. Step one for the import of nominal data is the selection of the master button in the software. In step 2 in Figure 5.6 the operator selects the nominal data: either by importing CAD or already generated cloud of points or by activating the option new master as shown. By activation of button 3 in Figure 5.6 the system will save the next generated cloud of points as its nominal data. All following measurements will be compared to the preselected data until another set of data is chosen.

## 5.5. Alignment

The focal point of comparison of nominal and actual data can be different from task to task. There are different possibilities of data registration. The standard procedure of alignment in the software is the best fit alignment. If required the software is capable to align nominal and actual data after the 3-2-1 rule. The 3-2-1 rule of Volkswagen is defined in detail in chapter 1.1. The following subsections will highlight the two different preregistrations in the software tool in detail.

### 5.5.1. Best fit registration

If the focal point of a measurement is on the relative geometrical conditions of an object the best fit registration can be used. The best fit registration is the standard alignment of the nominal data to the actual values. The best fit alignment considers the whole generated data and its geometrical relation. It will calculate the optimal alignment of the data to each other for comparison. For most single parts or components the best fit alignment will fulfil the requirements, but if one product has more than one component of interest the best fit alignment will reach its limits. Figure 5.7 shows a measurement result of a product with different components in detail. The central component has been lifted on one side from the ground.

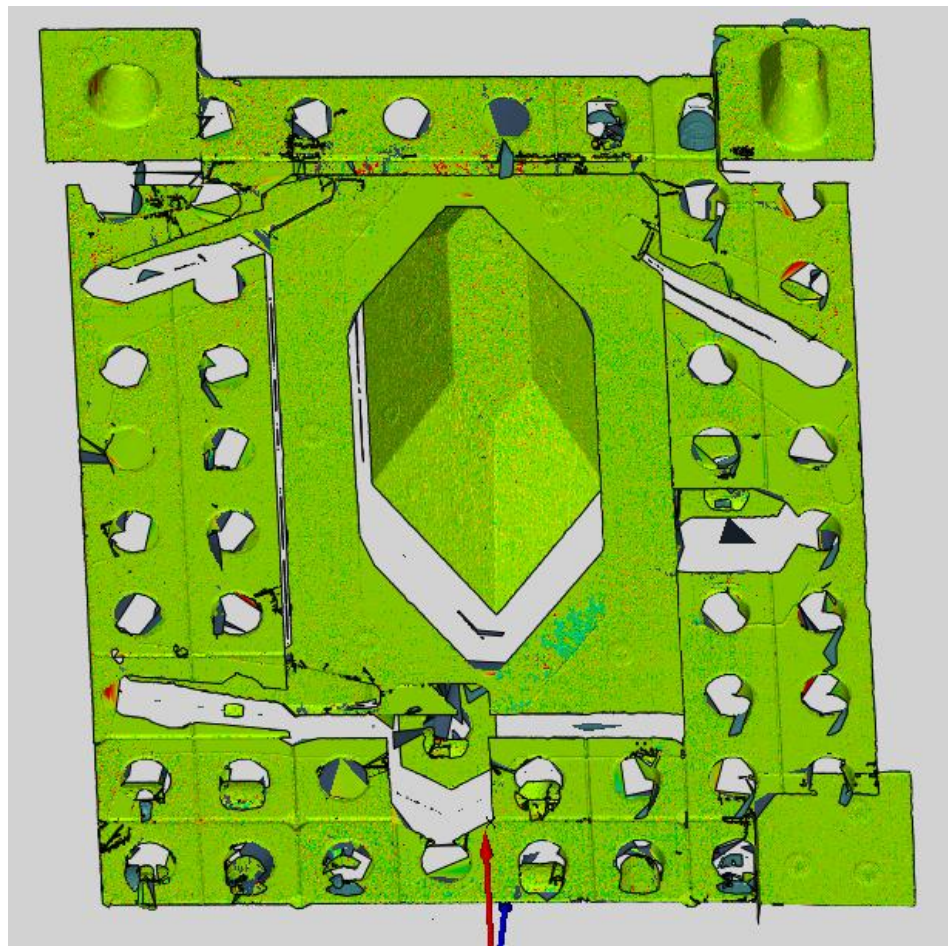
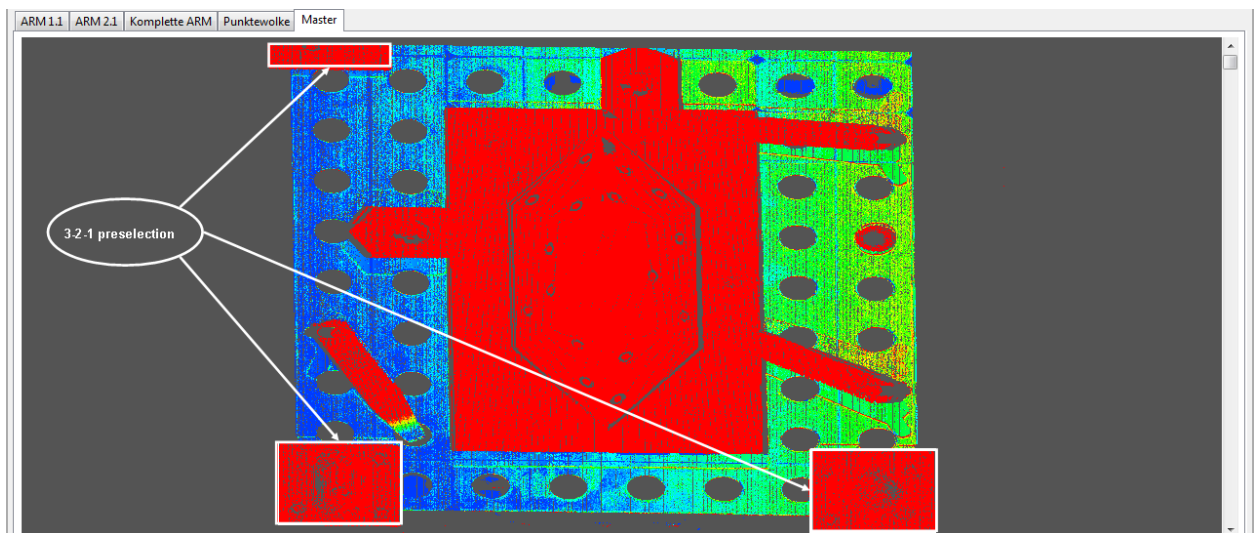


Figure 5.7: Best fit alignment

The best fit alignment will calculate the best possible concordance of the nominal and actual data. In the in Figure 5.7 shown result not only the central pattern shows deviations, whether it is the only component which changed its position. In cases where the relative orientation of different components to each other is of particular interest the best fit alignment will reach its limits.

### 5.5.2. 3-2-1 registration

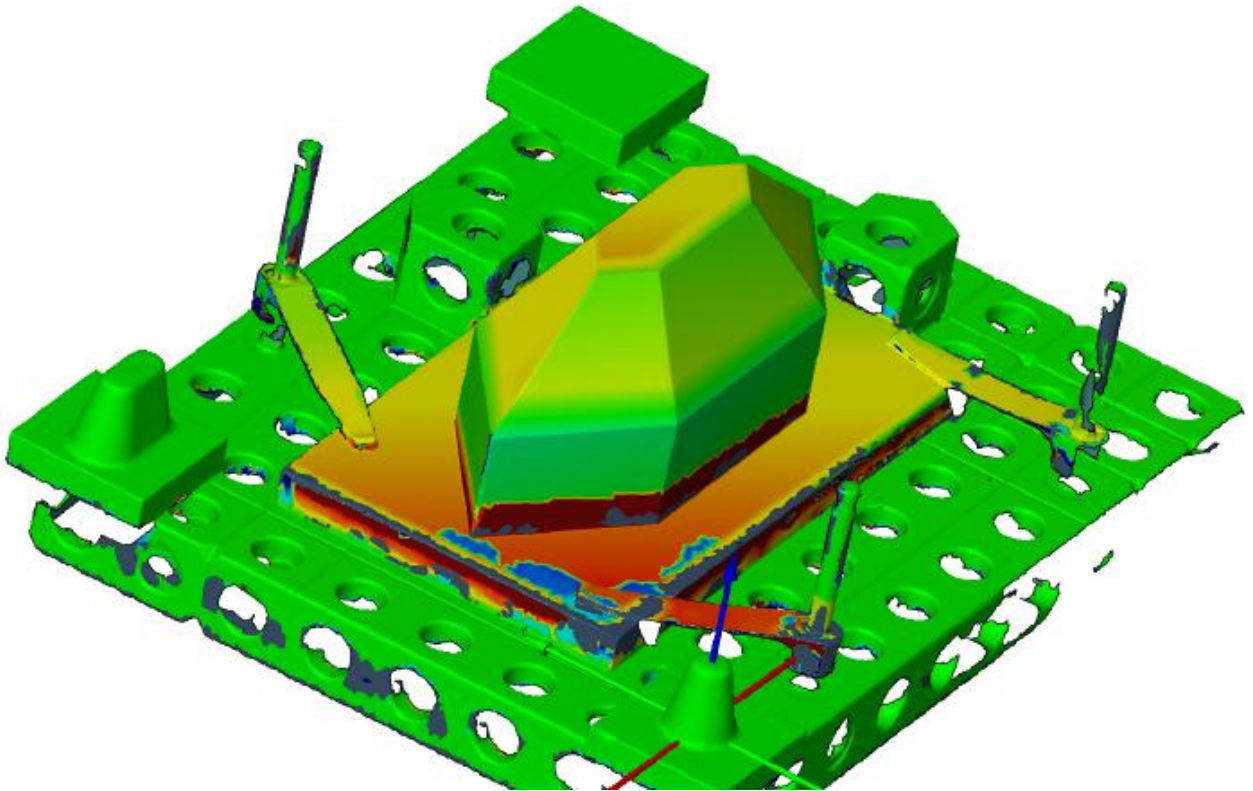
The implemented 3-2-1 registration is based on the RPS standard of Volkswagen. This form of registration has to be predefined in the software. If nominal data is selected the software tool provides the choice of alignment. Figure 5.8 shows a by the system generated cloud of point of nominal value.



**Figure 5.8: 3-2-1 preselection**

The object is identical to the in the previous chapter best fit aligned object. The operator preselects with the cursor the parts of the object which will be the basis for the future 3-2-1 alignment. In the in Figure 5.8 shown example the three marked object have been chosen for alignment purposes. If the central pattern is shifted the result will not effect these three elements but give the exact deviation of the central pattern in correlation to the preselected objects.





**Figure 5.9: Result with 3-2-1 registration**

In Figure 5.9 is the identical measurement from the best fit alignment shown. The two results only differ in their registration. It is shown in detail that the partial deviation of the whole object is highlighted indubitably. The deviations shown in the result only occurs on the central pattern, like prepared before measurements.

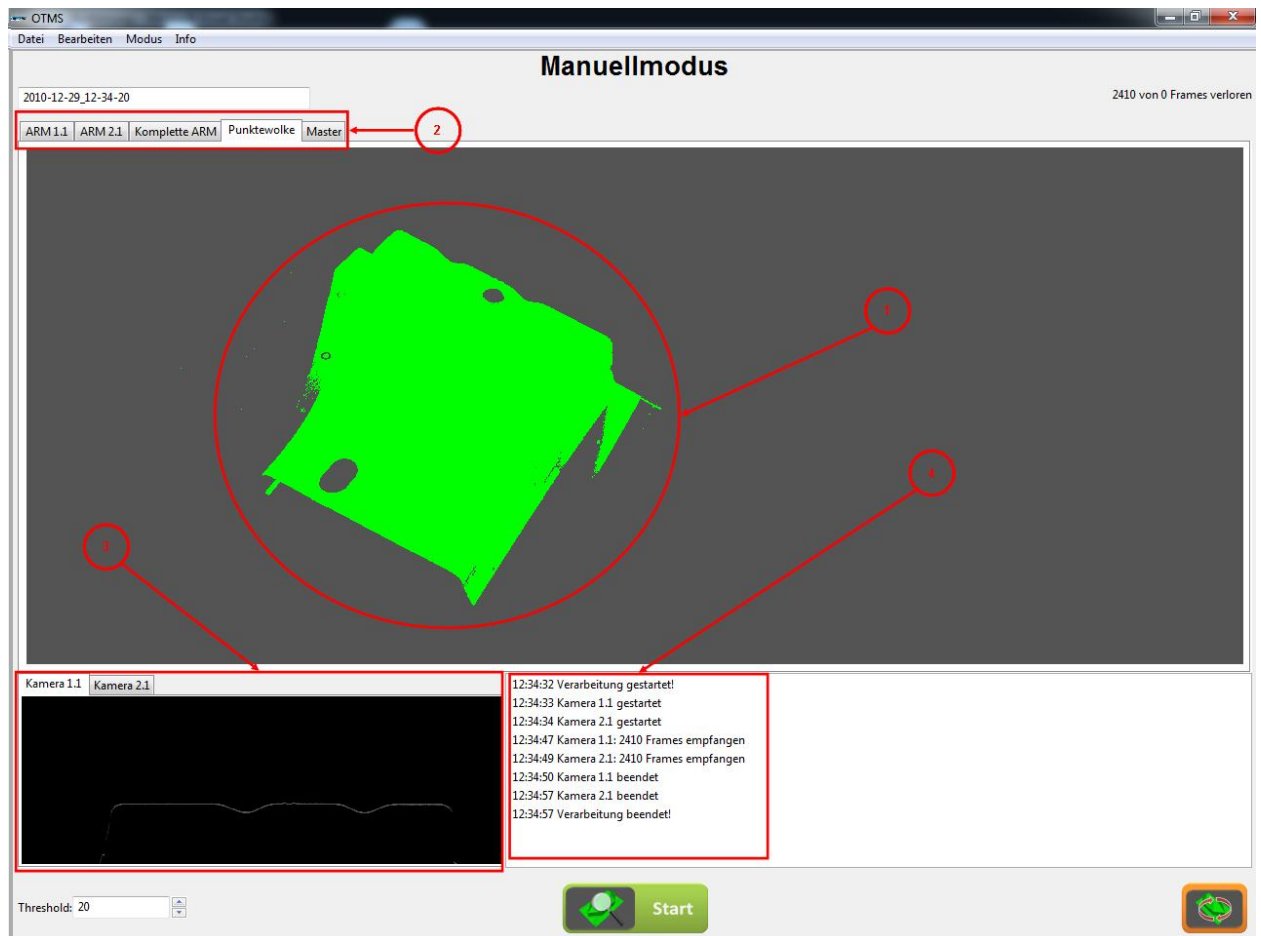
## **5.6. Measuring procedure**

The measurement system can be run in two different modes of operation. For single measurements a manual mode is available and for continuous repeating measurements the software provides an automated solution. The internal processes of calculation are identical in both modes. The difference is the automated restart function of the automatic modus. One measurement has three different phases: first the data is generated, secondly the actual data is compared to nominal values and finally the display of the result.

### **5.6.1. Manual measurements**

The manual measurement option is an implemented tool in the innovative measurement system for single measurements of objects. This mode can be used for system setup and for single measurements. Figure 5.10 shows the manual mode in detail.

If a new measurement tasks occurs or the results of the automation mode are not satisfying setup optimizations might be necessary.



**Figure 5.10: Manual mode**

The generated data is highlighted with position 1 in Figure 5.10. It is possible to check different stages of information of the object. Position 2 marks the options. There are four different options: information of the individual sensor, the merged information of all used sensors, the generated metric cloud of point and finally the aligned result of the measurement. The manual mode also gives a real time processing image from the individual sensors. Position 3 points out the real time processing image. Finally the operator receives a feedback of actual system status. Position 4 in Figure 5.10 shows the information window in detail. The system will show the actual state of each sensor and the complete measurement process.

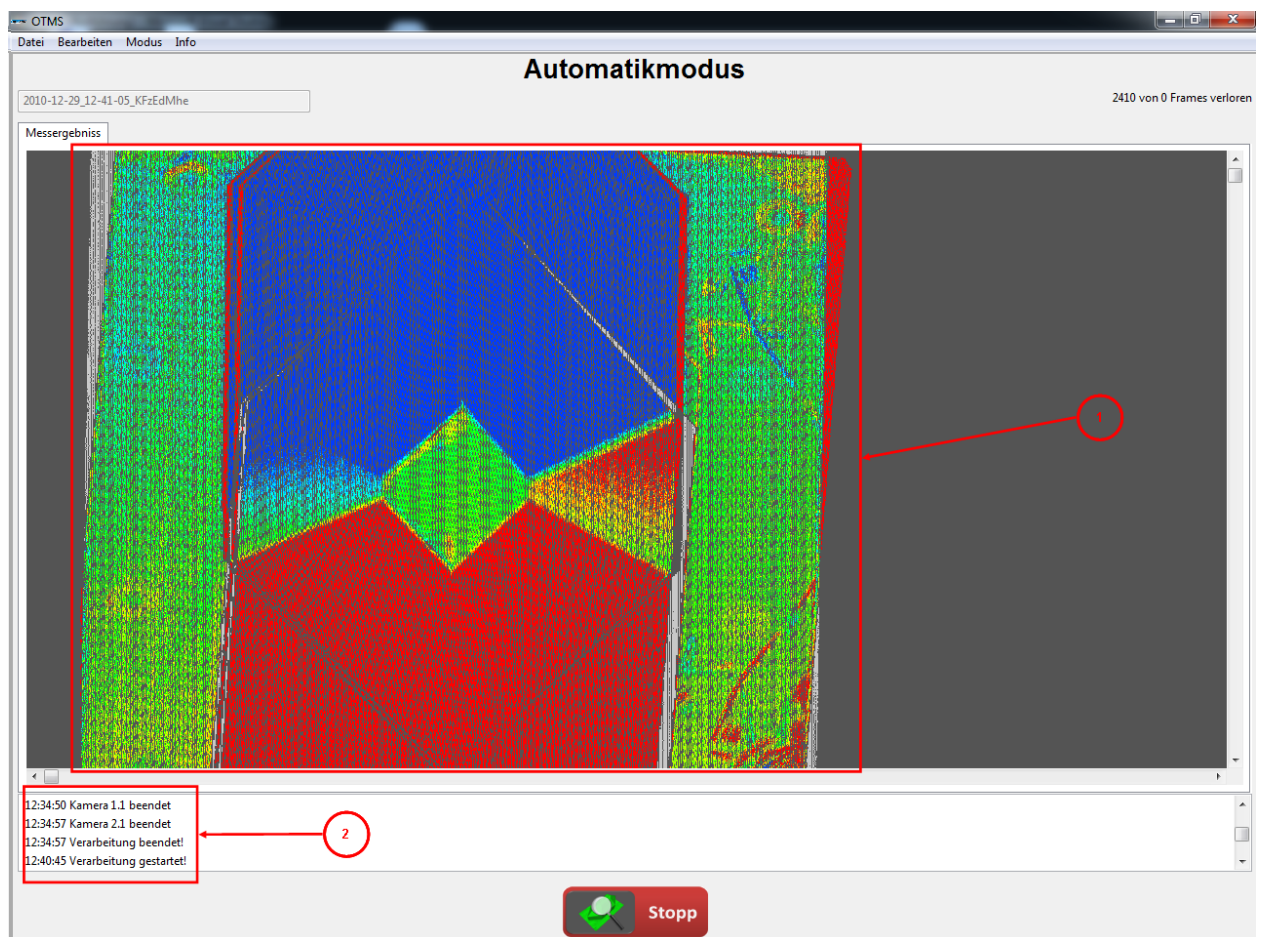
Furthermore the manual mode is designed for maintenance departments for tools. If a tool is manufactured with its geometrical values it is possible to generate three-dimensional data, which may deviate from CAD data, of the actual geometrical

conditions before it is installed into production. If after a while of production errors occur in combination with this particular tool a comparison to its initial state can be carried out. This is in particular interest for tools which are not controlled continuously.

The manual mode runs only for one sequence of received signals and has to be restarted before every measurement manually.

### 5.6.2. Automated measurements

The automatic mode is designed for continuous control of objects of interest. The graphical user interface differs from the manual mode. The graphical user interface of the automatic mode is shown in detail in Figure 5.11.



**Figure 5.11: Automatic mode**

The mode displays only two informations for the operator. One the one hand it shows the actual status of processing, marked with position 2 in Figure 5.11, and on the other hand it shows the result of the measurement in a false colours graphic, highlighted in position 1 in Figure 5.11.



The settings are set only once before the first measurement starts. The automatic mode will calculate a measurement result after every sequence of signals received. If the next sequence of signals occurs the software will restart the process automatically until the operator stops the automatic mode.

Additionally the automatic mode has the feature to handle more than one measurement task at a time. If the controller delivers additionally predefined signals the software is able to associate one signal with one measurement task. This occurs if one system measures sequentially different tools installed on one tool magazine.

The results of the measurements are continuously saved in a file. Therefore it is possible to track back creeping errors in the tool and to record the whole life cycle of one tool.

## 5.7. Display of the results

The generated data and the result of one measurement are displayed in different ways. The result of one measurement is displayed from a top view. The file is called Zmap. A typical result of a measurement is shown in detail in Figure 5.12.

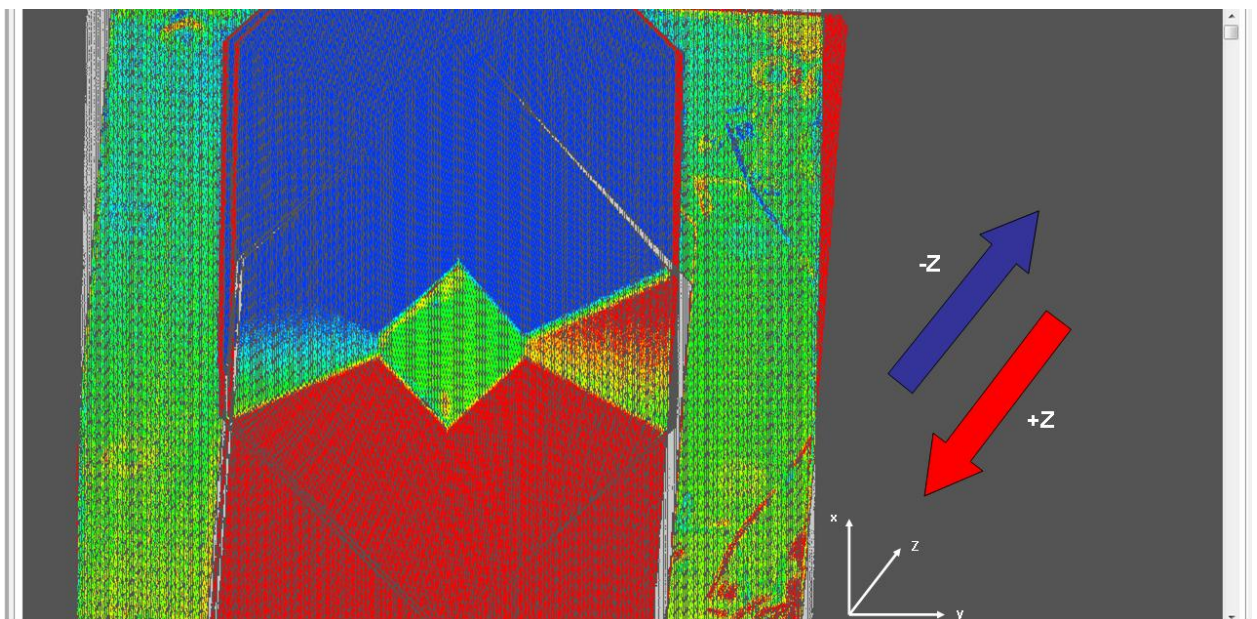


Figure 5.12: Display of Z deviation

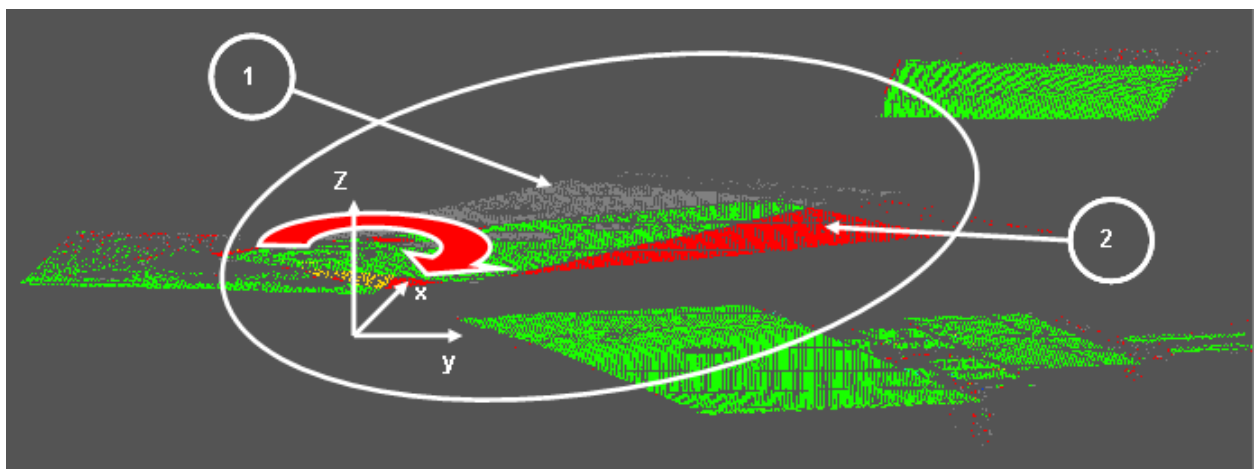
The two dimensional Zmap is a top view onto the X-Y-plane of the measurement. The third dimension is added by colouring of the result. The Zmap is a type of false colour



analysis. The result shown in Figure 5.12 includes three major colours: green, red and blue.

Green points out that there is no deviation above tolerance. If deviations occur above tolerance the area will be marked either red or blue. The blue colouration identifies a deviation in Z direction away from the perspective of the measurement sensors. Therefore the object moves away from the operator. The red colouration is the vice versa case, it highlights a deviation of the generated data of the nominal data towards the perspective of the sensors. If the operator needs metrical values of the occurring deviation the cursor will give information of every single point measured.

Furthermore errors can occur in X and Y direction. Figure 5.13 shows an example of a part distorted around the axis. The distortion will lead into a change of generated Z information around the object. Position 1 highlights in the example the area where Z information had been given before distortion. Since there cannot be generated no information it is classified as no information given and marked light grey.



**Figure 5.13: Display of X-Y deviation**

Position 2 in Figure 5.13 highlights the area of super saturation. Due to the distortion around the Z axis the component is detected and information is generated in an area where no nominal value is given. This is identified by the system and classified as information which comes towards the sensors and marked red.

So far the software cannot classify distortions directly, it highlights only the changes of Z in the X-Y plane. Therefore the operator has to be able to classify the by the system identified errors.

## 6. Testing and data analysis

The testing of the system focuses on different tasks. The testing will give information if the system will be able to generate adequate results in production conditions. Furthermore it will clarify if installed industrial robots can be used for measurements or if additional equipment has to be used. Finally the results will point out the achievable accuracies under the given circumstances. The following subsections will describe in detail how measuring results have been generated for further analysis and evaluation of the system accuracy. The measurements occur in the in chapter 4.1 described production cell. The measured test object is a pattern which also can be used for calibration purposes.

### 6.1. Test setup

The measurement system is installed in the production cell of the Volkswagen AG. For testing purposes an additional testing cycle is programmed in the robot control. In order to generate ideal measurement conditions the system and robot setup have to be in ideal conditions, too. System cooperation setup focuses on three major topics: focal distance, angle between robot and sensors and parallelism. Figure 6.1 shows exemplary the constellation of sensor and object. If the object is orientated parallel, the sensor will be able to generate the most data. If the object is not parallel as highlighted in case 2 in Figure 6.1, certain areas of the object can be invisible to the sensor and therefore no data can be generated.

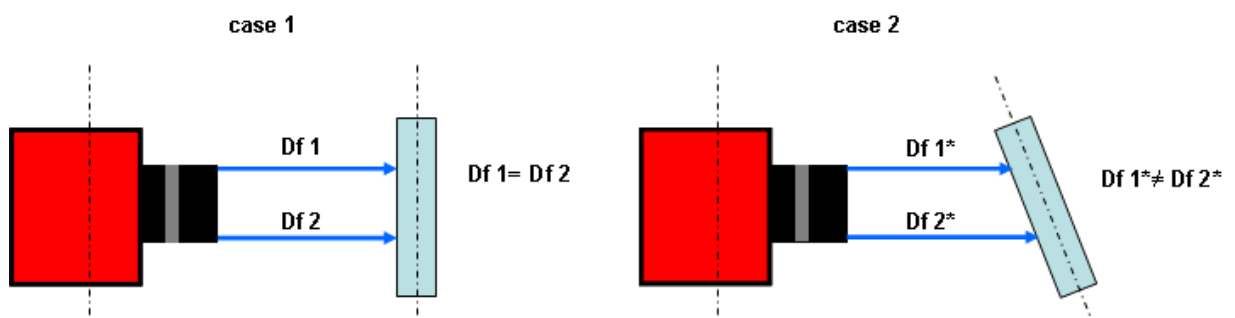
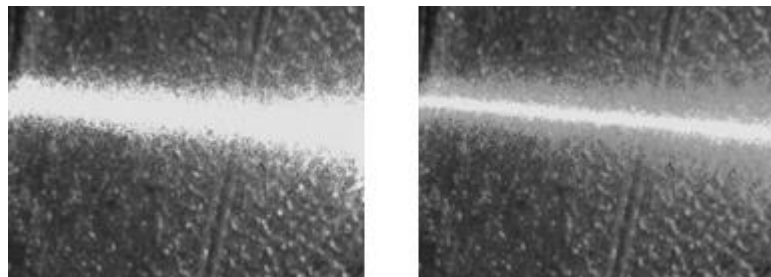


Figure 6.1: Angle between sensor and object

The identical parallelism is required in the moving direction of the robot. If deviations occur from a parallel movement, areas of the measured object can be invisible to the

sensors. Therefore no data will be generated and a lack of information occurs in the analysis of the data.

Another aspect for ideal measurements is the focal distance of the laser module and the sensors. Figure 6.1 shows the effect of dumping to the focal length. If the difference in the distance reaches a certain limit, measurements will be inaccurate. The range of focal distance depends on the used sensor and the focal length of the optical lenses. Furthermore has the laser module an ideal focal distance for an optimum laser line projection. If the distance between the measured object and the laser module is not within the depth of field of the laser module the line will not be sharp. This will lead to inaccuracy in the measuring process.



**Figure 6.2: Focusing of laser line**

Figure 6.2 shows the effect of focusing of the laser line. Both shots are from the identical sensor and the identical object. If the object is not within the depth of field of the sensors and the laser module the projection is not sharp and the projection becomes blurred.

## **6.2. Test object**

For testing a known geometrical constellation is used. The calibration pattern is installed into the grab of the robot and its dimensions are known in detail. The manufactured pattern was measured with the optical GOM ATOS scanner. The result is shown in detail in Figure 6.3. The analysis focuses on the position of the twelve major design points of the pattern. The nominal values are shown in detail in Appendix F.

The twelve points are shown with their XYZ position in the pattern. There are minor deviations appearing from manufacturing inaccuracies which will be neglected in the later verification of the results. The complete result of the ATOS measurement is shown in detail in Appendix G.

The pattern is manufactured with a synthetic material. The temperature strain of the material is minimal. The material is stiff with a faint white surface, which on the one hand reflects enough illumination and on the other hand does not absorb the light and shines from within the material.

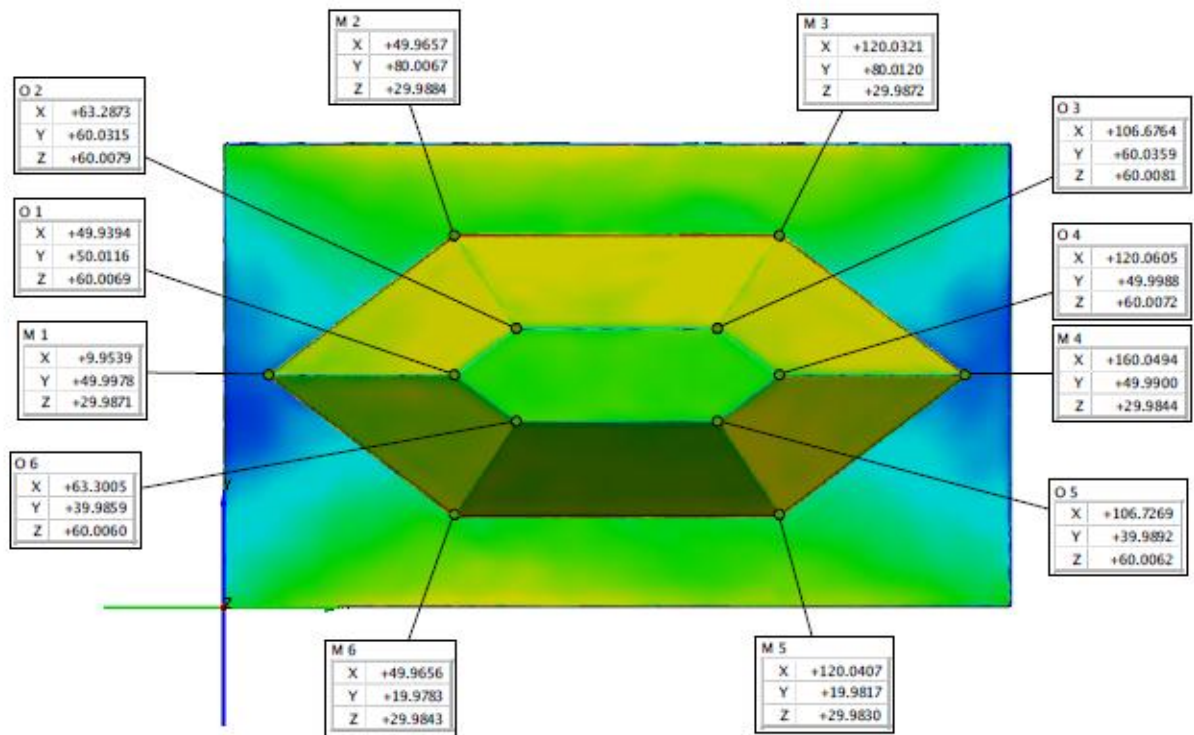
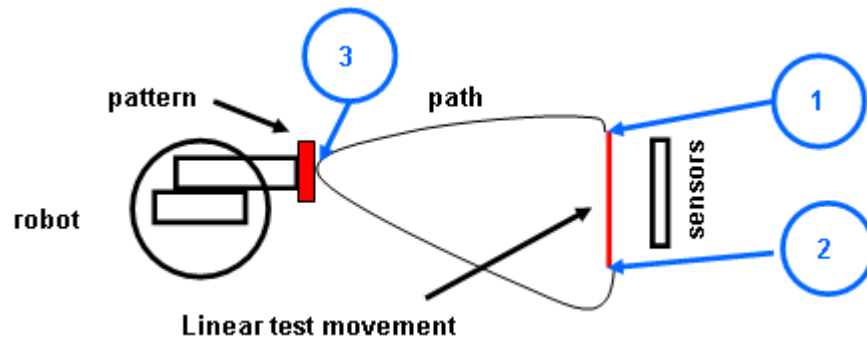


Figure 6.3: ATOS measurement result

### 6.3. Testing procedure

The robot repeats its programmed testing cycle continuously. The robot grab does not handle a part during measurements. The programmed robot path is shown schematic in Figure 6.4. The robot reaches point 1 with a not linear point to point movement. The distance between point 1 and point 1 performs the robot in a linear movement. Due to the ramp effect the linear movement is started before the first reflexion of the object of interest is detected by the sensors. In chapter 3.1.3 the different types of movement are explained in detail.



**Figure 6.4: Scheme of robot test cycle**

The robot provides a real time position signal for the period of linear movement in between point 1 and point 2. The signal is provided on a port of the robot controller which is connected to the designed atmel controller. After passing point 2 in Figure 6.4 the robot switches back to point to point movement and aims for its home position. The home position of the robot is highlighted with position 3 in Figure 6.4. In the home position the robot will stay in a hold position for five seconds before it repeats the test cycle.

The sensor and the laser module are only activated if the robot performs its linear movement. In this period the sensors generate triggered to the movement of the robot pictures of the projected laser line. If the robot leaves the linear mode the trigger signal is deactivated and the computer starts processing. The generated three- dimensional information are aligned with the nominal data and displayed as false colour graphic for the operator of the system. The generated data is saved in different file format. The procedure restarts with the next provided signal of the robot.

## **6.4. Data transformation**

The system generates three-dimensional information of an object. Mathematically describes the system every measured point with its three-dimensional coordinates individually. In further processes the sum of the generated punctual information is transferred into a cloud of points. For further analysis and validation of the generated data it has to be transferred into standard files.

In order to be able to analyse the system with the GOM Inspect professional tool the data is in the first step transferred into the American standard code for information interchange (ASCII). This format can be imported in common analyse tools from

different companies. With the GOM Inspect professional a polygonisation of the data is possible. The polygonized data can be inspected and analysed. For further processes the data is saved as a stereolithography file (STL). An STL file describes a raw unstructured triangulated surface by the unit normal and vertices of the triangles using a three-dimensional Cartesian coordinate system.

## 7. Verification of results

This chapter and its subsections will identify the received measurement results and point out the possible mistakes occurring in the measurements. Furthermore it will highlight the theoretical error determination and discuss possible reasons.

### 7.1. Points of interest for analysis

The system is integrated into the production for three-dimensional measurements. For the evaluation of the generated data the consideration of off all three measured axes is required. The measured pattern is designed with twelve defined points. These twelve points are in a particular interest for inspection. The position and the distances between these points will be informative for achievable accuracies in all three dimensions.

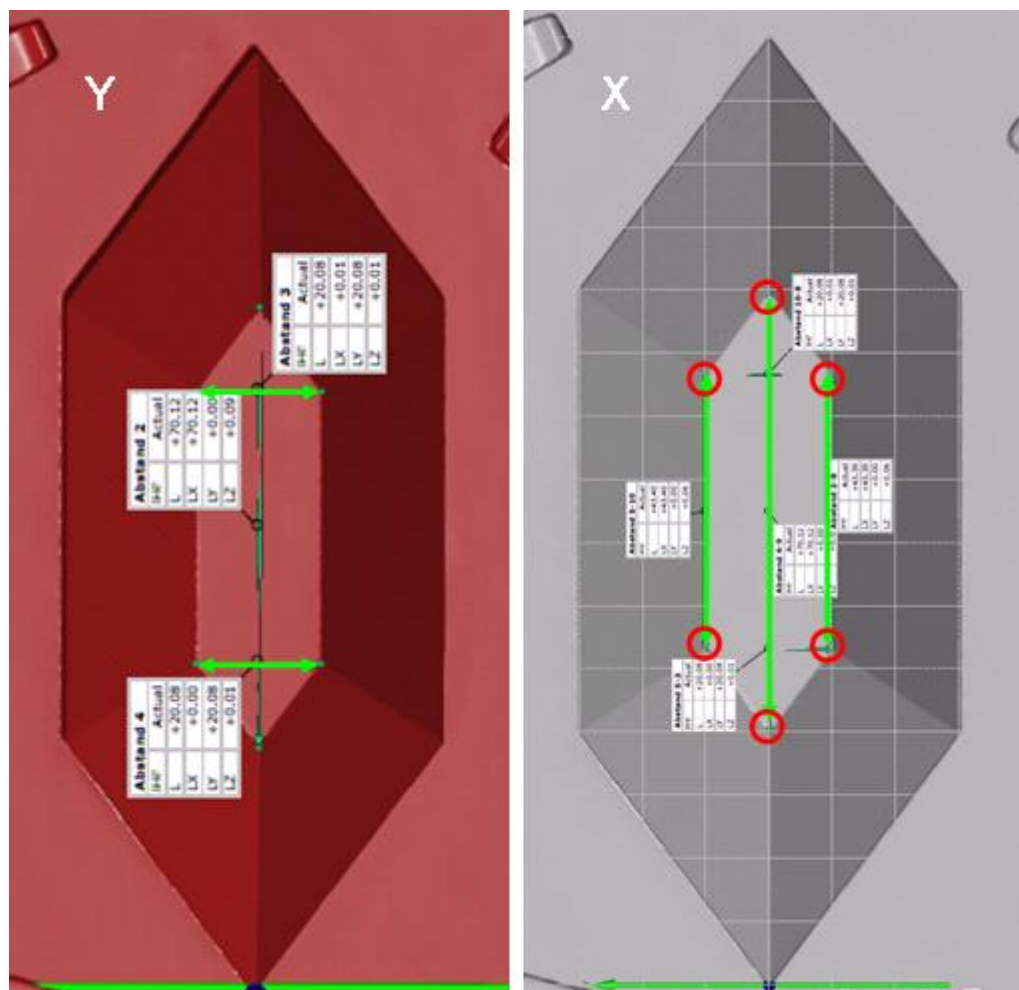


Figure 7.1: Points of interest

Figure 7.1 shows in detail the dimensions of the pattern which will be used for the evaluation of the results. The focus is on the six defined upper points of the pattern. The

six points will be analysed in their Z position. Furthermore will be the distance in between the points be calculated and compared to nominal values. The left hand part of Figure 7.1 shows the distances which will be considered for the evaluation of the Y dimensions. On the other hand the distances highlighted in the right part of Figure 7.1 will be considered for the evaluation of the X distances. The distances in X direction are from particular interest since this is the direction of relative movement between the measured object and the installed sensors.

## **7.2. Errors**

If data is generated in measurements errors might occur. The analysis considers three different types of errors; gross errors, accidental errors and systematic errors (Ait Tahar 2008). Gross errors are the types of errors which should be eliminated before an evaluation of results take place. The appearance of gross errors is in majority caused by operator errors, defects or unsuitable equipment or significant errors in the analysis of the generated data. If gross errors appear measurements or analysis will have to be repeated. Gross errors have to be identified by the operator and are neglected in the statistical analysis (Ait Tahar 2008).

The second type of error is the systematic error. Systematic errors manipulate the result of a measurement under identical conditions consistently in the same way (Hempel 2010). Systematic errors are identical in value and algebraic sign, therefore not to identify by repeating the measurement. Systematic errors can be caused by the usage of wrong equipment, leaving operational limits of equipment and ambient conditions. Systematic errors can be eliminated partly. In the evaluation of the results these errors will be identified.

Finally occur in measurements accidental errors. Even if all systematically caused errors are eliminated will the results of measurements of the same physical value vary. The achieved results will be located in a certain range of the true value. These deviations are considered in the statistical analysis.

## **7.3. Theoretical evaluation of measurements**

In order to evaluate the generated data and the accuracy of the system a statistical analyses is carried out. The statistical analysis with its tools of standard deviation and



average value is used for specifying the innovative measurement strategy. In order to evaluate the data different formulas are required. The statistical analysis concentrates on the single measurement  $x_i$ , the arithmetic average value  $\bar{x}$ , the standard deviation for a single measurement  $s_x$ , the standard deviation for a series of measurements  $s_{\bar{x}}$ , the confidence level  $\gamma$  and the confidence interval  $\vartheta$  and Gaussian error propagation. In the following the mentioned factors of the statistical analysis will be described in detail and the formulas for calculation will be pointed out.

The arithmetic average  $\bar{x}$  is calculated from a series of measurements in order to achieve the optimal value of measured data. The arithmetic average  $\bar{x}$  can be calculated with Equation 7:1:

$$\bar{X} = \frac{1}{n} \cdot \sum_{i=1}^n X_i$$

**Equation 7:1: Arithmetic average (Blüm 2002)**

The arithmetic average  $\bar{x}$  is calculated with the sum of all individual measurement results divided by the number of measurement considered in the calculation.

The standard deviation  $s_x$  defines the spreading of the result from a single measurement. Within a series of at least ten measurements the standard deviation  $s_x$  indicates the deviation of a single measurement from the arithmetic average (Kähler 2008). Equation 7:2 shows the formula for calculation in detail.

$$s_x = \sqrt{\frac{\sum_{i=1}^n (X_i - \bar{X})^2}{n-1}}$$

**Equation 7:2: Standard deviation (Bourier 2011)**

The standard deviation  $s_x$  of a series of measurements can be calculated by taking the square root of the deviation of a single measurement from the arithmetic average  $\bar{x}$  and sum them up. The sum will be divided by the number of measurements minus one and finally the square root of this result will lead to the standard deviation  $s_x$ .

Furthermore the standard deviation for a series of measurement  $s_{\bar{x}}$  has to be identified. It indicates the standard deviation of the average value. It correlates to the standard deviation by the factor  $\frac{1}{\sqrt{n}}$ . The standard deviation of the average value  $s_{\bar{x}}$  can be determined with Equation 7:3:

$$s_{\bar{x}} = \frac{s_x}{\sqrt{n}} = \sqrt{\frac{\sum_{i=1}^n (X_i - \bar{X})^2}{n(n-1)}}$$

**Equation 7:3: Average deviation (Papula 2003)**

With the standard deviation  $s_x$  it is possible to define an interval of confidence  $\vartheta$  in which a certain percentage of the measured values is expected. The interval of confidence  $\vartheta$  depends on the standard deviation  $s_x$  and additionally on the level of confidence  $\gamma$ . The level of confidence  $\gamma$  describes the probability of how many of the expected results will lie within the defined interval of confidence  $\vartheta$ . The level of confidence  $\gamma$  varies from 68.3 percent up to 99 percent (Papula 2003). The interval of confidence  $\vartheta$  can be calculated with Equation 7:4:

$$\vartheta = \bar{x} \pm t \cdot \frac{s_x}{\sqrt{n}} = \bar{x} \pm t \cdot \sqrt{\frac{\sum_{i=1}^n (X_i - \bar{X})^2}{n(n-1)}}$$

**Equation 7:4: Interval of confidence (Papula 2003)**

In Equation 7:4 the formula shows the involved parameters in detail: from the arithmetic average  $\bar{x}$  the product of the factor  $t$ , which correlates to the level of confidence  $\gamma$  and is shown in detail in Table 4 and the standard deviation  $s_x$  is either added or subtracted.

**Table 4: Level of confidence (Papula 2003)**

number of measurements	level of confidence (%)			
	68.3	90	95	99
2	1,84	6,31	12,71	63,66
5	1,15	2,13	2,78	4,00
10	1,06	1,83	2,26	3,25
50	1,01	1,68	2,01	2,68
100	1,00	1,66	1,98	2,63
infinite	1,00	1,65	1,96	2,58

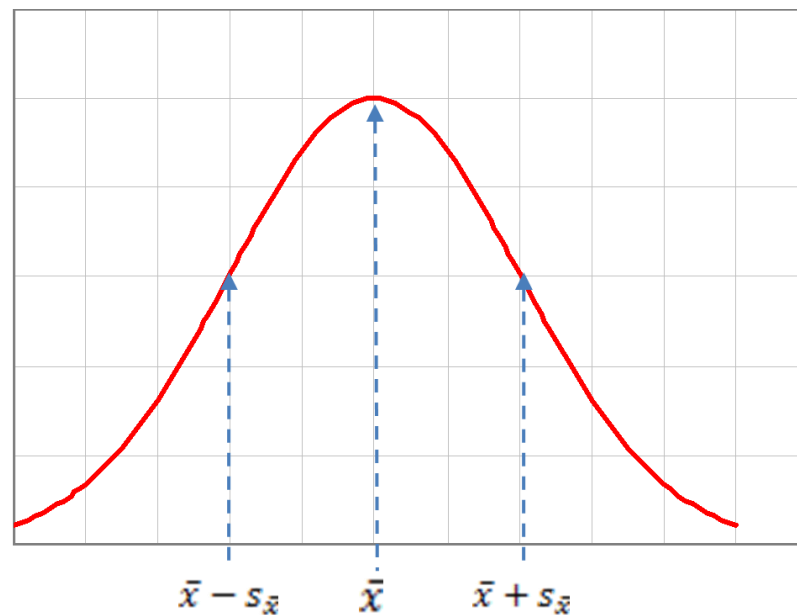
Table 4 shows the involved factor  $t$  for the calculation of the interval of confidence  $\vartheta$  for a defined number of measurements.

The results of measurements are given in the form  $x = \bar{x} \pm s_{\bar{x}}$ . The expected results of measurements can be described with the Gaussian distribution curve. The Gaussian distribution curve visualizes the correlation of the individual measurement to the nominal value. It describes the result density for a nominal value and a infinitive number of measurements. The distribution curve is defined with Equation 7:5:

$$\varphi(x) = \frac{1}{\sqrt{2\pi}s_x} \cdot e^{-\frac{1}{2}\left(\frac{x-\bar{x}}{s_x}\right)^2}$$

**Equation 7:5: Gaussian distribution curve (Papula 2003)**

Figure 7.2 shows exemplarily a Gaussian distribution curve of any measurement in detail. Highlighted are the measurement result  $\bar{x}$  and the standard deviation  $s_{\bar{x}}$ .



**Figure 7.2: Gaussian distribution curve**

It is not always possible to calculate the deviations of a system in the three-dimensional space directly. The measured values do not directly depend on each other and have accidental independent deviations. The inaccuracy of the complete system including all independently occurring individual deviations can be generated with the Gaussian error propagation. The Gaussian error propagation considers the individual deviation and

calculates a general deviation for the complete system. The error propagation is shown in detail in Equation 7:6:

$$\Delta G = \sqrt{\left(f_{x_1} \Delta x_1\right)^2 + \left(f_{x_2} \Delta x_2\right)^2 + \dots + \left(f_{x_n} \Delta x_n\right)^2}$$

**Equation 7:6: Gaussian error propagation (Papula 2003)**

The in Equation 7:6 shown equation allows the computation of the total deviation of the system in the three- dimensional space by considering the individual deviations of the axes.

## 7.4. Analysis of measurements

In the following sub sections a statistical analysis of the in chapter 7.1 described points of interest will be prosecuted. In the following inspection and theoretical analysis the three axes of the coordinate system are considered individually.

### 7.4.1. Arithmetic average of measurements

The calculation of the arithmetic average is shown only exemplarily since there have been 180 measurements carried out. The values are calculated with Equation 7:1. The prepared table of the results for the points of interest is shown in detail in Appendix H.

$$\begin{aligned}\bar{X} &= \frac{1}{n} \cdot \sum_{i=1}^n X_i \\ \bar{X} &= \frac{1}{540} \cdot \sum_1^{540} X_i \\ \bar{X} &= \frac{1}{540} \cdot 23128.80 \\ \underline{\underline{\bar{X} &= 42.83}}\end{aligned}$$

The arithmetic averages for the X,Y and Z coordinates are shown in detail in Table 5.

**Table 5: Arithmetic average**

Coordinate axis	abreviation	X	Y	Z
Arithmetic average	$\bar{x}$	42.831	19.951	60.002

#### 7.4.2. Standard deviation

With the in chapter 7.3 shown Equation 7:2 and Equation 7:3 the standard deviation and the deviation of the average is calculated. One calculation is shown exemplarily. The example is calculated with the generated Y data. First the standard deviation is calculated:

$$s_y = \sqrt{\frac{\sum_{i=1}^n (Y_i - \bar{Y})^2}{n-1}}$$

$$s_y = \sqrt{\frac{\sum_{i=1}^{360} (Y_i - \bar{Y})^2}{360-1}}$$

$$\underline{\underline{s_y = 0.01725}}$$

In the 180 measurements have been 360 information for the Y coordinate been generated. In the calculation the deviation from every single measurement to the arithmetic average is being considered.

Based on the calculations of the standard deviation the deviation of the arithmetic average can be calculated:

$$s_{\bar{y}} = \frac{s_y}{\sqrt{n}} = \sqrt{\frac{\sum_{i=1}^n (Y_i - \bar{Y})^2}{n(n-1)}}$$

$$s_{\bar{y}} = \frac{0.01725}{\sqrt{360}}$$

$$\underline{\underline{s_{\bar{y}} = 0.00091}}$$

Table 6 shows the results of the calculation of the standard deviation and the deviation of the arithmetic average in detail.

**Table 6: Standard deviation and deviation of average**

Coordinate axis	abbreviation	X	Y	Z
Arithmetic average	$\bar{x}$	42.831	19.951	60.002
Standard deviation	$s_x$	0.30605	0.01725	0.04082
Deviation of average	$s_{\bar{x}}$	0,01317	0,00091	0,00124

The calculated deviations in Table 6 show in detail on the one hand that there are only minor deviations in the Y and Z coordinates of the system but on the other hand the most deviations occur in X direction. In this coordinate system the X direction is the direction of movement. Furthermore the results lead to the result of a series of measurements X,Y,Z:

$$X = (42.831 \pm 0.01317) \text{ mm}$$

$$Y = (19.951 \pm 0.00091) \text{ mm}$$

$$Z = (60.002 \pm 0.00124) \text{ mm}$$

and for one single measurement x, y, z:

$$x = (x_i \pm 0.30605) \text{ mm}$$

$$y = (y_i \pm 0.01725) \text{ mm}$$

$$z = (z_i \pm 0.04082) \text{ mm}$$

#### **7.4.3. Interval of confidence**

The interval of confidence can be calculated with Equation 7:4. Depending on the level of confidence the interval of confidence will vary. The calculation is shown exemplarily and the results of all calculations are shown in Table 7: Interval of confidence for different level of confidence. The interval of confidence is calculated for three different levels of confidence: 68.3 percent, 95 percent and 99 percent. In the example the Z coordinate is considered and 68.3 percent of the results are supposed to be in the interval of confidence, therefore the factor  $t=1$ :

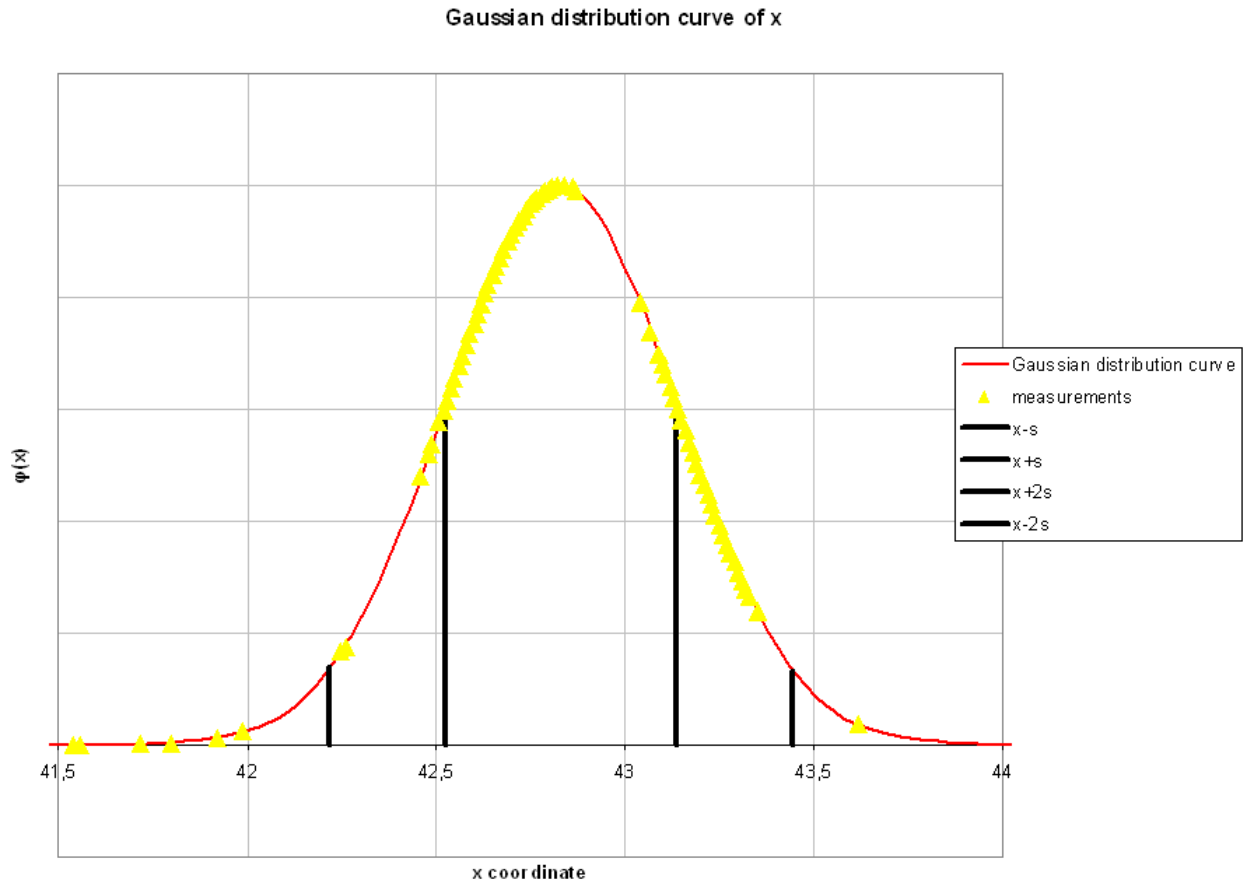
$$\begin{aligned}
\vartheta &= \bar{z} \pm t \cdot \frac{s_z}{\sqrt{n}} = \bar{z} \pm t \cdot \sqrt{\frac{\sum_{i=1}^n (Z_i - \bar{Z})^2}{n(n-1)}} \\
\vartheta &= \bar{z} \pm t \cdot \frac{s_z}{\sqrt{n}} \\
\vartheta &= 60.002 \pm 1 \cdot \frac{0.04082}{\sqrt{1080}} \\
\vartheta &= \underline{\underline{60.002 \pm 0.00124}}
\end{aligned}$$

Table 7: Interval of confidence for different level of confidence shows the results of the calculation of the interval of confidence in detail.

**Table 7: Interval of confidence for different level of confidence**

Coordinate axis	abbreviation	X	Y	Z
<b>Arithmetic average</b>	$\bar{x}$	42.831	19.951	60.002
<b>Standard deviation</b>	$s_x$	0.30605	0.01725	0.04082
<b>Deviation of average</b>	$s_{\bar{x}}$	0,01317	0,00091	0,00124
<b>confidence of 68%</b>	t=1	0,01317	0,00091	0,00124
<b>confidence of 90%</b>	t=1.98	0,02608	0,00180	0,00246
<b>confidence of 99%</b>	t=2.63	0,03464	0,00239	0,00327

With the calculated results it is possible to generate the Gaussian distribution curve. The curve describes the majority of the perspective measurement results considering the arithmetic average and the standard deviation of the measurements.

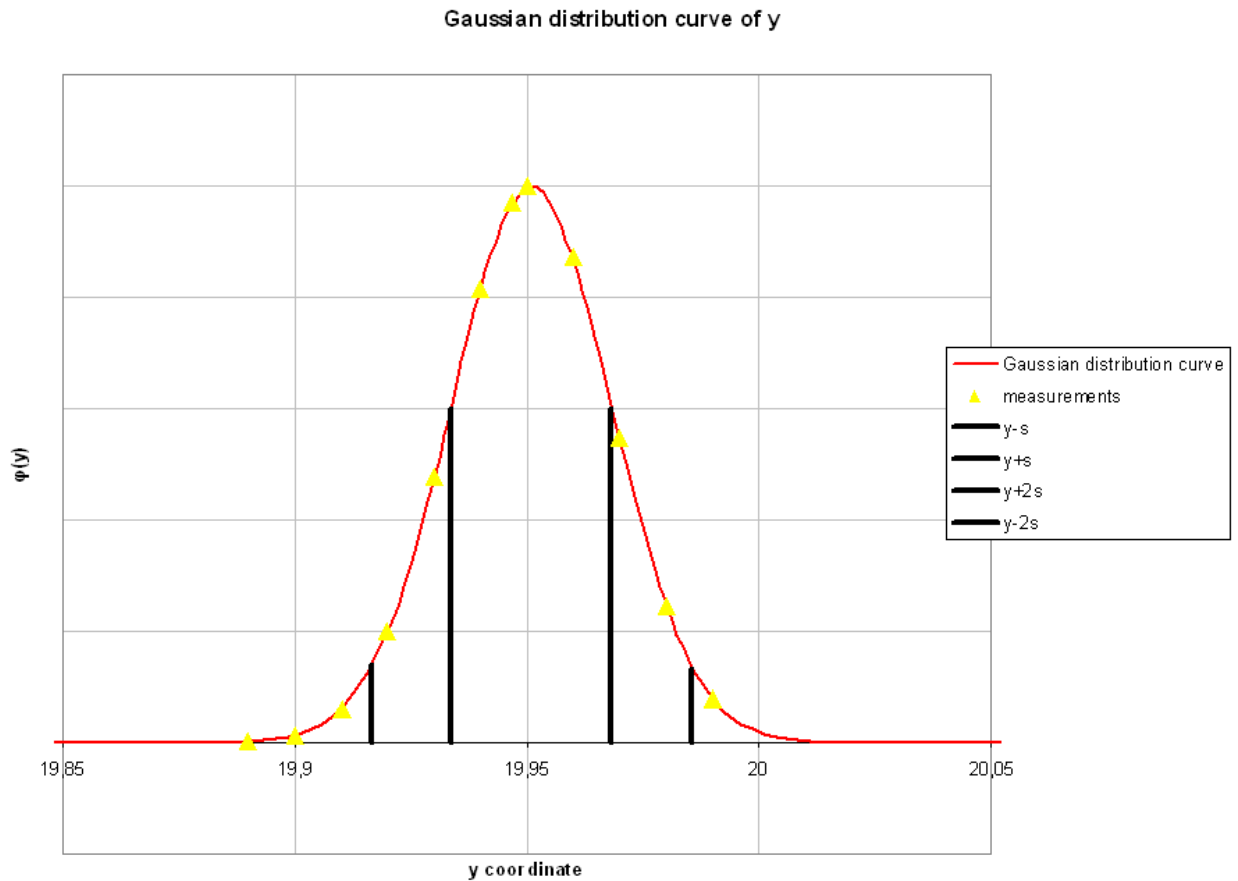


**Figure 7.3: Gaussian distribution curve x**

Figure 7.3 shows the Gaussian distribution curve for the series of measurements of X. The majority of the generated is located within the distribution curve. Most of the data is spread along the curve. The results differ in minimal values. Furthermore are the intervals of confidence for 68 percent and for 95 percent of the measurements highlighted in the figures.

Additionally the Gaussian distribution curve is generated for the measurement results of Y and Z.

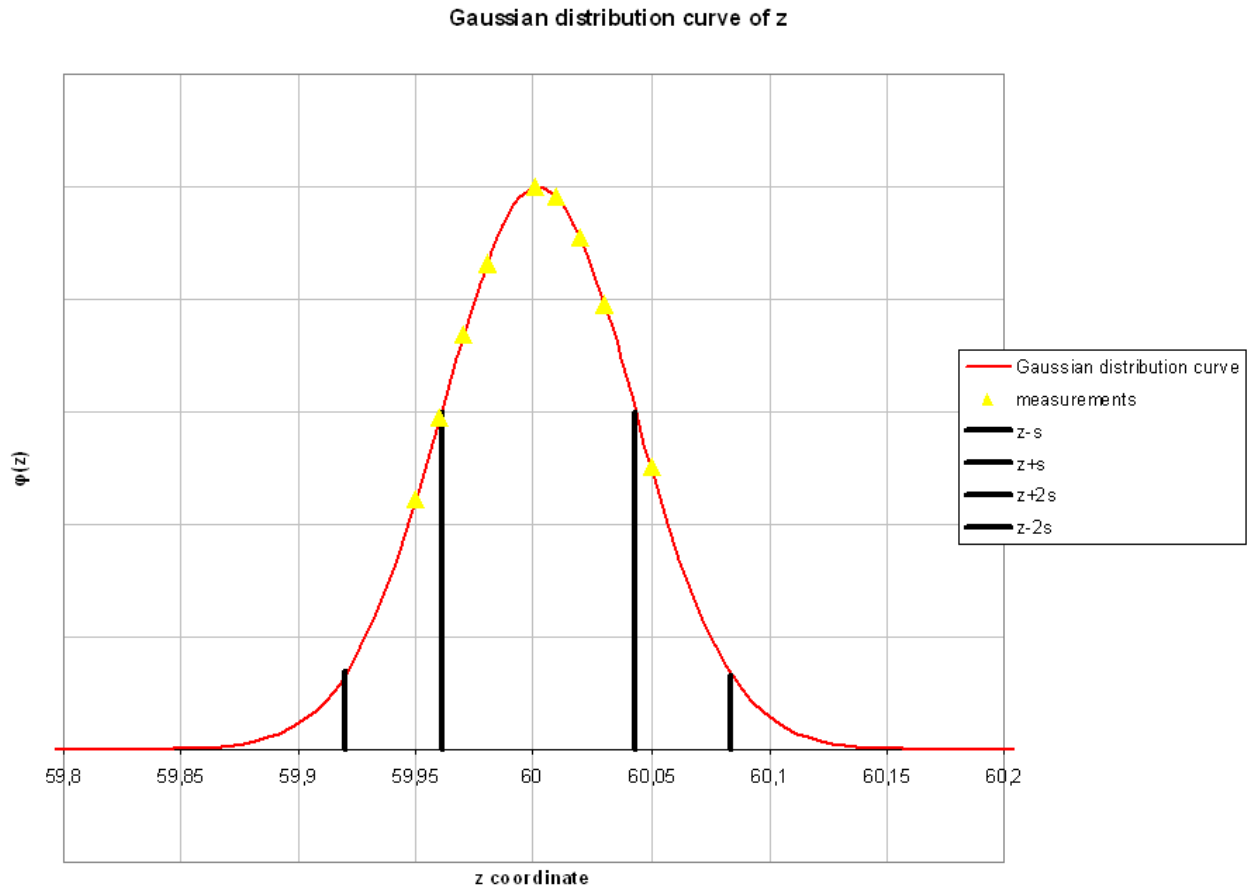




**Figure 7.4: Gaussian distribution curve Y**

Figure 7.4 shows the generated Gaussian distribution of the measured Y coordinate. Compared to the distribution curve of the X axis the results of the individual measurements are not spread along the curve but located in groups along the Gaussian distribution curve. The interval of confidence is in its modulus less than the interval of confidence of the X coordinate.

Figure 7.5 shows the Gaussian distribution curve for the measurements of the Z coordinate. As seen before in Figure 7.4 the measured values are located in little groups along the distribution curve. Furthermore has the standard deviation the smallest modulus of all three axes and therefore is the interval of confidence the smallest. As shown in detail in Figure 7.5 are the majority of the measured results are either within or close to the interval of 68 percent.



**Figure 7.5: Gaussian distribution curve Z**

The three distribution curves give an overview of the deviations of the individual axes. They show in detail the appearing spreading of the individual measurements and the expected spreading of results with the Gaussian distribution curve.

#### 7.4.4. Total deviation in three- dimensional space

The total deviation can be calculated with the Gaussian error propagation, which is shown in detail in chapter 7.3. The calculation will be prosecuted for the measurement series as well for an individual measurement:

$$\Delta G = \sqrt{(f_{x_1} \Delta x)^2 + (f_y \Delta y)^2 + (f_z \Delta z)^2}$$

$$\Delta G = \sqrt{(0,30605)^2 + (0,01725)^2 + (0,04082)^2}$$

$$\underline{\underline{\Delta G = 0,30924}}$$

The total deviation  $\Delta G$  for an individual measurement is  $\Delta G = 0,30924$ . For a series of measurements the total deviation  $\Delta G_s$  can be calculated with the identical formula:

$$\Delta G_s = \sqrt{(f_{x_i} \Delta x)^2 + (f_y \Delta y)^2 + (f_z \Delta z)^2}$$
$$\Delta G_s = \sqrt{(0,01317)^2 + (0,00091)^2 + (0,00124)^2}$$
$$\underline{\underline{\Delta G_s = 0,01326}}$$

The total deviation  $\Delta G_s$  in the three-dimensional space for the series of measurements with the innovative system is  $\Delta G_s = 0,01326$ .

The calculated total deviation considers only the relative error of the system, the absolute error of the measurements is neglected in this theoretical analysis.

## 8. Conclusion

The verification of the results shows the capabilities and limits of the innovative measurement strategy in detail. The innovative system is capable of generating three-dimensional information of objects of interest. The measurements have been fast and efficient. The time period for internal analysis of the generated data and their preparation for display to the operator is neglectable small.

The theoretical inspection of the data shows different results. Therefore the results for each axis will be discussed individually before finally the total deviation and the deviation from nominal data will be discussed.

The biggest deviations occurred in the X axis. This is the axis of relative movement between the measured object and the sensors installed into the production cell. The standard deviation of this axis is  $\underline{s_x = 0.30605\text{mm}}$ . This large deviation, compared to the deviations of the other axes, can be caused by different factors. The accuracy of the X axis depends on the one hand from the constancy of movement of the industrial robot and on the other hand on the density of profiles generated per moved distance. The deviation of the average for the series of measurement proofs the influence of the robot to be minimal. The deviation of the average reaches with  $\underline{s_x = 0.01317\text{mm}}$  almost the results of the other axes. Therefore the movement of the industrial robot can be seen as almost constant and the synchronisation of the movement and the trigger as accurate enough. More effect on the accuracy will have the density of the profiles generated per moved distance.

The Y axis reaches a deviation of  $\underline{s_y = 0.01725\text{mm}}$  for an individual measurement and a deviation of average for all measurements of  $\underline{s_y = 0.00091\text{mm}}$ . The results and the deviation for a single measurement in production conditions are very good. The deviation of the average is even the smallest throughout all axes. The accuracy depends in majority from three factors: the physical resolution of the sensor in the measured volume, the sharpness of the laser throughout the measured volume and finally the stability of movement. The results highlight unequivocally that the movement of

an industrial robot is stable enough in the Y direction for measurements which reach repeating accuracies smaller than its own accuracy. The laser module used in the measurements was not ideal for this application and will be replaced with a more adequate module. The physical resolution was set up for the grab of the robot, therefore it still can be optimized for smaller measuring volumes in order to achieve more accurate results.

The achieved results for the deviation for a single measurement in the Z axis of  $s_z = 0.04082\text{mm}$  and the deviation of the average of  $s_z = 0.00124\text{mm}$  are very good as well. The accuracy of the results in the Z axis mainly depends on four factors: the stability of movement of the industrial robot, the physical resolution of the sensor and the depth of field of the sensor and the laser module. In this case, again, the stability of the industrial is good enough to achieve measurement results and accuracies which are higher than its own accuracy. The physical resolution of the sensor changes with angle of perspective. If changes in resolution are required the angle can be changed. In the test setup the angle was minimized in order to minimize the physical resolution as much as possible in order to maximize the measurement speed. Another impact which should not be neglected is the depth sharpness of the focal lenses and the laser module. If one of these parameters is not ideal throughout the measuring depth the result will definitely be affected. If there are more accurate results are required the system setup definitely gives options for increasing the accuracy in Z direction.

Whether the discussed relative accuracies are acceptable the deviation to the real nominal data is especially in the X direction not optimal. Another series of measurements will have to be carried out with an increased density of profiles per moved distances. The deviations from nominal values are shown in detail in Appendix I

The developed software for the innovative measurement tool is an intuitive to handle, reliable software tool. The display of the results for the operator has to be optimized in order to achieve optimal results for quality assurance. The software has been parallel running an endurance test with more than 13.000 measurements, without major difficulties.

Summing up the discussed facts the innovative system is in general capable of measuring within production conditions with required accuracies. There still have to be made changes and improvements, which will be discussed in chapter **Fehler!**  
**Verweisquelle konnte nicht gefunden werden..** If the complete innovative strategy of quality assurance is been set up it will be a useful addition to the recent quality assurance. It will be the connection between quality of the product and geometrical conditions of the tools.

## 9. Discussion

The system is still in a prototype phase and improvements still have to be added to it. Future developments will include all areas of the system; the hardware and the software.

Major changes have been implemented in the change from the first software version to version two. Still there are more implementations and changes required. At the recent stadium the software is used by experts and software programmers who know the software by heart. The system will later be used in the production; therefore especially the display of the measurement result has to be understood intuitively. If an error is detected, it is shown in a coloured plot. The deviations are marked with colours and the metric values can be displayed with the cursor. If the system additionally is capable to classify errors it will be also possible to identify different types of errors and rate their impact on the processes.

As pointed out in this thesis the process of making result available to superior systems is complicated. The data has to be transferred through different stages for further processing with other systems. If the system is integrated into the production it is necessary to either generate or transfer the data into a compatible file format for superior analyse instruments.

In order to use the system efficiently more than one system has to be installed into the production processes. If multiple systems are installed the quality loop can be minimized. This leads to a sum of future work. At the recent stage one sensor unit runs with one computer, in order to be more efficient and to reduce cost multiple systems should be controlled by only one computer. This setup requires changes in the software as well in the hardware. So far the range of the computer and the sensor is limited. By integrating other sensors with another interface the range can be extended.

The developed controller fulfils its functions but it also can be optimized. The later used system should consist out of a minimum of single components. The ideal constellation is the computer and the sensor unit. In order to realize this step, the controller should be integrated into the computer, if possible.

The measuring speed and accuracy in moving direction is limited by the used sensors. Depending on the measurement task the usage of faster sensors is unalterable. This will have an impact on the measuring speed and the density of profiles per moved distance.

So far the software operates with two sensors at maximum. In order to solve more complex measurement tasks the integration of additional sensors will be required.

In order to increase the depth sharpness of the system, the implementation of the Scheimpflug phenomenon into the system is necessary.

These mentioned facts only give a general overview of the required future works, but they recommend a lot of effort and put them into reality. By processing these topics, other ideas and improvements will occur and give this system a final shape.

If these recommendations are realized this innovative system will be a fast, cost effective addition to the recent quality assurance in the automobile production. Furthermore it will give the opportunity to document a whole life constantly, from the first process to last production tact. So far tool setup occurs after CAD data, but tool changes will be made until the first product within quality requirements. The chances of documenting the actual geometrical of the tool at this stage is limited. This integrated quality tool can avoid this lack of information.

Finalizing this thesis, this innovative tool is the ideal instrument to link the product quality to the geometrical conditions of the tools manufacturing the product.



---

## 10. List of reference

- Ait Tahar, M. (2008) *Einführung in die Fehlerrechnung*. Unpublished booklet. Köln: Fachhochschule Köln
- Barthen, D. (2009) (dana.barthen@volkswagen.de) *Inlinemessung* [email an F. Viol] (f.viol@fh-wolfenbuettel.de) [15.06.2009]
- Bauer, H. (1991) *Lasertechnik: Grundlagen und Anwendungen*. Würzburg: Vogel Verlag und Druck KG
- Baumert, J. (2009) *Project meeting* [interview by F. Viol] Wolfsburg, 15.01.2009
- Blüm, P. (2002) *Einführung zur Fehlerrechnung im Praktikum*. Unpublished booklet. Karlsruhe: Universität Karlsruhe, Fakultät für Physik
- Bourier, G. (2011) *Wahrscheinlichkeitsrechnung und schließende Statistik 7. Auflage*. Regensburg: Gabler Verlag
- Dalsa (2010) *Product detail 4M60* [online] available from <<http://dalsa.com/mv/products/cameradetail.aspx?partNumber=PT-41-04M60>> [03.02.2010]
- Donges, A., Noll, R. (1993) *Lasermeßtechnik: Grundlagen und Anwendungen*. Heidelberg: Hüthig Buch Verlag GmbH
- Hempel, T. (2010) *Mathematische Grundlagen Fehlerrechnung* [oline] available from <[http://www.uni-magdeburg.de/exph/mathe\\_gl/fehlerrechnung.pdf](http://www.uni-magdeburg.de/exph/mathe_gl/fehlerrechnung.pdf)> [06.11.2010]
- Hexagon Metrology (2008) *Ihr Begleiter in der Welt der Messtechnik*. Switzerland: Hexagon Metrology
- Hoffmann, D. (2009) *Golf A5 side panel analysis*. [CD-Rom] Wolfsburg: Volkswagen AG [07.05.2010]
- Kähler, W.-M. (2008) *Statistische Datenanalyse*. Wiesbaden: Friedr. Vieweg & Sohn Verlag

- 
- Kaiter, M. (2006) *Electromagnetic Spectrum* [online] available from  
<[http://mail.colonial.net/~hkaiter/scienceimagesB/wavelength\\_figure.jpg](http://mail.colonial.net/~hkaiter/scienceimagesB/wavelength_figure.jpg)>  
[11.072010]
- Knoll, A., Christaller, T. (2003) *Robotik*. Frankfurt am Main: S.Fischer Verlag GmbH
- Krämer, W. (2010) *Statistik verstehen. Eine Gebrauchsanweisung 9. Auflage*. München:  
Piper Verlag GmbH
- Labahn, J. (2010) (joerg.labahn@volkswagen.de) *Prototypeninstallation*. [email to F.  
Viol] (f.viol@ostfalia.de) [13.07.2010]
- Lange, C. (2010) *Simulation of robot impacts on measuring procedure* [interview by F.  
Viol] Wolfsburg 15.07.2010
- Litwiller, D. (2001) 'CCD vs. CMOS: Facts and Fiction.' *Photonics Spectra* [online]  
available from <[http://www.dalsa.com/corp/markets/CCD\\_vs\\_CMOS.aspx](http://www.dalsa.com/corp/markets/CCD_vs_CMOS.aspx)>
- Luhmann, T. (2003) *Nahbereichsphotogrammetrie*. Heidelberg: Herbert Wichmann  
Verlag, Hüthig GmbH & Co. KG
- Neumann, H. J. (1990) *Koordinatenmeßtechnik Technologie und Anwendung*.  
Landsberg. Verlag moderne industrie AG &Co.
- Neumann, H. J. (2005) 'Grundlagen der Koordinatenmesstechnik.' In  
*Präzisionsmesstechnik in der Fertigung mit Koordinatenmessgeräten*. ed. by  
Neumann, H. J. Ehningen: Prof. Dr.-Ing. Dr.h.c. Bartz, Dipl.-Ing. Wippler
- Michels, B., Westerhoff, S. (2006) *Photogrammetrie Digitale Bildverarbeitung*.  
Unpublished booklet: Geodätisches Institut und Rechen- und  
Kommunikationszentrum der RWTH Aachen
- Papke, J. (2010) *Technische Mechanik 1 Statik*. Unpublished booklet. Wolfsburg:  
Ostfalia Hochschule für angewandte Wissenschaften
- Papula, L. (2003) *Mathematische Formelsammlung für Ingenieure und  
Naturwissenschaftler 8. Auflage*. Wiesbaden: Friedr. Vieweg & Sohn Verlag
-

- 
- Perceptron (2010) *Lasertriangulation* [online] available from  
<<http://perceptron.com/index.php/de/lasertriangulation.html>> [23.07.2010]
- Schießle, E. (1991) 'Berührungslose Abstandsmessung.' In *Messtechnik am Kraftfahrzeug, mobil und stationär*. ed. by Bartz, W. Böblingen: Expert Verlag
- Schlitter, F. (2010) *Project meeting* [interview by F. Viol] Wolfsburg, 15.10.2010
- Schnell, G. (1998) *Sensoren in der Automatisierungstechnik*. Wiesbaden: Friedr. Vieweg & Sohn / GWV Verlag
- Schulz, C. (2007) *Benchmarking im Bereich Inline-Messtechnik in der Automobilindustrie*. Unpublished dissertation: Fachhochschule Braunschweig/Wolfenbüttel
- Sipex (2007) *Sea Ice and physics and ecosystem experiment* [online] available from <<http://www.acecrc.sipex.aq/access/page/?page=811ccae0-b978-102a-8ea7-0019b9ea7c60>> [11.07.2010]
- Stemmer Imaging (2009) *C4 Series*. [CD ROM] Puchheim: Stemmer Imaging [21.03.2009]
- Viol, F. (2009) *Konzeptionierung und Realisierung einer Inline - Prozessüberwachung*. Unpublished thesis, Fachhochschule Braunschweig/Wolfenbüttel
- Volkswagen AG (1996) *Reference Point System -RPS-*. VW Norm 010 55:1996. Wolfsburg: Volkswagen AG
- Wäldele, F. (1988) 'Überblick über den technischen Stand und die Anwendung der Koordinatenmesstechnik.' In *CNC- Koordinatenmesstechnik*. ed. by Neumann, H. J. Ehningen: Prof. Dr.-Ing. Dr.h.c. Bartz, Dipl.-Ing. Wippler
- Warnecke, B. (2009) *Project meeting* [interview by F. Viol] Wolfsburg, 04.06.2009
- Weber, W. (2009) *Industrieroboter*. Darmstadt: Carl Hanser Verlag München

# Appendix A

Klass.-Nr./Class. No. 02 24 5

December 1996

<b>VOLKSWAGEN AG</b>	<b>Reference Point System - RPS -</b> Drawings	<b>VW</b> <b>010 55</b>
<b>Konzernnorm</b>		

Contents

Page

1	Scope and Aim .....	1
2	Theoretical Principles .....	2
2.1	Component-Oriented Reference System .....	2
2.2	Standard Sizes/Characteristics for RPS Mountings .....	3
3	The 3-2-1 Rule .....	4
4	Designation and Drawing Representation .....	5
4.1	RPS Designation .....	5
4.2	Drawing Representation .....	6
4.3	Procedure for Assemblies (ASSY) with Components with no Separate Drawing (ND): .....	6
5	Dimensioning and Tolerancing .....	7
5.1	General .....	7
5.2	Component-Oriented Reference Systems Parallel to the Coordinate System .....	7
5.3	Rotated, Component-Oriented Reference Systems .....	7
6	Universal Use .....	11
6.1	General .....	11
6.2	Specification of Reference Points .....	11
6.3	Specification of Function Sectors .....	11
7	Referenced Standards .....	12

1 Scope and Aim

This standard applies to dimensioning and to manufacturing and inspecting single parts or assemblies (ASSY) in all product creation phases for

- uniform positioning throughout the manufacturing and inspection areas
- assurance of identical dimensional references

Fortsetzung Seite 2 bis 14

Fachverantwortung/Responsibility	Normung/Standards (EZTN, 1733)
AK "RPS-Systematik" Lürer Vonau	Lürer Tel: +49-5361-929063 Sobanski

Confidential. All rights reserved. No part of this document may be transmitted or reproduced without the prior written permission of a Standards Department of the Volkswagen Group.  
Parties to a contract can only obtain this standard via the responsible procurement department.

© VOLKSWAGEN AG

QUELLE: NOLIS

The English translation is believed to be accurate. In case of discrepancies the German version shall govern.

Norm vor Anwendung auf Aktualität prüfen / Check standard for current issue prior to usage.

Form FE 41 - 12.00

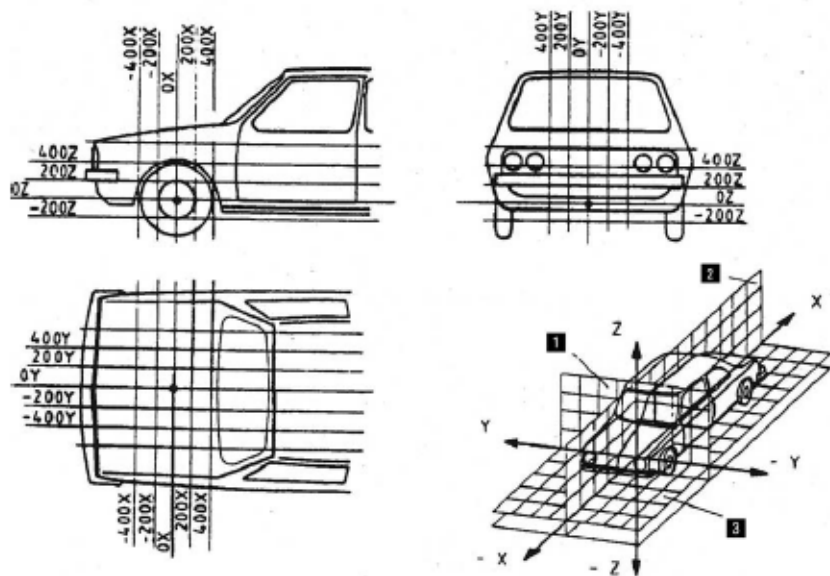
Page 2  
VW 010 55: 1996-12

## 2 Theoretical Principles

### 2.1 Component-Oriented Reference System

One of the basic ideas forming the basis for the reference point system is the component-oriented coordinate system according to VW 010 52.

A vehicle is dimensioned by means of a global coordinate system (mathematical vehicle coordinate system), the origin of which is defined to be in the center at the level of the front axle of a vehicle (see VW 010 59 Part 1; VW 010 52 is the binding reference for the vehicle coordinate system), Figure 1.



A Vertical plane    S Longitudinal center plane    D Horizontal plane  
Figure 1. Global coordinate system for vehicles

Starting from the axes of this coordinate system, grid lines are spread out parallel to the axes. These grid lines, spaced 100 mm apart, theoretically penetrate the vehicle. These grid lines serve to find all points on the vehicle. In other words, they help to determine the position of each vehicle component. Dimensioning is also performed with the aid of these grid lines.

The reference point system is based on a component-oriented reference system.

The origin of the component reference system is defined by the intersection point of three reference planes. The reference planes are formed via the RPS main mountings defined on the component.

When several parts are assembled, these parts are toleranced with respect to each other.

After the parts are joined, the ASSY is described by a combined component-oriented reference system. This is formed

- by adoption of one of the existing reference systems or
- by forming a new reference system using the existing reference points.

The specification of the new reference system depends on the function of the ASSY.

**2.2 Standard Sizes/Characteristics for RPS Mountings**

Multiple-use location holes with high precision requirements must be adequately strong.

In general, the standard sizes according to Table 1 and Table 2 shall be used. In case of holes in RPS surfaces, it must be ensured that the bearing surfaces are of adequate size and provide process assurance.

The specified dimensions shall be projected – parallel to the axes – onto the component.

Table 1. Recommended standard values

For further standard sizes see VW 010 77


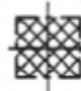
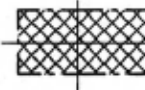

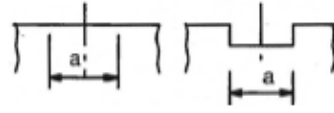
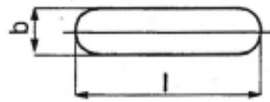
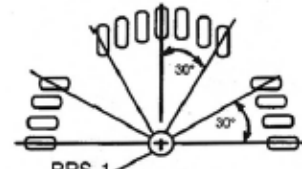
Designation		Nominal dimension	Tol.	Graphical representation
Location holes, pluggable	Round hole	see VW 01077		
	Square	10 15 20 25	+1	
Surfaces	Rectangle	6 x 20 10 x 20 15 x 20	+1	
	Circle	Ø 15 Ø 20 Ø 25	+1	
Edges	Edge length "a"	10 20 25	+1	

Table 2. Recommended standard values

For further standard sizes see VW 010 78

Designation		Nominal dimension w x l	Tol.	Graphical representation
Location holes, pluggable	Long hole	see VW 01078		
	Long hole in angle position			

Page 4  
VW 010 55: 1996-12

### 3 The 3-2-1 Rule

Every rigid body possesses six degrees of freedom in three-dimensional space: three translational degrees parallel to the axes of a reference system and three rotatory degrees around the axes, Figure 2.

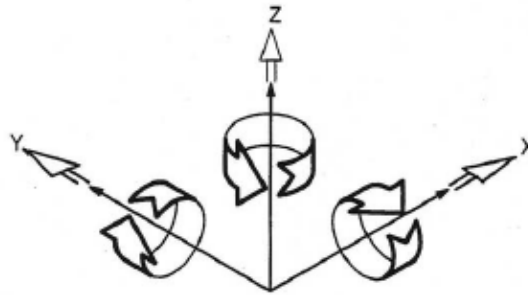


Figure 2. The degrees of freedom in three-dimensional space

In order to support a non-rotationally-symmetric body in a uniquely determinate manner, it must be fixed in all six possible directions of movement. The 3-2-1-rule provides for such unique fixing. It determines the following main-mounting distribution:

E.g.    3 mountings            in z direction  
          2 mountings            in y direction  
          1 mounting            in x direction

Implementation of this rule is shown based on the following representation, Figure 3.

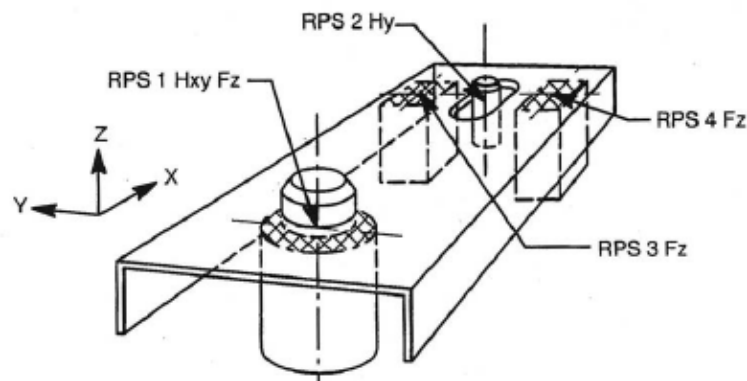


Figure 3. Application of the 3-2-1 rule

The three mountings in z direction restrict three degrees of freedom: translation in z direction and rotation around the x and y axes. The pin in the round hole prevents motion parallel to the axes in the x and y directions and, finally, the pin in the long hole prevents rotation around the z axis, Figure 3.

This rule applies equally to any other rigid component, even if its structure is much more complex. With a system of rigid bodies, the elements of which are interconnected by joints or guides, more than 6 degrees of freedom must be fixed using additional main mountings.

For non-rigid components, additional support points must be defined for supporting the components according to RPS aspects.

RPS 1 shall be the point that binds the most degrees of freedom.

## 4 Designation and Drawing Representation

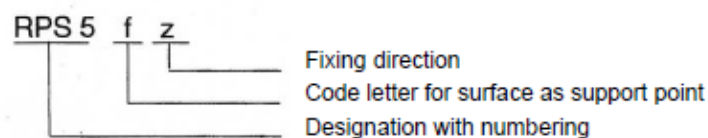
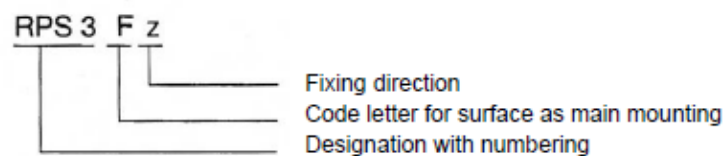
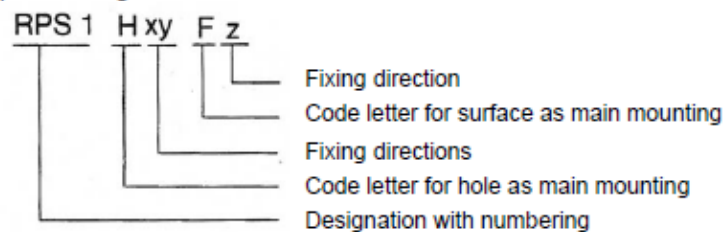
### 4.1 RPS Designation

All RPS points must be included in the part drawing.

The designation is subdivided as follows:

- Main mounting points = Capitals
  - H = Hole
  - F = Surface
  - T = Theoretical point  
is the mean of two support points
- Support points = Small letters
  - h = Hole
  - f = Surface
  - t = Theoretical point  
is the mean of two support points
- Mounting types
  - Location holes/pins = Code letter H,h
  - Surfaces/edges/ball/tip = Code letter F,f
  - Theoretical point = Code letter T,t
- Fixing directions = Small letters
  - x, y, z for component-oriented reference systems parallel to the coordinate system
  - a, b, c for rotated, component-oriented reference systems

Examples of designation:



Numbering begins with the RPS 1 point for each single part and for each assembly.



Page 6  
VW 010 55: 1996-12

#### 4.2 Drawing Representation

Drawing representation takes place according to the valid drawing guidelines.

The RPS surfaces shall be identified by means of cross-hatching.

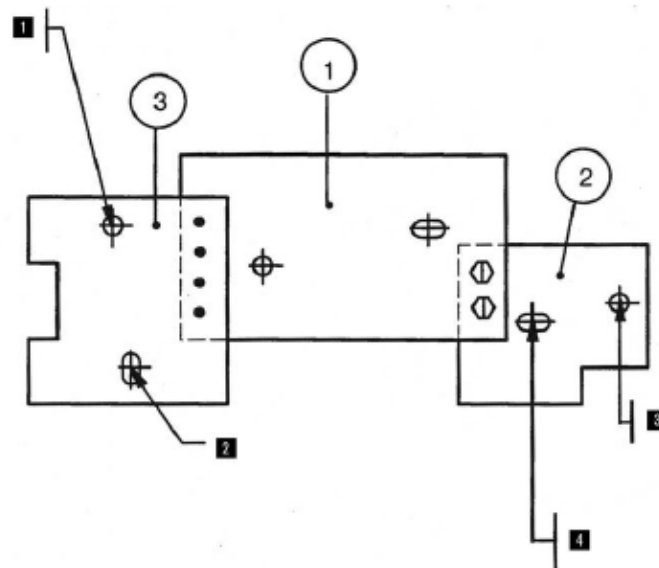
If a part drawing does not exist yet, RPS Dimensions Sheet FE 515 <sup>1)</sup> shall be used.

As soon as the part drawing exists, the specifications from the RPS Dimensions Sheet are adopted directly in the drawing or adopted in text macro NO-F23 <sup>2)</sup>. Administration of these specifications in the text macro is mandatory.

#### 4.3 Procedure for Assemblies (ASSY) with Components with no Separate Drawing (ND):

The RPS points for components with no drawing (ND) must be identified by specifying the item number or part number.

A drawing exists for part 1; ND for parts 2 and 3, Figure 4.



A RPS 1 Hxy; RPS 1 Hxy for Item 3  
D RPS 1 Hxy only for Item 2

S RPS 2 Hx only for Item 3  
F RPS 2 Hy; RPS 2 Hy for Item 2

Fig. 4 ASSY with RPS points  
Graphical representation, not adopted in drawing

<sup>1)</sup> Stored in design data administration system under FEO 000 515

<sup>2)</sup> Stored in design data administration system under NOF 000 023

## 5 Dimensioning and Tolerancing

### 5.1 General

Dimensions and tolerances can be entered directly in the drawing or via the table, Figure 5.

The starting point for dimensioning the components is generally the origin of the reference system.

Form and functional dimensions with tolerances shall always be referenced to the origin of the reference system.

Example: The holes within a hole group are dimensioned with respect to each other. The position of the hole group is dimensioned with respect to the reference planes.

In the fixing direction, the main mountings are positioned without tolerance with respect to the vehicle coordinate system / reference system.

The origin/reference point is shown in the drawing or table. If two or three fixing directions are bound at one point, tolerancing must be separated according to the hole or surface. In this case, the surface must be identified one line lower in the table. Here, the surface is set to zero in the tolerance zone. In the line in which the hole is set to zero, the tolerance zone for the surface shall be identified with a horizontal line, see the table in Figure 5.

The support-point tolerances shall be defined according to the requirements.

### 5.2 Component-Oriented Reference Systems Parallel to the Coordinate System

The origin of the reference system is defined without tolerances in the global vehicle coordinate system by means of a translation, Figure 5

### 5.3 Rotated, Component-Oriented Reference Systems

With rotated reference systems, the theoretical angles of rotation must be specified in RPS Dimensions Sheet FE 515 <sup>1)</sup> or in the drawing table text macro NO-F23 <sup>2)</sup>.

If there are several angles of rotation, the angle specification and thus the sequence of rotations shall be obtained from the drawing. "See drawing" must be added to the table instead of the angle entry.

The position of the reference point is determined by means of its x, y and z coordinates in the global vehicle coordinate system.

Angles of rotation around the x, y and z axes are entered using mathematically positive or negative values. Positive angles are specified counterclockwise and negative angles clockwise.

In the coordinate system, the horizontal axis is assigned an angle of zero.

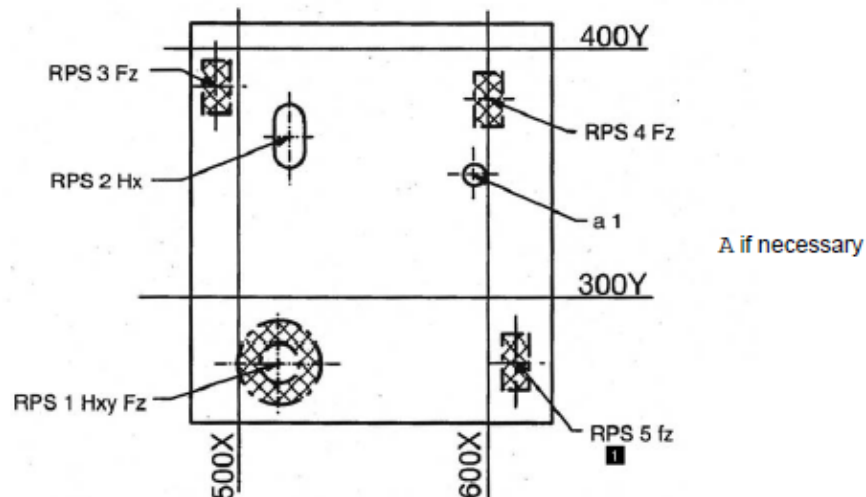
Nominal dimensions and tolerances are specified in a, b and c values in the RPS table.

The fixing directions of the RPS points are specified as a, b and c values in the table and/or drawing, e.g. RPS 1 HabFc, Figure 6 and Figure 7.

---

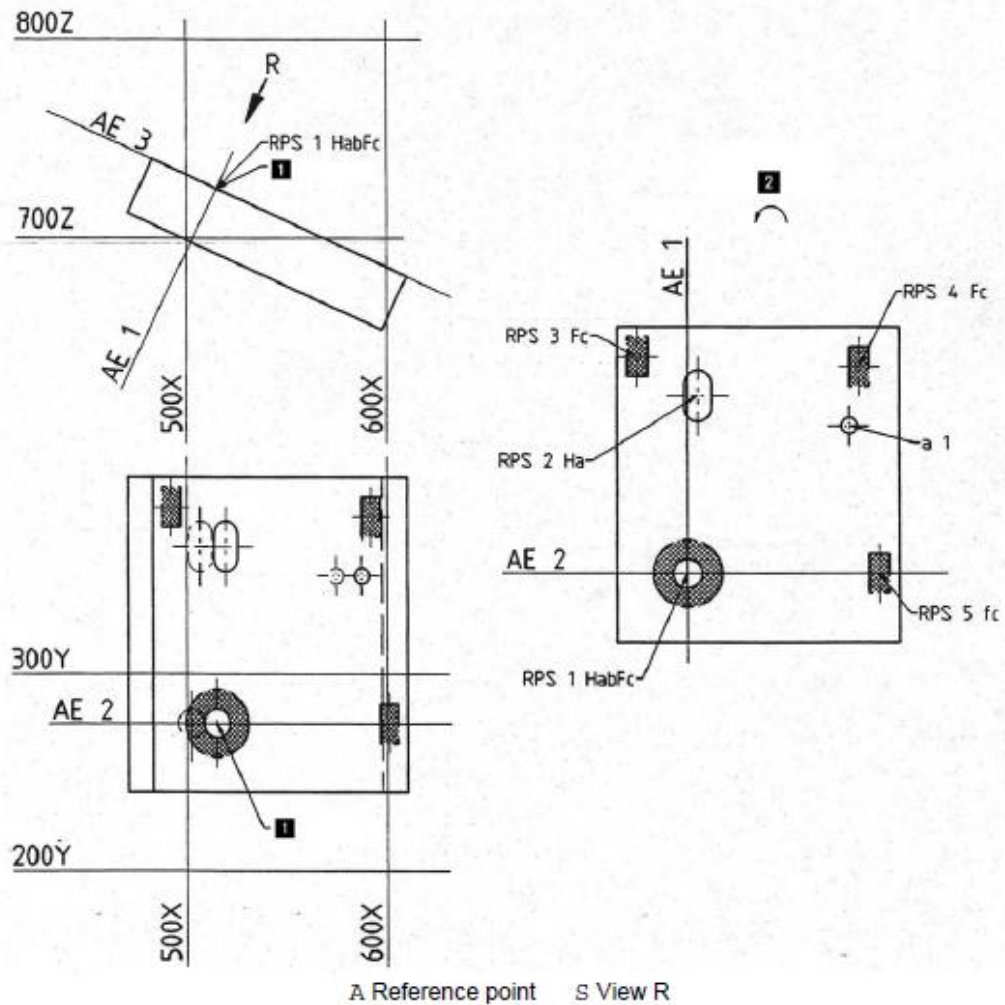
<sup>1), 2)</sup> see page 6

Page 8  
VW 010 55: 1996-12



Feld Sect.	RPS F.- Pkt./ Funct. point	Globale Koordinaten Global coordinates			Aufnahmeart/ Bemerkung Mounting type/ note	Bezugspunkt: Reference point: Theor. Drehwinkel um Achse: Theor. angle of rotat. around axis:			Toleranzen/ Tolerances			Zusatz Addition
		x	y	z		x:	y:	z:	AE x/a	AE y/b	AE z/c	
	1HxyFz	515	275	725	Hole Ø 14.5+0.2				0	0	0	
	...	...	...	...	Surface Ø 34.5+1				±1	±1	0	
	2Hx . .	520	385	725	Long hole 13+0.2 x 26+0.4	5	90	0	0	±0.5	.	.
	3F . . z	490	385	725	Surface 10+1 x 20+1	25	110	0	±1	±1	0	.
	4F . . z	600	380	725	Surface 10+1 x 20+1	85	105	0	±1	±1	0	.
	5F . . z	610	275	725	Surface 10+1 x 20+1	95	0	0	±1	±1	±0.5	.
	a 1	595	350	725	Hole Ø 8+0.2				.	.	.	0.2

Fig. 5 Dimensioning with text macro NO-F23




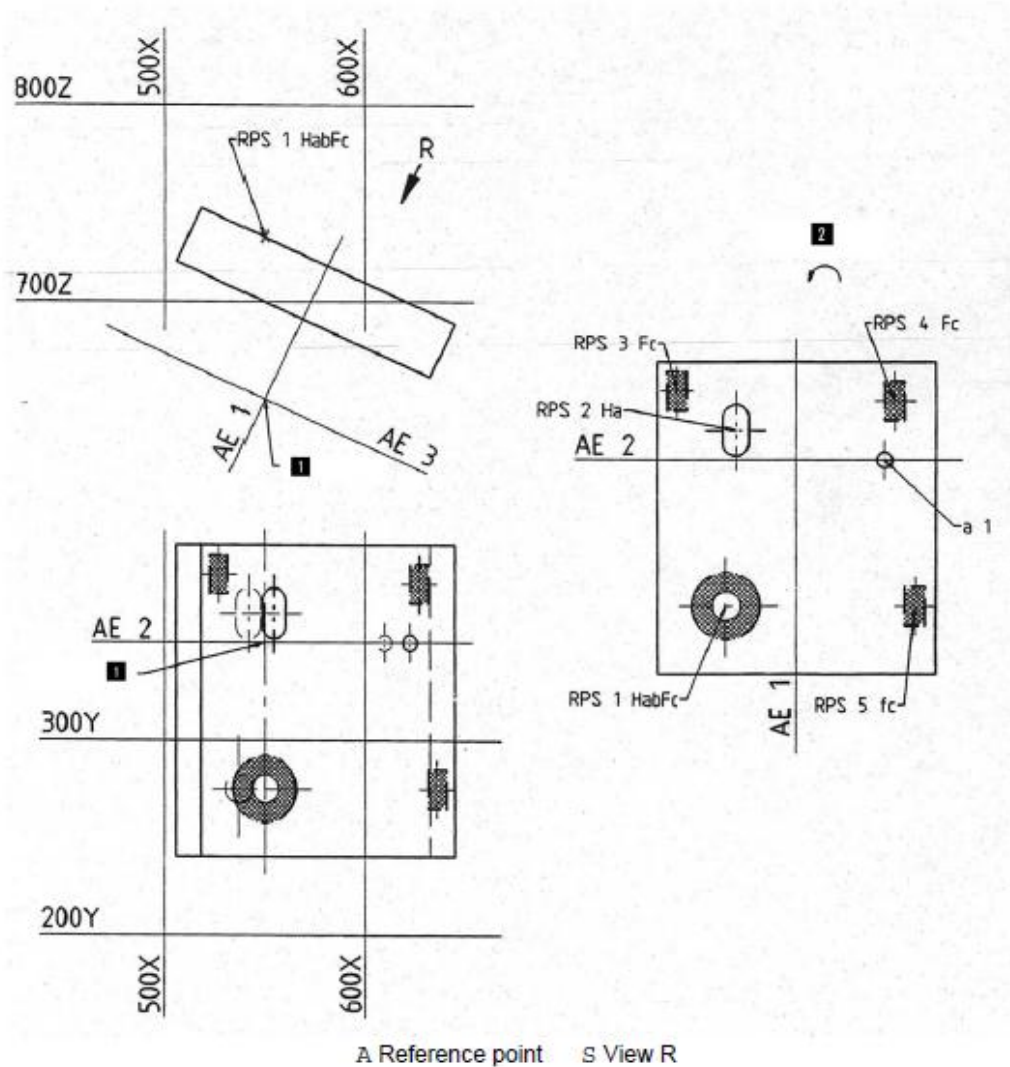
Feld Sect.	RPS  F.- Pkt./ Funct. point	Globale Koordinaten Global coordinates			Aufnahmeart/ Bemerkung Mounting type/ note	Bezugspunkt: Reference point: x: 515 y: 275 z: 725 Theor. Drehwinkel um Achse: Theor. angle of rotat. around axis: x: 0° y: 25° z: 0°						
						Nennmasse/ Nominal sizes			Toleranzen/ Tolerances			
		AE1 x/a	AE2 y/b	AE3 z/c		x/a	y/b	z/c				
	1HabFc	515	275	725	Hole Ø 14.5+0.2	0	0	0	0	0	-	.
	.....	.	.	.	Surface Ø 34.5+1	.	.	.	±1	±1	0	.
	2Ha . .	519.5	385	722.9	Long hole 13+0.2 x 26+0.4	5	90	0	0	±0.5	.	.
	3F . . c	492.3	385	735.6	Surface 10+1 x 20+1	25	110	0	±1	±1	0	.
	4F . . c	592	380	689.1	Surface 10+1 x 20+1	85	105	0	±1	±1	0	.
	5f . . c	601.1	275	684.8	Surface 10+1 x 20+1	95	0	0	±1	±1	±0.5	.
	a 1	587.5	350	691.2	Hole Ø 8+0.2	.	.	.	.	.	.	0.2

Fig. 6 Reference point is formed directly via RPS main mountings.

Page 10  
VW 010 55: 1996-12




Feld Sect.	RPS F.- Pkt./ Funct. point	Globale Koordinaten Global coordinates			Aufnahmeart/ Bemerkung Mounting type/ note	Bezugspunkt: Reference point: x: 550 y: 350 z: 650 Theor. Drehwinkel um Achse: Theor. angle of rotat. around axis: x: 0° y: 25° z: 0°						
		x	y	z		Nennmasse/ Nominal sizes			Toleranzen/ Tolerances			
						AE1 x/a	AE2 y/b	AE3 z/c	x/a	y/b	z/c	
	1HabFc	550	275	732.8	Hole Ø 14.5+0.2	35	75	75	0	0	-	.
	.....	.	.	.	Surface Ø 34.5+1	.	.	.	±1	±1	0	.
	2Ha ..	554.5	365	730.6	Long hole 13+0.2 x 26+0.4	30	15	75	0	±0.5	.	.
	3F ...c	527.3	385	743.3	Surface 10+1 x 20+1	60	35	75	±1	±1	0	.
	4F ...c	627	380	696.8	Surface 10+1 x 20+1	50	30	75	±1	±1	0	.
	5f ...c	636.1	275	692.6	Surface 10+1 x 20+1	60	75	75	±1	±1	±0.5	.
	a 1	622.5	350	699	Hole Ø 8+0.2			-	-	-	-	0.2

Fig. 7 Reference point is formed via RPS main mountings with defined distances



## 6 Universal Use

### 6.1 General

The purpose of the RPS is to provide process assurance/capability and repeat accuracy for the procedures in order to make them independent of setting work performed by the worker.

The reference points must be used in all manufacturing, assembly, inspection and installation processes.

In case of self-contained function sectors such as the side panel tank flap, a reference change in combination with functional dimensions to RPS planes is permissible.

Prior to the specification of RPS points, it is absolutely necessary to define the functions of the single part and the relevant assemblies with their required functional tolerances.

Reference points that were established at the beginning of a process must be kept for as long as possible. In order to avoid changes to arranged reference points, they are jointly defined – as early as possible in the design and development process – in consultation with all departments participating in the production process.

Reference points must be positioned at stable areas of a component that will remain unchanged even in further development and/or production processes.

Reference points on components that move relative to the body during driving operation can be considered according to the 3-2-1 rule only in the actual design position.

The RPS points on components that are used several times in vehicles and thus have multiple references to the global coordinate system can be shown without a global coordinate reference in the technical drawing.

The reference point system is equally oriented toward the production process, toward the function sectors and toward the strategic quality goals, e.g. audit, process capability.

### 6.2 Specification of Reference Points

Parallelism to the coordinate system (holes and surfaces) must be observed when entering the reference points. In the case of rotated systems, parallelism to the reference planes must be observed.

The RPS points must be produced in the tool sequence in which the greatest dimensional stability is attained.

Whenever possible, reference points must be produced with a standardized shape (hole, surface), which must be defined in detail.

If holes cannot be made in a component, surfaces or edges must be used to specify reference points.

In the case of COP parts (transfer parts), the respective reference-point positions arise in the ASSY.

### 6.3 Specification of Function Sectors

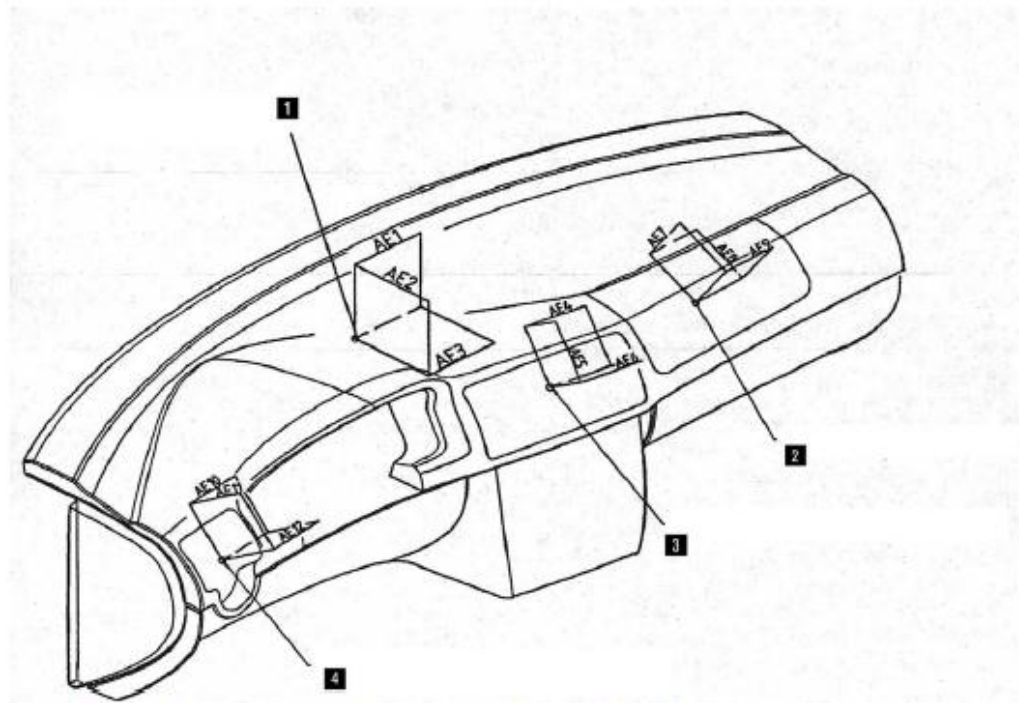
Use of the RPS on a complex portion of the vehicle such as the dashboard requires a structure that addresses the development and design engineering systems and includes all parts, single parts and assemblies.

A function sector includes all components in the visible and covered areas that directly affect their surroundings with their function points.

The specification of reference planes depends on the spatial and geometric position relationship of a component with its surroundings.

The reference planes are identical for a function sector. In other words, components or component groups and the surroundings have the same starting basis, Figure 8.

Page 12  
VW 010 55: 1996-12



A Dashboard ASSY function sector  
D Center-vent function sector  
Fig. 8

S Airbag function sector  
F Air outlet vent function sector FS

#### 7 Referenced Standards

VW 010 52  
VW 010 59 T1  
VW 010 77  
VW 010 78

[illegible]



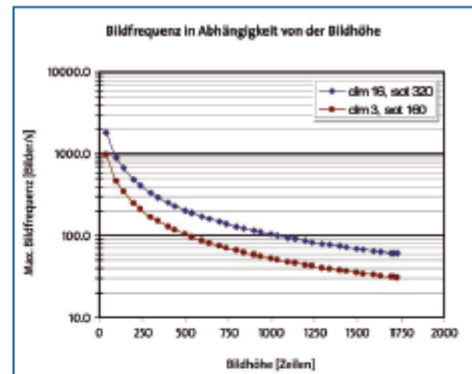


## Appendix B



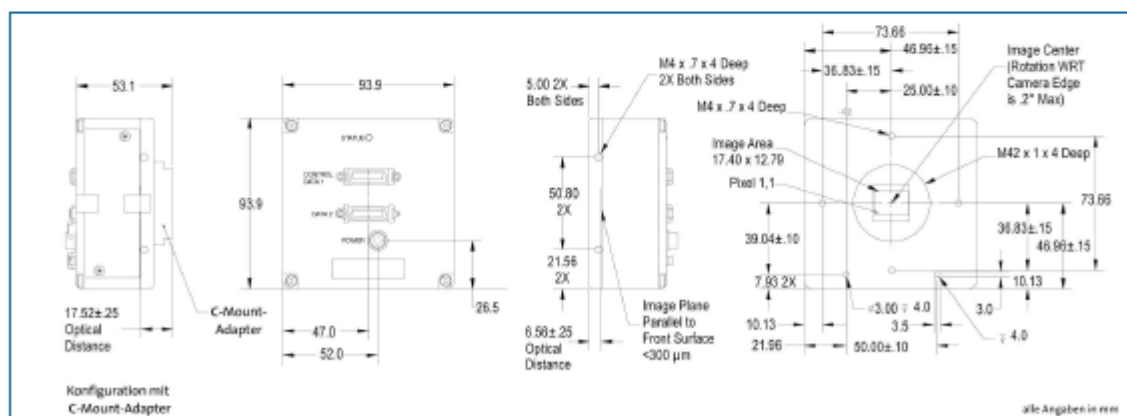
### ► Technische Daten

Spezifikationen	DALSA Falcon 4M30 Color	DALSA Falcon 4M60 Color
Kamera-Klasse	Flächenkamera, Farbe	
Sensor-Klasse	1.2" Global Shutter-CMOS	
Spektrale Empfindlichkeit	400 - 800 nm	
Fill-Faktor	60 %	
Sensorfläche (effektiv)	17,4 x 12,8 (H x V in mm)	
Auflösung (effektiv)	2352 x 1728 (H x V)	
Pixelgröße	7,4 x 7,4 (H x V in µm)	
Bildfrequenz (Standard)	30,6 Hz	60,4 Hz
Datenrate	80 MHz	
Ausgangskanäle (max.)	2	4
Empfindlichkeit	18,4 DN/(el/cm <sup>2</sup> )	
Signal-/Rausch-Abstand	57 dB	
Bit pro Pixel	8 or 10 bit	
Digitales Interface	CameraLink-Base	CameraLink-Medium
Spannungsversorgung	12 - 15 V	
Leistungsaufnahme	10 W	
Externe Konfiguration	Steuerung der Kamera-Funktionen via CameraLink	
Anschlüsse	MD8-26, Hirose (6-polig)	
Funktionen	Anti-Blooming, Integrationszeit einstellbar, Flat-Field-Korrektur	
Objektivanschluss	M42x1, F-Mount	
Abmessungen	94 x 94 x 48 (H x H x T in mm)	
Gewicht	<550 g	
Betriebstemperatur	0 - 50 °C	
Zertifikate	RoHS, CE	



Durch Verkleinerung der Bildhöhe (vertical windowing) kann die Bildfrequenz deutlich gesteigert werden

### ► Abmessungen



WWW.STEMMER-IMAGING.COM • IMAGING IS OUR PASSION

DEUTSCHLAND  
Telefon: +49 89 309002-0  
info@stemmer-imaging.de

GROSSBRITANNIEN  
Telefon: +44 1252 780000  
info@stemmer-imaging.co.uk

FRANKREICH  
Telefon: +33 1 45069560  
info@stemmer-imaging.fr

SCHWEIZ  
Telefon: +41 55 4159090  
info@stemmer-imaging.ch

**STEMMER®**  
IMAGING

K-DAL21-09/2009 • Technische Änderungen und Fehler vorbehalten.

## Appendix C

	<i>microEnable IV AS1-PoCL</i>	<i>microEnable IV AD1-CL</i>	<i>microEnable IV AD1-PoCL</i>
Host interface	PCIe x1	PCIe x1	PCIe x1
DMA channels	1	2	2
Bandwidth (theo.)	250 Mbyte/s per direction on PCIe bus	250 Mbyte/s per direction on PCIe bus	250 Mbyte/s per direction on PCIe bus
Bandwidth (typ.)	200 Mbyte/s	200 Mbyte/s	200 Mbyte/s
On-board memory	128 Mbyte	128 Mbyte	128 Mbyte
On-board FPGA processing	Acquisition Applets	Acquisition Applets	Acquisition Applets
Voltage, max. Current (actual values dependant on processing)	+3.3V, 200 mA +12V, 300 mA	+3.3V, 225 mA +12V, 300 mA	+3.3V, 225 mA +12V, 300 mA
Dimensions	Standard height, half length card: 167.64 mm length x 111.15 mm height	Standard height, half length card: 167.64 mm length x 111.15 mm height	Standard height, half length card: 167.64 mm length x 111.15 mm height
Weight	110 g	115 g	117 g
Camera interface	CameraLink 1 x Base (Port A)	CameraLink 2 x Base, Medium	CameraLink 2 x Base, Medium PoCL SafePower
Camera interface connector	MDR Connector	MDR Connector	MDR Connector
Operating Temperature	0°C - 50°C	0°C - 50°C	0°C - 50°C
Storage Temperature	-50°C - 80°C	-50°C - 80°C	-50°C - 80°C
CE conformity	yes	yes	yes
FCC		verification class B*	
	<i>microEnable IV AD1-mPoCL</i>	<i>microEnable IV AD4-CL</i>	<i>microEnable IV AQ4-GE</i>
Host interface	PCIe x1	PCIe x4	PCIe x4
DMA channels	2	2	4
Bandwidth (theo.)	250 Mbyte/s per direction on PCIe bus	1 Gbyte/s per direction on PCIe bus	1 Gbyte/s per direction on PCIe bus
Bandwidth (typ.)	200 Mbyte/s	750 Mbyte/s	750 Mbyte/s
On-board memory	128 Mbyte	256 Mbyte	256 Mbyte
On-board FPGA processing	Acquisition Applets	Acquisition Applets	Acquisition Applets
Voltage, max. Current (actual values dependant on processing)	+3.3V, 225 mA +12V, 300 mA	+3.3V, 250 mA +12V, 1000 mA	+3.3V, <100 mA +12V, 1.4 A
Dimensions	Standard height, half length card: 167.64 mm length x 111.15 mm height	Standard height, half length card: 167.64 mm length x 111.15 mm height	Standard height, half length card: 167.64 mm length x 111.15 mm height
Weight	115 g	123 g	136 g
Camera interface	CameraLink 2 x Base, Medium PoCL SafePower	CameraLink 2 x Base, Medium, Full	4x GigabitEthernet
Camera interface connector	SDR Connector	MDR Connector	4x GigabitEthernet RJ45 Jack
Operating Temperature	0°C - 50°C	0°C - 40°C **	0°C - 40°C
Storage Temperature	-50°C - 80°C	-50°C - 80°C	-50°C - 80°C
CE conformity	yes	yes	yes
FCC			

\*This equipment has been tested and found to comply with the limits for a class B digital device, pursuant to Part 15 of the FCC Rules and meets all requirements of the Canadian Interference-Causing Equipment Standard ICES-003 for digital apparatus. These limits are designed to provide reasonable protection against harmful interference in a residential installation. This equipment generates, uses, and can radiate radio frequency energy and, if not installed and used in accordance with the instructions, may cause harmful interference to radio communications.

However, there is no guarantee that interference will not occur in a particular installation. If this equipment does cause harmful interference to radio or television reception, which can be determined by turning the equipment off and on, the user is encouraged to try to correct the interference by one or more of the following measures:

- Reorient or relocate the receiving antenna.
- Increase the separation between the equipment and receiver.
- Connect the equipment into an outlet on a circuit different from that to which the receiver is connected.
- Consult the dealer or an experienced radio/T.V. technician for help.

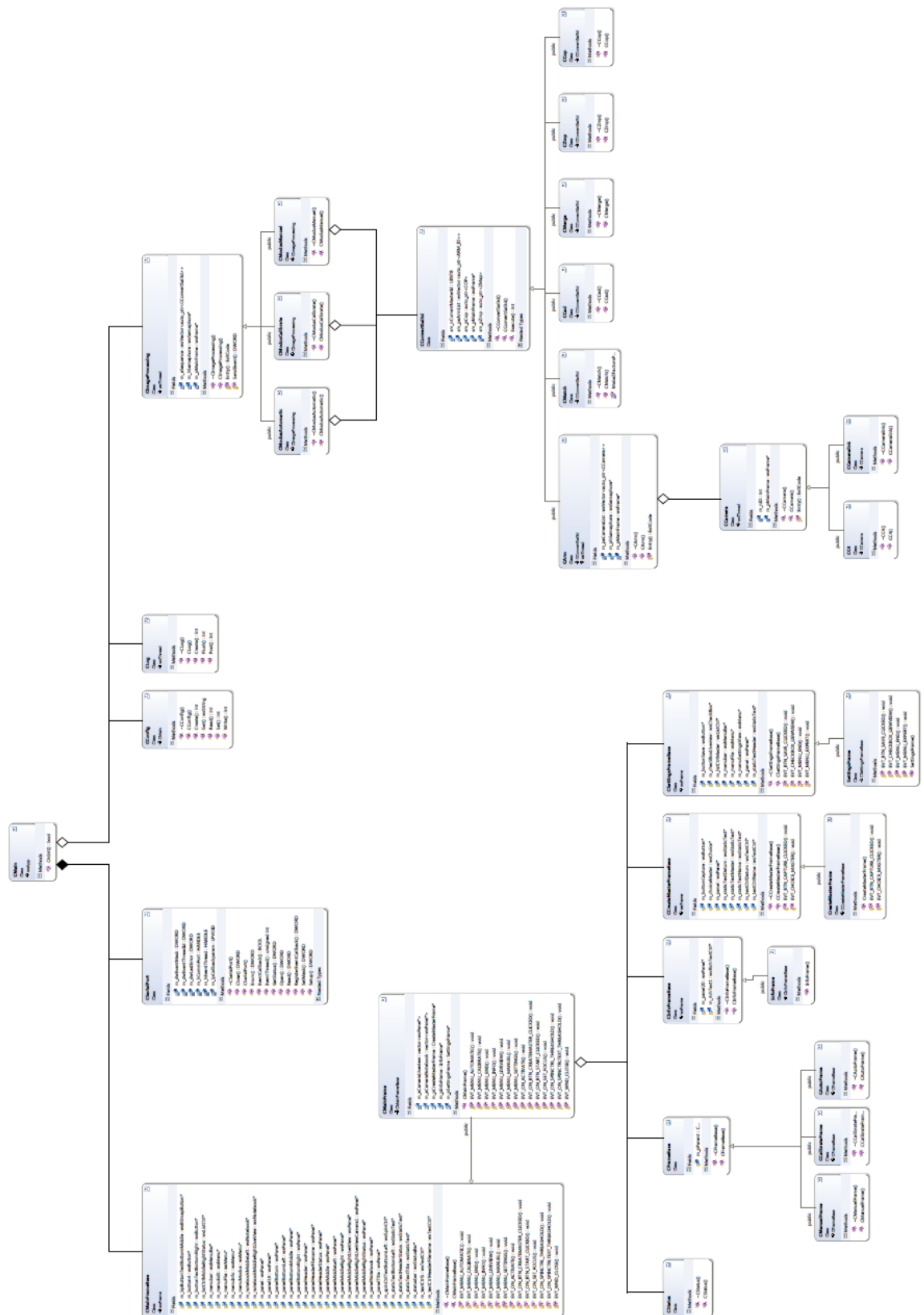
Silicon Software GmbH is not responsible for any radio television inter-ference caused by unauthorized modifications of this equipment or the substitution or attachment of connecting cables and equipment other than those specified by Silicon Software GmbH. The correction of interference caused by such unauthorized modification, substitution or attachment will be the responsibility of the user. The use of shielded I/O cables is required when connecting this equipment to any and all optional peripheral or host devices. Failure to do so may violate FCC and ICES rules.

\*\* A minimal airflow is required.

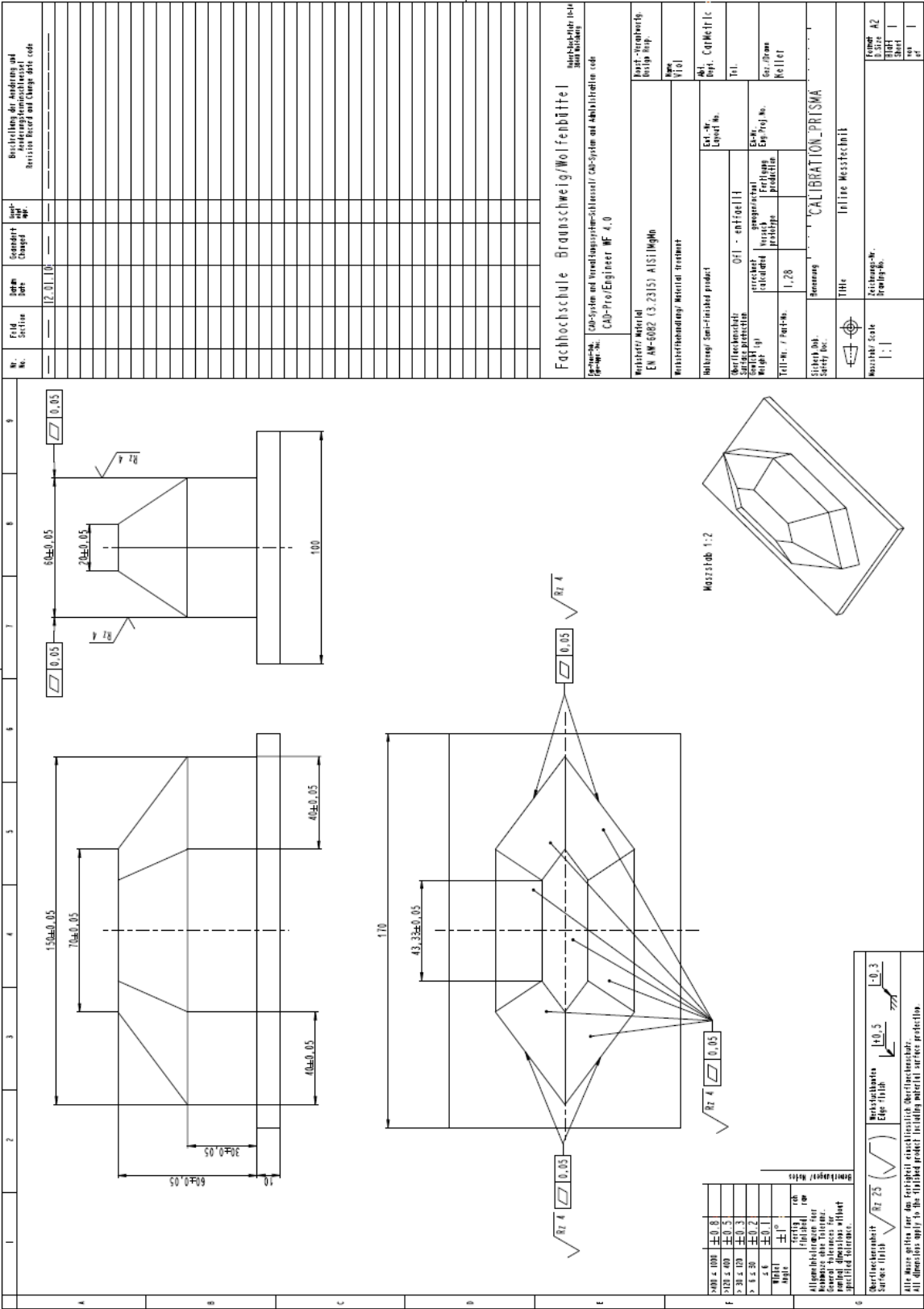
## Appendix D

Anforderungen	Klasse1	Klasse1M	Klasse2	Klasse2M	Klasse3R	Klasse3B
Laserschutz-beauftragter	Nicht erforderlich, aber empfohlen bei Anwendungen, die den direkten Blick in den Laserstrahl erfordern				Nicht erforderlich für sichtbare Emissionen	Erforderlich
Fernbedienbare Verriegelung	Nicht erforderlich					An Raum- oder Türstromkreisen anzuschließen
Schlüsselschalter	Nicht erforderlich					Schlüssel abziehen, wenn außer Betrieb
Strahlabschwächer	Nicht erforderlich					Vermeidet unabsichtliche Bestrahlung, wenn in Betrieb
Strahlanzeige	Nicht erforderlich				Zeigt an, wenn der Laser mit unsichtbarer Strahlung in Betrieb ist	Zeigt an, wenn der Laser in Betrieb ist
Laserwarnschild	Nicht erforderlich					Den Hinweisen auf Warnschildern ist Folge zu leisten
Strahlwege	Nicht erforderlich	Siehe 2M, 3R und 3B	Nicht erforderlich	Der Strahl ist am Ende seines zweckdienlichen Weges zu beenden		
Spiegelnde Reflexion	Nicht erforderlich	Unbeabsichtigte Reflexionen sind zu vermeiden	Nicht erforderlich	Unbeabsichtigte Reflexionen sind zu vermeiden		
Augenschutz	Nicht erforderlich					Erforderlich, wenn konstruktive oder organisatorische Maßnahmen nicht praktikabel zum MZB Wert überschritten
Schutzkleidung	Nicht erforderlich					
Ausbildung	Nicht erforderlich				Erforderlich für Bedienungs- und Wartungsperson	

## Florian Viol

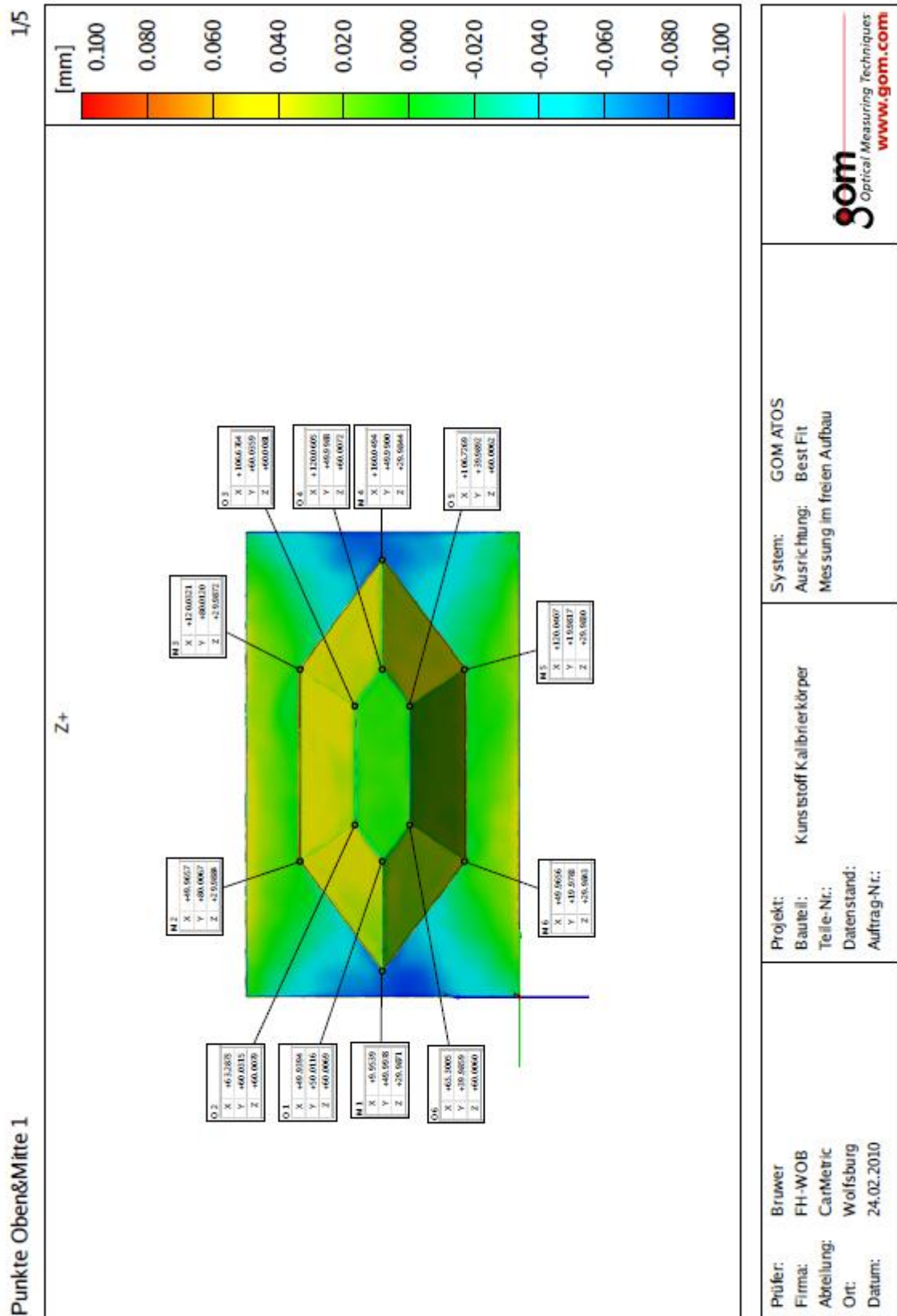


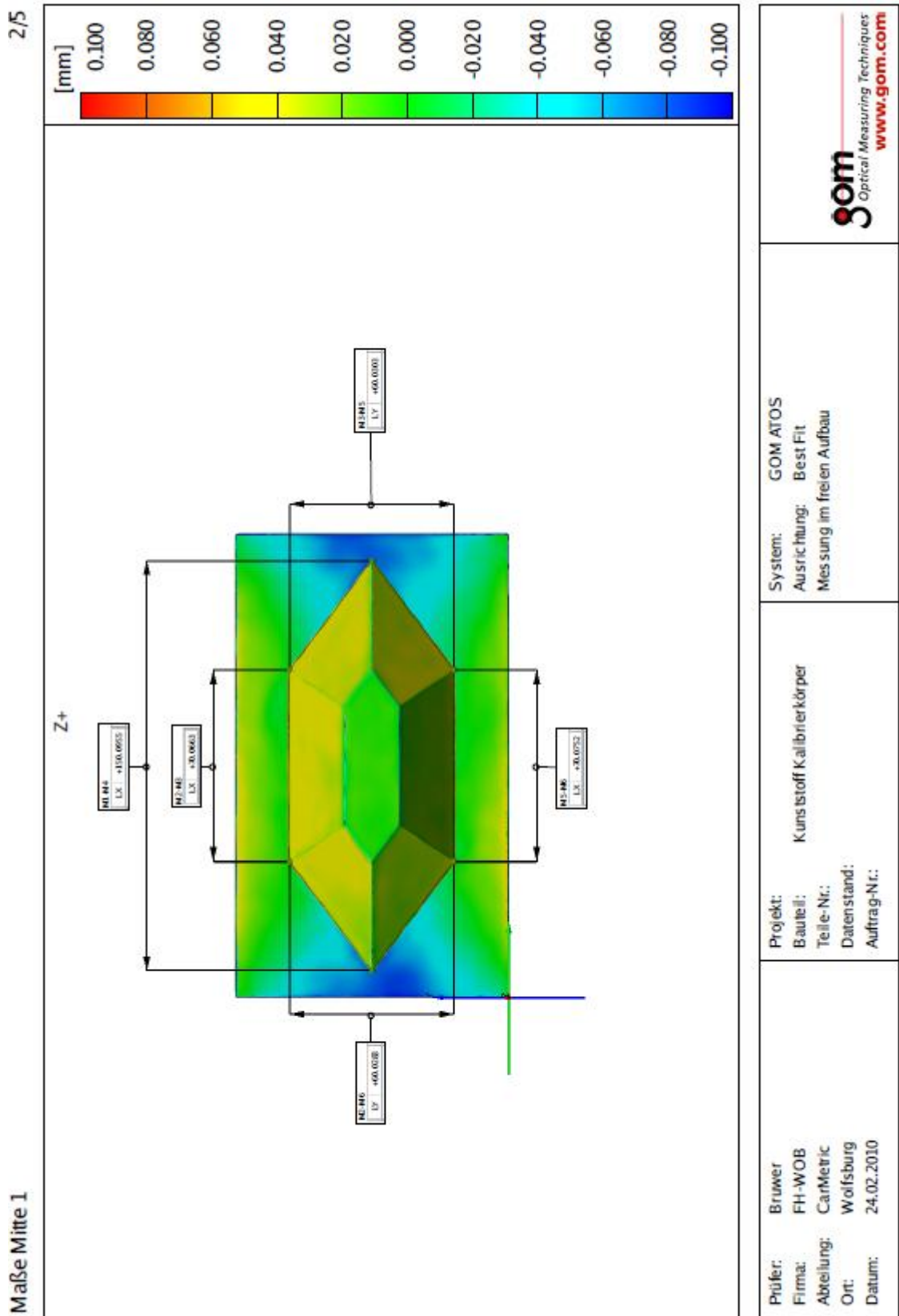
Appendix F



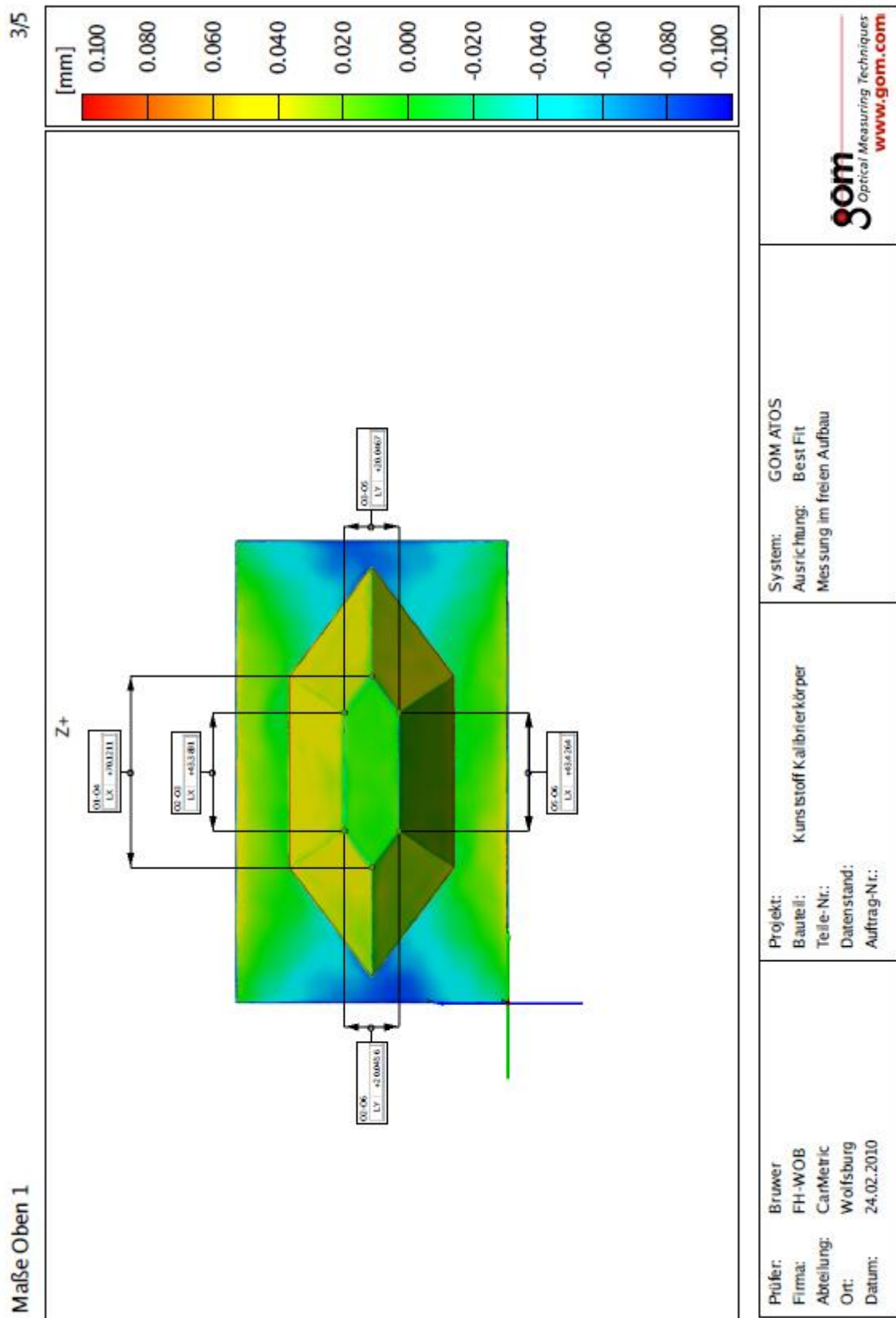


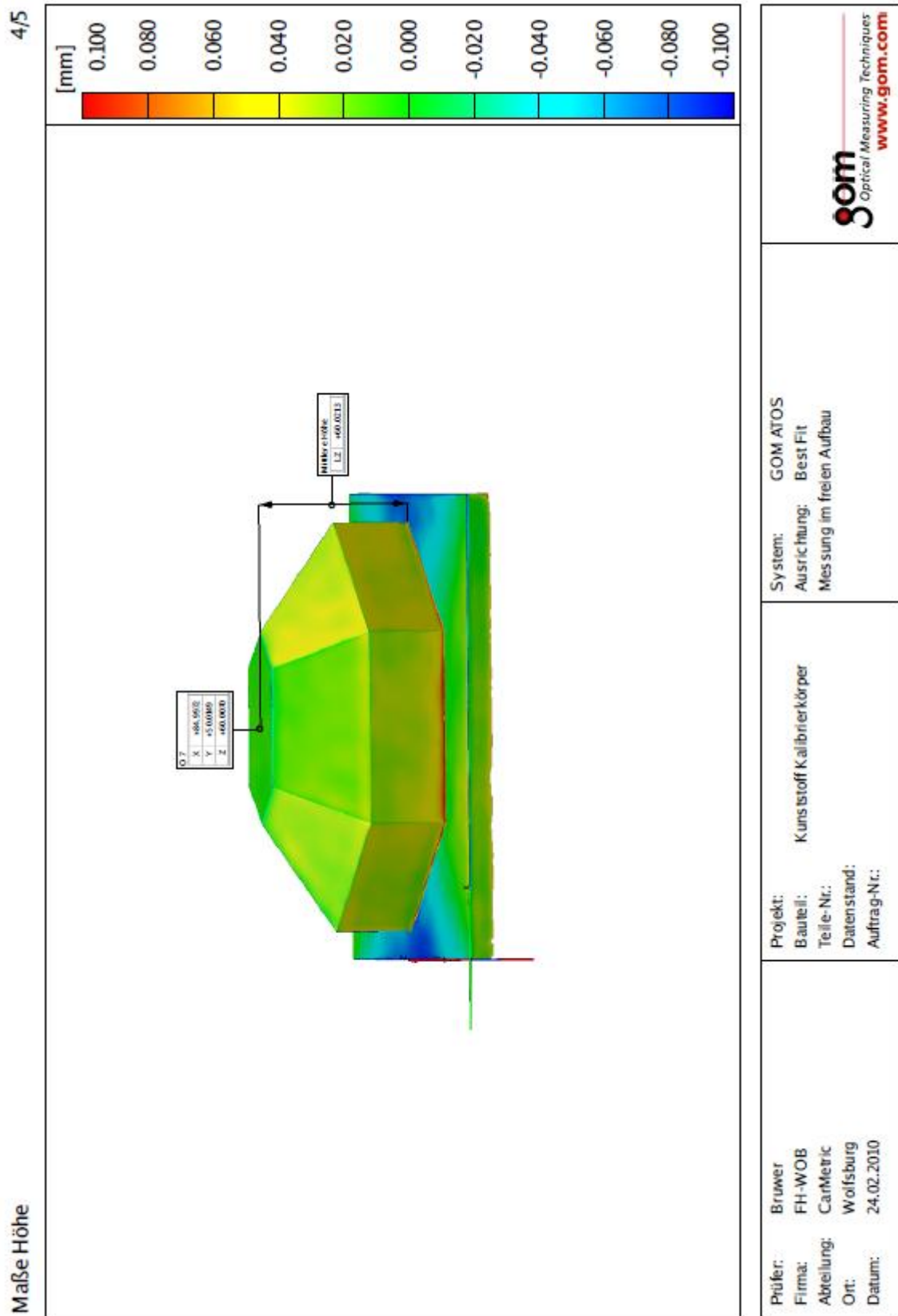
## Appendix G











## Appendix H

STL	LX4-9	Lx5-10	Lx3-8	Ly3-5	Ly8-10	Z5	Z10	Z4	Z9	Z3	Z8
1	69,88	42,62	42,72	19,96	19,95	19,95	59,95	59,95	60,00	60,00	60,05
3	69,93	42,80	42,75	19,97	19,94	19,94	59,95	59,95	60,00	60,00	60,05
4	69,88	42,62	42,72	19,96	19,95	19,95	59,95	59,95	60,00	60,00	60,05
6	69,53	41,72	42,46	19,97	19,95	19,95	59,95	59,95	60,00	60,00	60,05
7	69,86	42,58	42,75	19,97	19,94	19,94	59,95	59,95	60,00	60,00	60,05
9	70,00	42,73	42,75	19,97	19,95	19,95	59,95	59,95	60,00	60,00	60,05
10	69,94	42,66	42,78	19,96	19,96	19,96	59,95	59,95	60,00	60,00	60,05
11	68,23	40,01	42,73	19,96	19,95	19,95	59,95	59,95	60,01	60,00	60,05
12	69,83	42,72	42,63	19,95	19,93	19,93	59,95	59,95	60,00	60,00	60,05
13	69,92	42,63	42,79	19,95	19,96	19,96	59,95	59,95	60,00	60,00	60,05
14	69,89	42,66	42,82	19,97	19,95	19,95	59,95	59,95	60,00	60,00	60,05
15	69,89	42,67	42,65	19,96	19,95	19,95	59,95	59,95	60,00	60,00	60,05
17	69,92	42,71	42,78	19,95	19,93	19,93	59,95	59,95	60,00	60,00	60,05
18	69,88	42,79	42,66	19,95	19,95	19,95	59,95	59,95	60,00	60,00	60,05
19	69,88	42,58	42,86	19,95	19,93	19,93	59,95	59,95	60,00	60,00	60,05
20	69,97	42,71	42,72	19,98	19,95	19,95	59,95	59,95	60,00	60,00	60,05
21	69,83	42,68	42,62	19,97	19,96	19,96	59,95	59,95	60,00	60,00	60,05
22	69,80	42,60	42,71	19,95	19,93	19,93	59,95	59,95	60,00	60,00	60,05
23	69,86	42,61	42,63	19,96	19,94	19,94	59,95	59,95	60,00	60,00	60,05
24	69,98	42,73	42,80	19,96	19,95	19,95	59,95	59,95	60,00	60,00	60,05
25	69,91	42,75	42,64	19,98	19,94	19,94	59,95	59,95	60,00	60,00	60,05
26	69,92	42,69	42,76	19,97	19,95	19,95	59,95	59,95	60,00	60,00	60,05
27	69,90	42,56	42,73	19,96	19,94	19,94	59,95	59,95	60,00	60,00	60,05
28	69,19	43,16	41,54	19,96	19,92	19,92	59,95	59,95	60,00	60,00	60,05
30	69,88	42,70	42,67	19,96	19,95	19,95	59,95	59,95	60,00	60,00	60,05
32	69,85	42,71	42,52	19,95	19,96	19,96	59,95	59,95	60,00	60,00	60,05
33	69,85	42,71	42,52	19,95	19,96	19,96	59,95	59,95	60,00	60,00	60,05
34	69,85	42,71	42,57	19,94	19,94	19,94	59,95	59,95	60,00	60,00	60,05
35	69,89	42,57	42,73	19,96	19,96	19,96	59,95	59,95	60,00	60,00	60,05
37	69,80	42,52	42,58	19,95	19,95	19,95	59,95	59,95	60,00	60,00	60,05
39	69,84	42,55	42,74	19,96	19,96	19,96	59,95	59,95	60,00	60,00	60,05
41	69,87	42,65	42,67	19,97	19,95	19,95	59,95	59,95	60,00	60,00	60,05
42	69,84	42,62	42,71	19,94	19,94	19,94	59,95	59,95	60,00	60,00	60,05
43	69,93	42,74	42,79	19,96	19,94	19,94	59,95	59,95	60,00	60,00	60,05
45	69,87	42,68	42,70	19,97	19,95	19,95	59,95	59,95	60,00	60,00	60,05

STL	47	69,80	42,62	42,77	19,95	19,95	59,95	59,95	60,00	60,05	60,05
	48	69,86	42,78	42,57	19,96	19,96	59,95	59,95	60,00	60,05	60,05
	49	69,88	42,62	42,72	19,96	19,95	59,95	59,95	60,00	60,05	60,05
	50	69,83	42,74	42,56	19,95	19,94	59,95	59,95	60,00	60,05	60,05
	51	69,83	42,61	42,72	19,95	19,97	59,95	59,95	60,00	60,05	60,05
	53	69,84	42,74	42,56	19,98	19,97	59,95	59,95	60,00	60,05	60,05
	56	69,89	42,68	42,66	19,97	19,96	59,95	59,95	60,00	60,05	60,05
	57	69,93	42,68	42,59	19,95	19,94	59,95	59,95	60,00	60,05	60,05
	58	69,81	42,58	42,72	19,98	19,95	59,95	59,95	60,00	60,05	60,05
	59	69,81	42,64	42,62	19,96	19,95	59,95	59,95	60,00	60,05	60,05
	61	69,86	42,55	42,78	19,96	19,94	59,95	59,95	60,00	60,05	60,05
	63	69,87	42,51	42,81	19,96	19,95	59,95	59,95	60,00	60,05	60,05
	65	69,85	42,63	42,63	19,99	19,95	59,95	59,95	60,00	60,05	60,05
	66	69,85	42,53	42,77	19,98	19,95	59,95	59,95	60,00	60,05	60,05
	67	69,84	42,58	42,74	19,97	19,94	59,95	59,95	60,00	60,05	60,05
	68	69,79	42,58	42,75	19,94	19,95	59,95	59,95	60,00	60,05	60,05
	69	69,89	42,61	42,74	19,97	19,95	59,95	59,95	60,00	60,05	60,05
	70	69,88	42,71	42,63	19,95	19,95	59,95	59,95	60,00	60,05	60,05
	76	69,80	42,54	42,73	19,96	19,94	59,95	59,95	60,00	60,05	60,05
	77	69,82	42,59	42,72	19,96	19,94	59,95	59,95	60,00	60,05	60,05
	78	69,97	42,73	42,74	19,97	19,94	59,95	59,95	60,00	60,05	60,05
	79	69,80	42,75	42,51	19,96	19,93	59,95	59,95	60,00	60,05	60,05
	80	69,86	42,69	42,66	19,97	19,95	59,95	59,95	60,00	60,05	60,05
	85	69,87	42,67	42,76	19,96	19,95	59,95	59,95	60,00	60,05	60,05
	86	69,88	42,60	42,71	19,97	19,94	59,95	59,95	60,00	60,05	60,05
	88	69,84	42,75	42,58	19,94	19,95	59,95	59,95	60,00	60,05	60,05
	89	69,80	42,61	42,66	19,95	19,95	59,95	59,95	60,00	60,05	60,05
	90	69,95	42,61	42,77	19,97	19,94	59,95	59,95	60,00	60,05	60,05
	93	69,88	42,59	42,74	19,95	19,94	59,95	59,95	60,00	60,05	60,05
	94	69,86	42,64	42,70	19,96	19,94	59,95	59,95	60,00	60,05	60,05
	95	69,88	42,71	42,73	19,95	19,94	59,95	59,95	60,00	60,05	60,05
	96	69,90	42,57	42,59	19,97	19,92	59,95	59,95	60,00	60,05	60,05
	97	69,76	42,68	42,49	19,95	19,94	59,95	59,95	60,00	60,05	60,05
	98	69,82	42,66	42,59	19,96	19,94	59,95	59,95	60,00	60,05	60,05
	99	69,85	42,63	42,68	19,97	19,93	59,95	59,95	60,00	60,05	60,05
	100	69,94	42,58	42,86	19,97	19,95	59,95	59,95	60,00	60,05	60,05

STL	101	69,81	42,60	42,66	19,97	19,94	59,95	59,95	60,00	60,05	60,05
	102	69,93	42,59	42,73	19,95	19,94	59,95	59,95	60,00	60,05	60,05
	103	69,87	42,70	42,66	19,95	19,95	59,95	59,95	60,00	60,05	60,05
	104	69,88	42,64	42,80	19,96	19,94	59,95	59,95	60,00	60,05	60,05
	105	69,94	42,65	42,75	19,97	19,95	59,95	59,95	60,00	60,05	60,05
	106	69,78	42,73	42,54	19,96	19,94	59,95	59,95	60,00	60,05	60,05
	107	69,81	42,67	42,60	19,94	19,94	59,95	59,95	60,00	60,05	60,05
	110	69,84	42,56	42,79	19,95	19,95	59,95	59,95	60,00	60,05	60,05
	111	69,77	42,66	42,58	19,96	19,94	59,95	59,95	60,00	60,05	60,05
	113	69,94	41,99	42,68	19,94	19,96	59,95	59,95	60,00	60,05	60,05
	114	69,78	42,64	42,65	19,96	19,95	59,95	59,95	60,00	60,05	60,05
	115	69,87	42,69	42,65	19,97	19,94	59,95	59,95	60,00	60,05	60,05
	116	69,87	42,71	42,71	19,93	19,97	59,95	59,95	60,00	60,05	60,05
	117	69,87	42,71	42,69	19,96	19,93	59,95	59,95	60,00	60,05	60,05
	118	69,84	42,70	42,65	19,96	19,95	59,95	59,95	60,00	60,05	60,05
	119	69,88	42,65	42,74	19,96	19,95	59,95	59,95	60,00	60,05	60,05
	122	69,92	42,63	42,80	19,96	19,95	59,95	59,95	60,00	60,05	60,05
	123	69,86	42,70	42,73	19,94	19,95	59,95	59,95	60,00	60,05	60,05
	124	69,88	42,70	42,67	19,96	19,95	59,95	59,95	60,00	60,05	60,05
	125	69,84	42,61	42,74	19,96	19,90	59,96	60,01	59,98	60,05	60,06
	126	69,85	42,64	42,74	19,96	19,94	59,95	59,95	60,00	60,05	60,05
	127	69,90	42,59	42,84	19,98	19,93	59,95	59,95	60,00	60,05	60,05
	128	69,88	42,58	42,79	19,97	19,95	59,95	59,95	60,00	60,05	60,05
	129	69,84	42,62	42,64	19,96	19,94	59,95	59,95	60,00	60,05	60,05
	130	69,81	42,59	42,72	19,97	19,95	59,95	59,95	60,00	60,05	60,05
	131	69,89	42,66	42,66	19,97	19,95	59,95	59,95	60,00	60,05	60,05
	132	69,71	42,62	42,62	19,96	19,90	60,00	60,03	60,00	60,05	60,06
	133	69,80	42,69	42,53	19,97	19,95	59,95	59,95	60,00	60,05	60,05
	134	69,90	42,79	42,64	19,97	19,95	59,95	59,95	60,00	60,05	60,05
	135	69,87	42,68	42,70	19,96	19,95	59,95	59,95	60,00	60,05	60,05
	136	69,86	42,67	42,72	19,97	19,93	59,95	59,95	60,00	60,05	60,05
	137	69,80	42,59	42,77	19,95	19,93	59,95	59,95	60,00	60,05	60,05
	138	69,84	42,75	42,62	19,95	19,95	59,95	59,95	60,00	60,05	60,05
	139	69,86	42,69	42,72	19,99	19,95	59,95	59,95	60,00	60,05	60,05
	140	69,91	42,69	42,68	19,97	19,94	59,95	59,95	60,00	60,05	60,05
	141	69,84	42,53	42,74	19,95	19,90	60,01	60,03	60,02	60,05	60,05



STL	142	69,93	42,73	42,69	19,97	19,96	59,95	59,95	60,00	60,00	60,05	60,05
	143	69,86	42,65	42,66	19,96	19,95	59,95	59,95	60,00	60,00	60,05	60,05
	144	69,84	42,68	42,65	19,96	19,94	59,95	59,95	60,00	60,00	60,05	60,05
	145	69,83	42,62	42,72	19,97	19,92	59,95	59,95	60,00	60,00	60,05	60,05
	147	69,95	42,63	42,80	19,95	19,94	59,95	59,95	60,00	60,00	60,05	60,05
	148	69,82	42,70	42,60	19,95	19,95	59,95	59,95	60,00	60,00	60,05	60,05
	149	69,83	42,65	42,66	19,96	19,94	59,95	59,95	60,00	60,00	60,05	60,05
	150	69,36	41,80	43,62	19,94	19,94	59,95	59,95	60,00	60,00	60,05	60,05
	151	69,78	42,67	42,58	19,95	19,95	59,95	59,95	60,00	60,00	60,05	60,05
	152	69,92	42,74	42,75	19,95	19,94	59,95	59,95	60,00	60,00	60,05	60,05
	153	69,91	42,58	42,76	19,96	19,94	59,95	59,95	60,00	60,00	60,05	60,05
	154	69,89	42,64	42,79	19,97	19,93	59,95	59,95	60,00	60,00	60,05	60,05
	155	69,84	42,60	42,71	19,96	19,93	59,95	59,95	60,00	60,00	60,05	60,05
	156	69,99	42,61	42,78	19,98	19,92	59,95	59,95	60,00	60,00	60,05	60,05
	157	69,74	42,53	42,72	19,96	19,89	60,01	60,05	60,00	60,07	60,02	60,06
	158	69,85	42,60	42,74	19,96	19,95	59,95	59,95	60,00	60,00	60,05	60,05
	161	69,81	42,66	42,66	19,97	19,95	59,95	59,95	60,00	60,00	60,05	60,05
	162	69,88	42,54	42,79	19,97	19,89	60,00	60,03	60,00	60,06	60,02	60,06
	163	69,87	42,63	42,75	19,96	19,95	59,95	59,95	60,00	60,00	60,05	60,05
	165	70,02	42,70	42,86	19,96	19,95	59,95	59,95	60,00	60,00	60,05	60,05
	166	70,02	42,70	42,86	19,96	19,95	59,95	59,95	60,00	60,00	60,05	60,05
	167	69,81	42,60	42,73	19,93	19,91	59,95	59,95	60,00	60,00	60,05	60,05
	169	69,82	42,58	42,72	19,96	19,90	59,97	60,02	59,98	60,05	60,02	60,06
	170	69,84	42,70	42,73	19,95	19,95	59,95	59,95	60,00	60,00	60,05	60,05
	171	69,94	42,72	42,73	19,95	19,94	59,95	59,95	60,00	60,00	60,05	60,05
	172	69,78	42,65	42,62	19,97	19,94	59,95	59,95	60,00	60,00	60,05	60,05
	173	69,74	42,57	42,70	19,96	19,89	59,98	60,05	59,97	60,08	60,01	60,07
	174	69,88	42,68	42,77	19,97	19,95	59,95	59,95	60,00	60,00	60,05	60,05
	175	69,87	42,74	42,65	19,96	19,95	59,95	59,95	60,00	60,00	60,05	60,05
	176	69,80	42,67	42,66	19,95	19,90	60,01	60,03	60,02	60,05	60,03	60,05
	177	69,87	42,62	42,68	19,97	19,94	59,95	59,95	60,00	60,00	60,05	60,05
	178	69,78	42,68	42,62	19,95	19,96	59,95	59,95	60,00	60,00	60,05	60,05
	179	69,87	42,65	42,77	19,95	19,94	59,95	59,95	60,00	60,00	60,05	60,05
	180	69,86	42,66	42,68	19,95	19,94	59,95	59,95	60,00	60,00	60,05	60,05
	181	69,87	42,63	42,75	19,97	19,94	59,95	59,95	60,00	60,00	60,05	60,05
	182	69,90	42,73	42,70	19,96	19,95	59,95	59,95	60,00	60,00	60,05	60,05

STL	183	69,83	42,61	42,70	19,98	19,90	59,97	60,01	59,98	60,04	60,02	60,06
	185	69,86	42,61	42,76	19,95	19,94	59,95	59,95	60,00	60,00	60,05	60,05
	186	69,93	42,64	42,80	19,96	19,95	59,95	59,95	60,00	60,00	60,05	60,05
	187	69,80	42,69	42,60	19,94	19,95	59,95	59,95	60,00	60,00	60,05	60,05
	188	69,79	42,64	42,65	19,95	19,95	59,95	59,95	60,00	60,00	60,05	60,05
	189	69,94	42,48	42,77	19,95	19,96	59,95	59,95	60,00	60,00	60,05	60,05
	190	69,89	42,71	42,69	19,94	19,94	59,95	59,95	60,00	60,00	60,05	60,05
	191	69,85	42,65	42,77	19,96	19,94	59,95	59,95	60,00	60,00	60,05	60,05
	192	69,80	42,53	42,72	19,94	19,93	59,95	59,95	60,00	60,00	60,05	60,05
	193	69,81	42,73	42,70	19,96	19,94	59,95	59,95	60,00	60,00	60,05	60,05
	194	69,81	42,67	42,62	19,97	19,95	59,95	59,95	60,00	60,00	60,05	60,05
	195	69,88	42,25	42,74	19,94	19,95	59,95	59,95	60,00	60,00	60,05	60,05
	196	69,79	42,56	42,71	19,95	19,93	59,95	59,95	60,00	60,00	60,05	60,05
	197	69,88	42,68	42,75	19,96	19,94	59,95	59,95	60,00	60,00	60,05	60,05
	198	69,83	42,26	42,71	19,98	19,93	59,95	59,95	60,00	60,00	60,05	60,05
	200	69,90	42,71	42,77	19,97	19,95	59,95	59,95	60,00	60,00	60,05	60,05
	202	69,80	42,69	42,65	19,96	19,89	60,00	60,03	60,00	60,05	60,02	60,06
	203	69,88	42,65	42,81	19,95	19,94	59,95	59,95	60,00	60,00	60,05	60,05
	204	69,86	42,63	42,70	19,96	19,95	59,95	59,95	60,00	60,00	60,05	60,05
	206	69,79	42,66	42,66	19,95	19,95	59,95	59,95	60,00	60,00	60,05	60,05
	208	69,85	42,65	42,77	19,98	19,95	59,95	59,95	60,00	60,00	60,05	60,05
	209	69,82	42,60	42,73	19,96	19,95	59,95	59,95	60,00	60,00	60,05	60,05
	210	69,86	42,58	42,74	19,96	19,90	59,97	60,02	59,97	60,06	60,03	60,07
	212	69,82	42,70	42,67	19,95	19,95	59,95	59,95	60,00	60,00	60,05	60,05
	214	69,96	42,78	42,78	19,95	19,96	59,95	59,95	60,00	60,00	60,05	60,05
	215	69,88	42,60	42,77	19,97	19,96	59,95	59,95	60,00	60,00	60,05	60,05
	216	69,95	42,67	42,73	19,96	19,96	59,95	59,95	60,00	60,00	60,05	60,05
	219	69,87	41,92	42,80	19,97	19,89	59,96	60,01	59,97	60,05	60,02	60,06
	220	69,85	42,56	42,75	19,96	19,96	59,95	59,95	60,00	60,00	60,05	60,05
	221	69,90	42,62	42,81	19,97	19,96	59,95	59,95	60,00	60,00	60,05	60,05
	223	69,85	42,64	42,69	19,96	19,96	59,95	59,95	60,00	60,00	60,05	60,05
	225	69,94	42,60	42,87	19,99	19,89	59,96	60,02	59,97	60,07	60,01	60,07
	227	69,84	42,56	42,80	19,98	19,89	59,96	60,03	59,96	60,08	60,01	60,08
	228	69,92	42,59	42,81	19,98	19,90	59,97	60,03	59,97	60,07	60,01	60,07
	229	69,83	42,61	42,74	19,96	19,96	59,95	59,95	60,00	60,00	60,05	60,05
	230	69,90	42,66	42,69	19,97	19,97	59,95	59,95	60,00	60,00	60,05	60,05

STL	247	69,86	42,71	42,70	19,97	19,94	59,95	59,95	60,00	60,05	60,05
	248	69,86	42,76	42,66	19,96	19,95	59,95	59,95	60,00	60,05	60,05
	250	69,82	42,65	42,80	19,98	19,89	59,98	60,04	60,07	60,01	60,07
	251	69,79	42,68	42,67	19,98	19,88	59,96	60,02	60,07	60,01	60,08
	253	69,88	42,63	42,75	19,97	19,93	59,99	59,97	59,99	60,04	60,03
	254	69,93	42,68	42,90	19,98	19,96	59,95	59,95	60,00	60,05	60,05
	255	69,79	42,56	42,76	19,96	19,89	60,00	60,03	60,05	60,03	60,06



## Appendix I

